GL013604

EXPLORATION CRITERIA FOR LOW PERMEABILITY GEOTHERMAL RESOURCES

Final Report

by

D. Norton
University of Arizona

October 1977

Prepared for

The U.S. Energy Research and Development Administration
Under Contract No. EY-76-S-02-2763

The studies reported are the result of research conducted by:

D. Norton, Principal Investigator
T. Gerlach, Research Associate
R. Knapp, Research Assistant
J. Knight, Research Assistant
W. Leinhard, Research Assistant
B. Moskowitz, Research Assistant.

Technical support for the project was also provided by the University Computer Center personnel. The final report was typed and edited by Lynn McLean, and figures were prepared by Janis Blainer and 4015.

I

Statement of Problem

Recognition that energy resources occur in finite quantities, that they are nonrenewable, and that consumption of energy is required in order to recover these resources has resulted in programs whose objectives are: (1) assessment of the magnitude and (2) recoverability of these resources. A viable resource assessment program for geothermal energy requires description of the unique features of the subsurface thermal energy resources and development of methods useful in direct or indirect detection of these features. Since geothermal energy resources occur in subsurface environments which are inaccessible to direct observation, the tasks which would, potentially, fulfill these program objectives are often poorly defined.

Geothermal resources occur as a natural consequence of processes which disperse anomalous concentrations of thermal energy in the earth's upper crust. These heat and mass transport processes are active around thermal anomalies, such as igneous or metamorphic intrusions, for long periods of time, and they affect large volumes of rocks. Characteristics of these resources have been deduced from data collected over an extremely short time interval, as compared to the total age of the resource, or from data on fossil systems which represent the total integrated history of the resources at only a few locations within a larger system. As a consequence, observations made on active geothermal systems are usually not extensive enough to be representative of the entire system.

In response to human crises, the need to expand the energy resource base and to evaluate the utilization of new and novel resources, such as geothermal energy, has arisen. Historically, responses have followed the sequence of events outlined in the flow chart depicted in figure 1, exclusive of

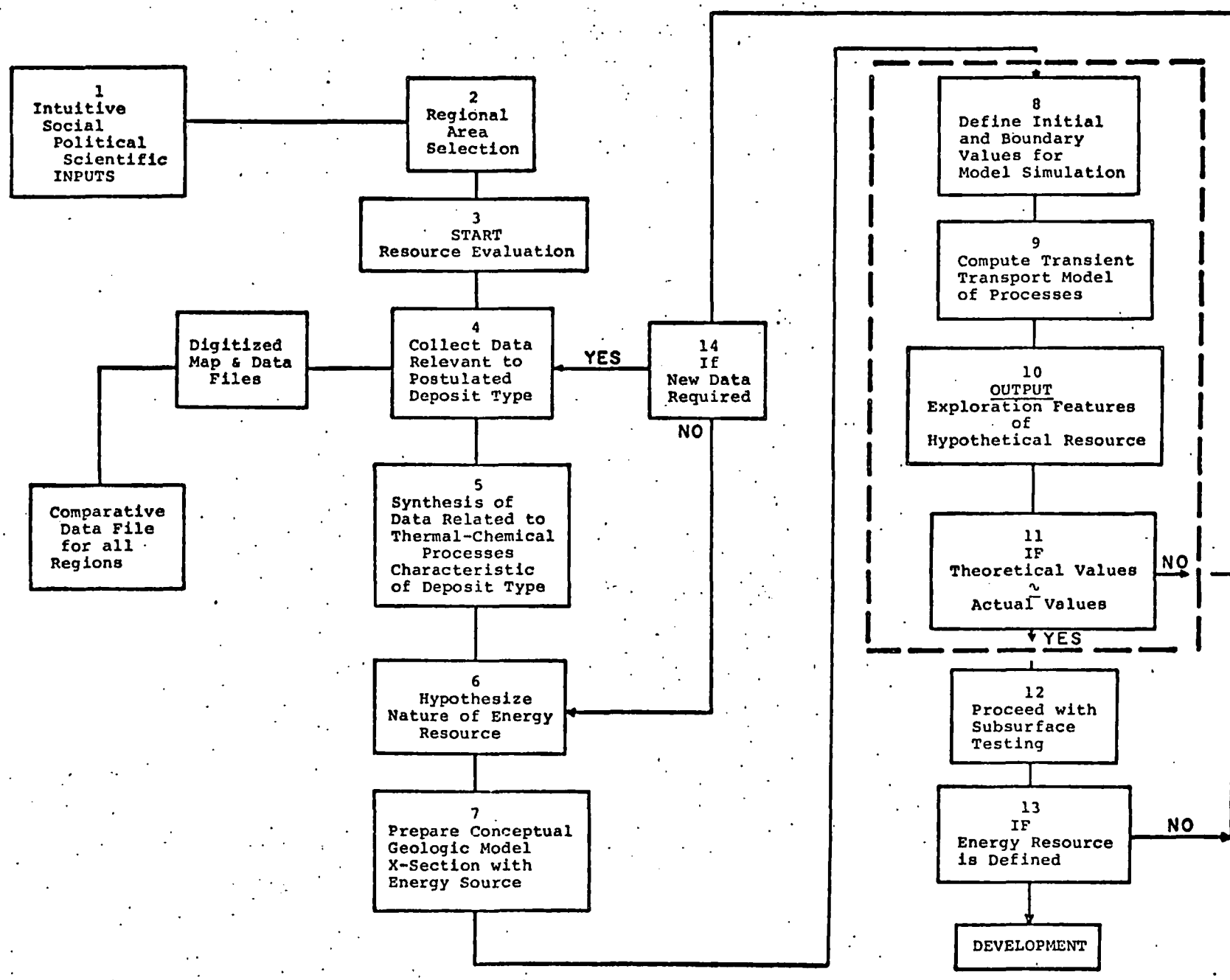

Figure 1
Resource Assessment

the operations detailed within the dashed box. A general problem in the decision sequence has traditionally been that the conceptual geologic x-section (step 7) can not be tested by methods other than drilling, which is ultimately necessary but which often detracts from the project objective. Furthermore, negative results from a single drill hole often totally destroy confidence in the prospective regions.

Geothermal energy resources are formed by processes which transport thermal energy to shallow depths in the crust. Simulation of heat and mass transport processes which occur in and around thermal anomalies in the upper crust provides a key to understanding the geologic past and the extent of hydrothermal systems. Basic mathematical equations representing the processes, and numerical approximations of these equations, permit computer simulation of large and long-lived natural systems. An analysis of the transport equations which simulate these processes reveals those parameters and variables that are characteristic of the system. Numerical approximations of idealised systems provide a first order approximation of the magnitude of the variables.

This novel technology is incorporated into a decision-making sequence which permits an objective evaluation of data and hypotheses prior to drilling, allows reliability factors to be assigned to various data, and demands more effective data collection. Since the decision to drill implicitly includes a conceptual model of energy resources in the subsurface, this decision is also a qualitative statement of initial and boundary conditions related to the prospective energy resource, figure 1 (8). These conditions can be quantitatively described for various thermal sources, and, consequently, a set of quantitative conditions, sufficient for analysis by heat and mass transport theory, is defined.

Energy resources are transient features in the earth's crust, usually existing for 10^5 - 10^6 years, and are distributed over large volumes of the crust, $\sim$ 100's km^3. Direct

measurement is, therefore, impossible, but with high-speed, large-memory computers the systems can be simulated within a few hours, figure 1 (9). The results of these computations contain the quantitative values of parameters directly related to the energy resource, figure 1 (10), e.g., the relevant exploration features are quantitatively defined.

The explorationist, then, can enjoy the situation of having both measured and theoretical values for his hypothesized resource. A comparative study of these data permits refinement of the hypothesis, regarding its location, or insight into additional data required prior to drilling, figure 1 (11). At some confidence level, drilling and subsurface data collection proceed, figure 1 (12), with the option to interpret the subsurface data in a similar method, figure 1 (12-13-14).

Objective of Study

The overall project objective was to analyze low permeability geothermal systems related to high temperature plutons in the upper crust in order to ascertain those characteristics of these systems which could be detected by surface and shallow subsurface exploration methods. Analyses were designed to integrate data and concepts from the literature, which relate to the transport processes, together with computer simulation of idealised systems.

Methods of Analysis

Notions of energy distribution in geothermal systems are primarily derived from temperature and pressures, measured in production or exploration wells, and are usually restricted to small portions of the total system. In order to predict the size, grade, and life expectancy of the resource, knowledge of these parameters over a large portion of the hydrothermal system is necessary. Time dependence of transport variables in the region of an energy source, such as a cooling pluton, can be simulated by numerical methods.

Fluid flow caused by thermal anomalies related to igneous plutons is effectively scaled and represented in a two-dimensional infinite half-space by partial differential equations representing the conservation of mass, momentum, and energy for the fluid-rock system, Norton and Knight, 1977:

$$(1)\quad \gamma\frac{\partial T}{\partial t} + q\nabla H = \nabla\cdot\kappa\nabla T \qquad \text{(conservation of energy)}$$

and

$$(2)\quad \frac{\nu\nabla\cdot\mu}{k}\,\nabla\Psi = R\,\frac{\partial\rho}{\partial y} \qquad \text{(conservation of momentum)}$$

where T is the temperature, Ψ the streamfunction, q the fluid flux, t the time, H, ρ, and ν are the enthalpy, density, and viscosity of the fluid, k is the permeability of the rock, κ the thermal conductivity and γ the volumetric heat capacity of the fluid saturated media, R the Rayleigh number, ∇ the gradient operator, and y the horizontal distance in the two-dimensional section to which these equations apply.

Fluid mass fluxes, $\vec{q}$, are derived from the streamfunction gradient where $q_z = -\frac{\partial\Psi}{\partial y}$; $q_y = \frac{\partial\Psi}{\partial z}$. The pressure throughout the system is obtained by integration of Darcy's Law:

$$(3)\quad P - P_o = \int_o^z [\rho g - q_z\,\frac{k}{\nu}]dz.$$

Equations (1), (2), and (3) are approximated by finite difference numerical equations which permit computation of the values of the dependent variables at discrete points from initial and boundary values specified for the system. These numerical equations account for variable transport properties of the fluid (H_2O-system) and rock, general boundary and initial conditions, and radioactive and volumetric heat sources. Transport processes related to transient thermal anomalies

are approximated by a time sequence of steady state numerical solutions to (1) and (2), computed at explicitly stable time intervals. An alternating-direction-implicit finite difference method, which accounts for the transportive characteristics of the system, is used to approximate the spatial derivatives at discrete intervals on the order of 0.1 to 0.5 of the system height. Fluid pressure in the system is computed at each steady state step using (3), in which the fluid properties, viscosity and density, are expressed as a function of temperature and pressure. The numerical methods used generally approximated the governing partial differential equations within 10% in space and time. Overall geologic reality of the analyses depends on the degree to which parameters used approximated natural conditions and was, therefore, more difficult to evaluate. Temperature, pressure, and fluid flux described in the simulated systems form the basis for predicting the magnitude and distribution of related characteristics. Heat flux (conductive and convective), energy content and distribution, porosity, temperature gradients, electrical resistivity, permeability, in-situ stress, and surface uplifts were predicted for the systems.

One objective was to analyze geothermal systems by systematically varying input parameters in order to understand their affect on the variables which might be measured in an exploration-assessment program. A second objective was to apply the methods to a prospective system in its early stages of evaluation; the Coso system was picked for this portion of the study.

This study represents a first-order approximation to transport processes in geothermal systems, which consist of high temperature intrusions, host rocks, and fluids. The results of these studies can be most effectively used as a tool for understanding the uniqueness of certain exploration data and for understanding some of the gross characteristics of the system, as a guide in the collection and interpretation of data, and as a basis for more refined and sophisticated numerical studies.

II

First Objective

Discussion of Results

Permeability of rocks is apparently the single most important parameter affecting the characteristics of geothermal resources, both in terms of locating the resource and recovering the energy. Production of geothermal energy by conventional means requires reservoirs with permeabilities $\geq 10^{-11}$ cm^2. However, systems which have bulk permeabilities as low as 10^{-14} cm^2 may have exploration characteristics which result from the circulation of large volumes of fluid, Norton and Knight, 1977.

Conductive transfer of thermal energy is defined by

$$(4) \quad \vec{q}_{cond} = - K\vec{\nabla T},$$

where K, cal sec^{-1} cm^{-1} $^oC^{-1}$, is the average thermal conductivity of the system, e.g., fluid and rock, T, ^oC, the temperature, and ∇ the gradient operator, whereas conductive — convective transport of thermal energy is

$$(5) \quad \vec{q}_{conv} = \frac{H(T,P)\ k}{\nu(T,P)} \nabla\Phi,$$

where H(T,P) is the heat content of the fluid, cal gr^{-1}, at the local temperature and pressure reference to H = 0 at T = .01^oC, P = .006 bars, k is the intrinsic rock permeability, cm^2, and $\nu(T,P)$ is the fluid viscosity, cm^2 sec^{-1}. Convective transport of thermal energy inevitably occurs in systems where lateral density anomalies are present in fluids contained in the flow porosity. The magnitude of fluid transport is determined principally by permeability since the fluid enthalpy, viscosity, and density, as well as the magnitude of the initial thermal anomaly, are similar for most igneous

environments. As can be seen in equations (4) and (5), the temperature gradient in any system will be strongly affected by the convective transport of energy such that conductive transfer is actually decreased along the principal flow channels in the direction of fluid flow. The relative ratios of convective to conductive transport as a function of host rock permeability have been calculated for several pluton-host rock systems, figure 2.

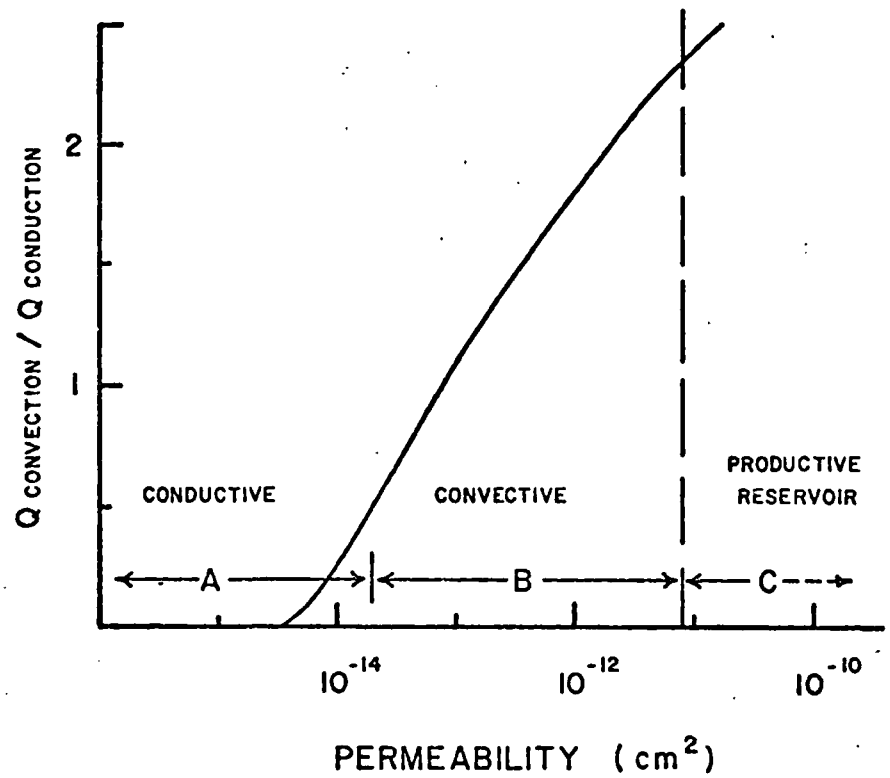

Figure 2

Geothermal resources in regions of igneous activity have been classified into three types, as defined by the processes which tend to disperse the anomalous thermal energy: (1) Thermal energy in rocks whose bulk permeability is sufficiently large, $\geq 10^{-11}$ cm^2, figure 2, region C, that fluids (liquid or vapor) can be recovered from conventional production wells. Examples of this resource are the rocks from which energy is being recovered today, e.g., Wairakei, Larderello, Geyser, etc. (2) Thermal energy in rocks which have permeabilities too small,

$< 10^{-11}$ cm^2, for direct production of energy by conventional wells but whose permeabilities are greater than the minimum value ($\sim 10^{-14}$ cm^2) at which heat transport by fluid convection predominates over heat transport by conduction, figure 2, region B. (3) Thermal energy in rocks whose permeabilities are less than the value at which heat transport by convection predominates over heat transport by conduction ($Q_{conv}/Q_{cond} \sim 0.5$), figure 2, region A.

Relatively impermeable but high-energy-content rocks are expected to occur within the fractured regions of either A or B type resources, as well as in C. This is certainly evident in the producing geothermal systems where drill holes have missed the zones of abundant fracturing; they are hot and dry. "Hot-dry-rock" geothermal energy is considered to be a production method useful where resources have permeabilities too low for conventional production methods. Rocks apparently contain pore fluids in their flow porosity from the groundwater table to several kilometer depths in the crust, Brace, 1971; Norton, 1977, albeit insufficient for conventional production of energy, and evidence exists that fluid circulation is characteristic of most shallow pluton environments, Taylor, 1974; Helgeson, 1970; Norton, 1972; Norton, 1978. As a consequence, thermal resources associated with plutons have characteristics that are not uniquely interpreted by conventional methods that assume the presence of a steady heat source which cools by conductive transfer of thermal energy to surrounding rocks.

There appear to be several advantages to identifying these systems at various stages of their development since their geologic age has a direct affect on the type of exploration methods which can be used to effectively detect these resources. The age of the geothermal resource, with respect to the causative thermal anomaly, is important in all types of systems, but it is particularly relevant for systems in which fluid circulation contributes to heat transport. The latter is apparently a general feature of virtually all igneous systems at depths

< 10 km in the crust.

Systems are discussed with respect to three age intervals, Stages I, II, and III, defined on the basis of major differences in their characteristics. The elapsed age obviously depends on geologic conditions in the subsurface; so, for purposes of discussion, the near-surface (1 - 3 km) thermal characteristics of a 4.5 km tall, ∿ 2 km wide, semi-infinite pluton emplaced at 4.5 km will be considered. The surface boundary condition is conductive to heat but impermeable to fluid, consistent with either an impermeable rock layer or an unsaturated zone at the surface of natural systems.

Plutons emplaced at ∿ 4.5 km depths will not cause temperature perturbations at 1 km depths for tens of thousands of years after emplacement of the pluton; the time of initial emplacement to the time at which perturbations in temperature are detectable at shallow depths is referred to as Stage I. Near-surface thermal perturbations then tend to a maximum, at which point the energy resource is nearest to the surface, Stage II, and, finally, the system decays to background temperatures, Stage III. This concept of time evaluation of geothermal resources is used to examine the predicted distribution of temperature in the following schematic diagrams.

Temperature as a function of depth, directly above the causative pluton, in three systems, A, B, and C, corresponding to permeability increments A, B, and C in figure 1, at an elapsed time equivalent to Stage II is summarized below. Differences between these thermal profiles are simply a function of permeability of the host rocks surrounding the thermal anomaly. Large values of permeability produce thermal profiles which are very steep near the top boundary; below this region of large temperature gradients, temperature increases slightly with depth then increases sharply to the current temperature of the causative pluton. The style of perturbations above the normal geothermal gradient, dashed line, appears to be unique

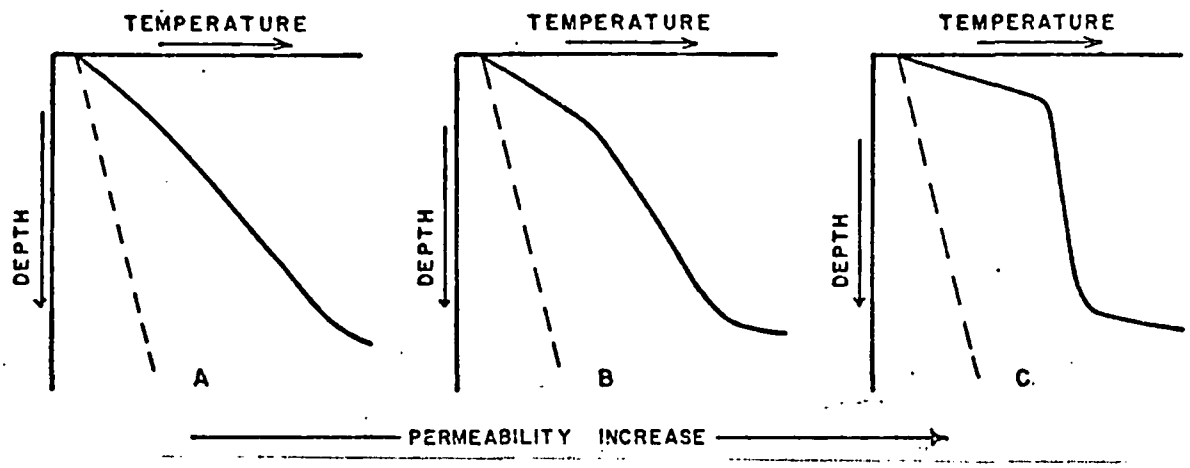

Figure 3

for natural systems. The interval of nearly constant temperature, figure 3C, results from convective heat transported by circulating fluids and may extend for several kilometers and persist for tens of thousands of years in the system. This type of thermal gradient has long been recognized as characteristic of active geothermal systems, and as a consequence of its overall nonlinear character, temperatures cannot be accurately predicted at depth on the basis of near-surface temperature gradient data. More significantly, temperatures are grossly over-estimated by conventional heat flow interpretation methods.

The variation in temperature as a function of depth with time in a system with permeabilities represented by the B-increment of figure 1 can be seen in figure 4. Note that the large near-surface temperature gradients occur during Stage II and the end stages of the thermal anomaly, Stage III. Independent evidence regarding subsurface energy content and distribution is required for these "older" systems, whereas in Stage I systems the gradients will predict temperatures at depth which are much lower than actual temperatures.

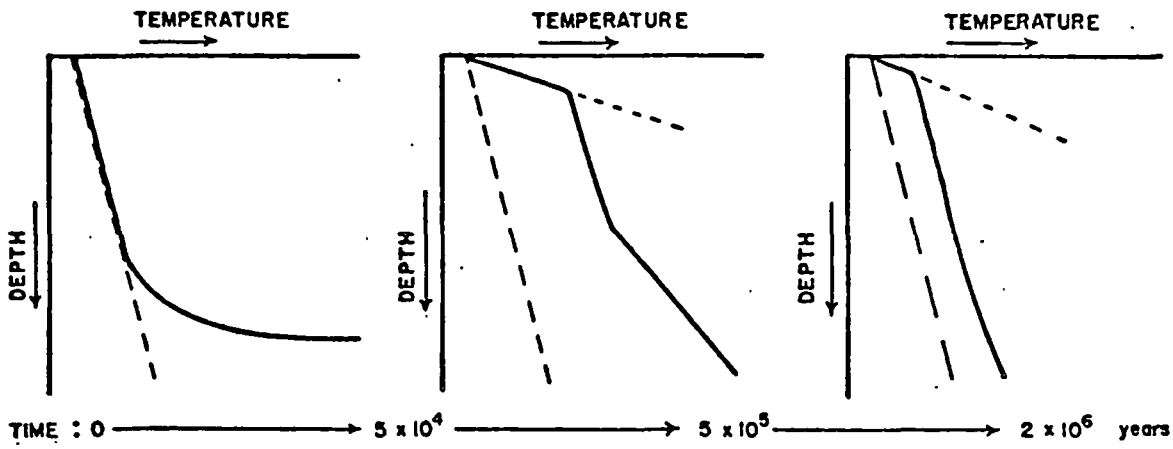

Figure 4

Prospecting methods detect (1) currently active processes related directly to the heat transport process of (2) spatial variations in rock or fluid properties which are a consequence of the process operating over some period of time. As can be seen in the temperature survey data, a significant lag time between events at depth and the detection of a perturbation near the surface is characteristic of the data collected in (1). In order to uniquely interpret time integrated properties (2), independent data regarding the magnitude and duration of the transport processes are required. Since all the features ultimately relate to dispersion of the thermal anomaly, the nature of various anomalies detected by methods (1) and (2) was predicted on the theory of thermal transport in idealised systems. In-situ values of electrical resistivity, stress, porosity, fluid velocity, and energy distribution, as well as microseismic activity, are summarized in the following discussions, in the perspective of the time evolution of geothermal systems defined above (Stages I-III).

Redistribution of thermal energy closely mimics the rock temperature for systems containing liquid H_2O at temperatures

< 350°C. As a consequence of the fracture controlled permeability and porosity characteristics of pluton environments, the thermal energy of the bulk system is defined by

$$(6) \quad Q_T = \int_v [\phi_T \rho_f H_f + (1 - \phi_T)\rho_r H_r] dV,$$

where ϕ_T is the total porosity, ρ_f and H_f the density and enthalpy of the fluid phase, and ρ_r and H_r the density and enthalpy of the solid phases where $H_r \simeq c_p T$ and $c_p = 0.26$ cal $^oC^{-1}$ g^{-1}. But the energy content of the "recoverable" fluid, e.g., fluid which is present in the flow porosity, ϕ_F, of the fractured matrix, is defined by

$$(7) \quad Q_R \doteq \int_v \phi_F \rho_f H_f \, dV.$$

Flow porosities range from 10^{-3} - 10^{-5} for fractured media, Norton and Knapp, 1977, and, therefore, a small fraction of the energy in the fluid phase is recoverable without recharge since total porosities are usually on the order of 10^{-1} - 10^{-2}. The in-situ energy content of the resource is essentially the energy content of the solid phases. Recoverability of the resource is not considered, but one can see from the predicted low flow porosities that recovery rates might be considerably lower than generally assumed, cf. White and Williams, 1975, if fluid recharge is slow.

In systems which include high permeability host rocks, $k > 10^{-14}$ cm^2, the transport of thermal energy upward toward the top boundary (surface) is more rapid and results in higher energy concentrations than in those systems whose host rock permeabilities are < 10^{-14} cm^2. Thermal energy content, size and location, and the correlation of these resource features with near-surface conductive heat flow and thermal gradients are summarized in the following discussion for an impermeable pluton emplaced into 10^{-11} cm^2 permeability host rocks, figure 5.

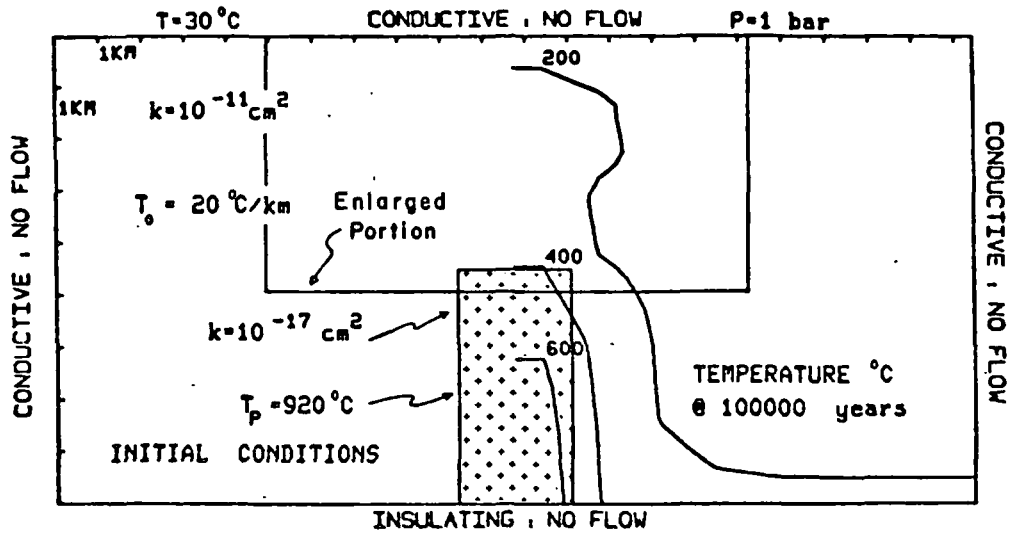

Figure 5

Temperature variations in the system along vertical profile 1-2 in figure 5 can be seen, figure 6, to reflect the stages of evolution discussed above.

A prospective resource is defined for this system as that region above 3 km and having temperatures greater than 200°C. Variation in the size, energy content, and depth of this resource is related to the age of the thermal anomaly, figure 7.[1] The resource is shown for an enlarged portion of the system, cf. figure 5.

Distribution of the hypothetical energy resource changes with time, as can be seen in figure 7. Transport of the resource toward the surface is accompanied by lateral spreading as a consequence of uniform horizontal and vertical permeability and an impermeable (no flow) top boundary condition. The maximum development of the resource can be seen to occur during the final portion of Stage I and during Stage II, during which time the resource is closest to the surface, has

[1]The reader should note that the thermal computations are for a two-dimensional cross-section of an infinitely long heat source; therefore, data are reported with respect to 1 km strike length of the source into the infinite half space.

STAGE I

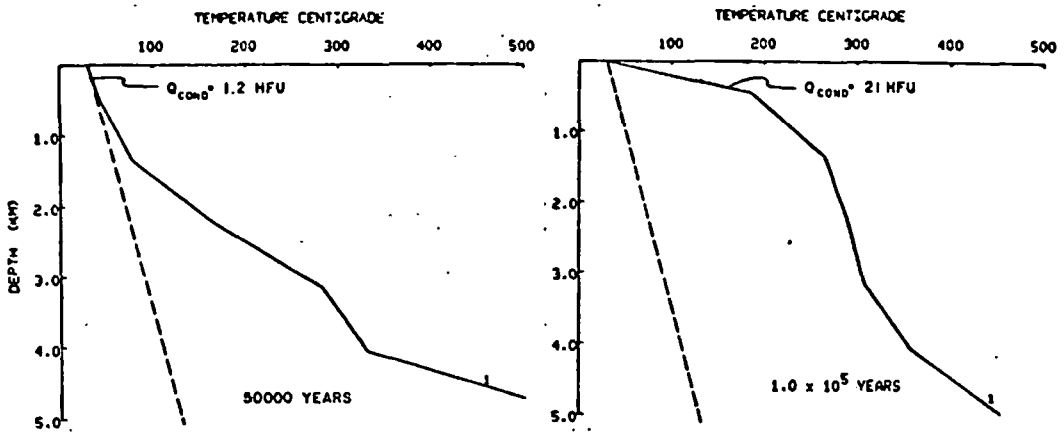

STAGE II

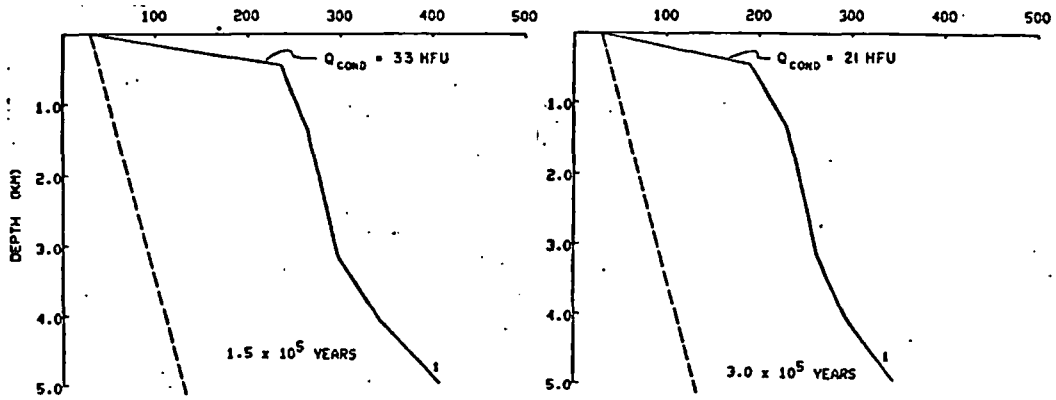

STAGE III

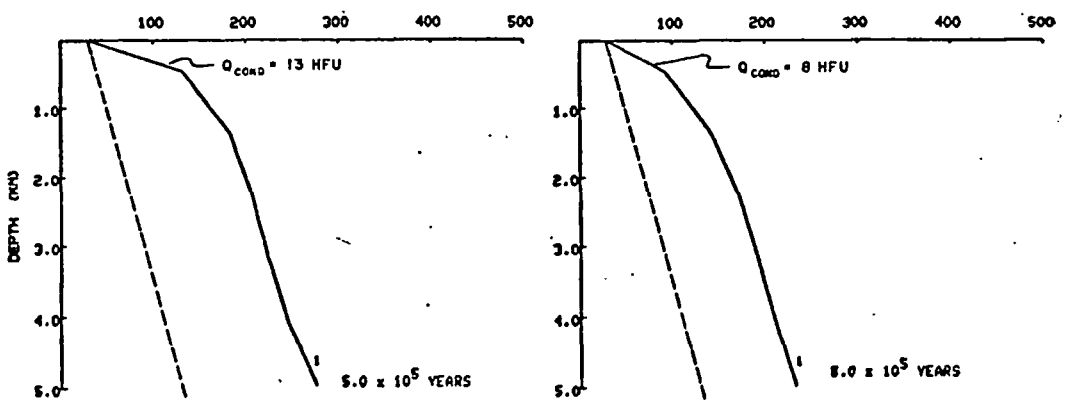

Figure 6

STAGE I

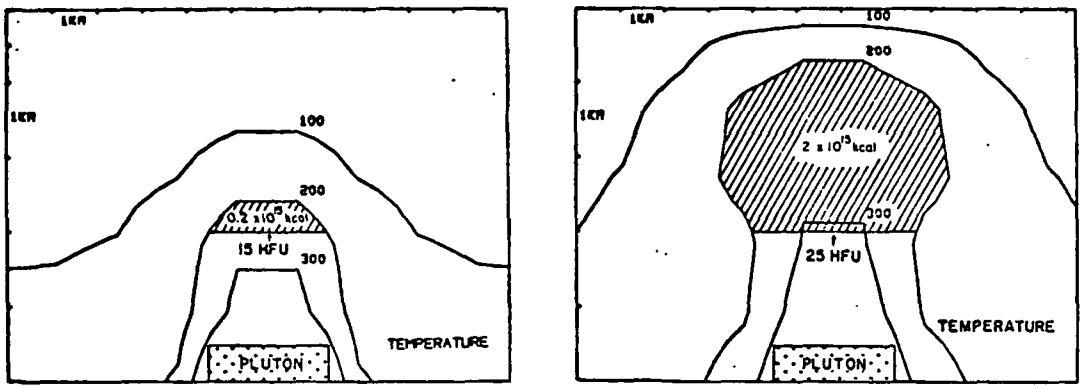

50000 YEARS

1.0×10^5 YEARS

STAGE II

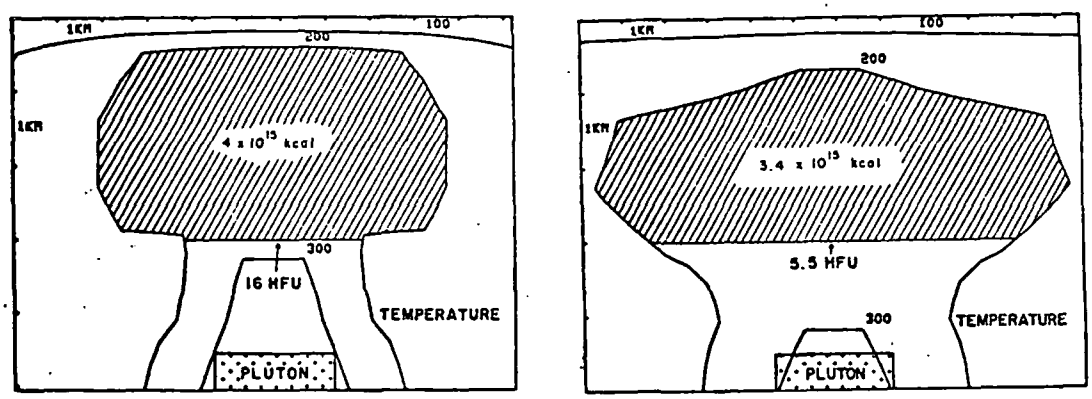

1.5×10^5 YEARS

3.0×10^5 YEARS

STAGE III

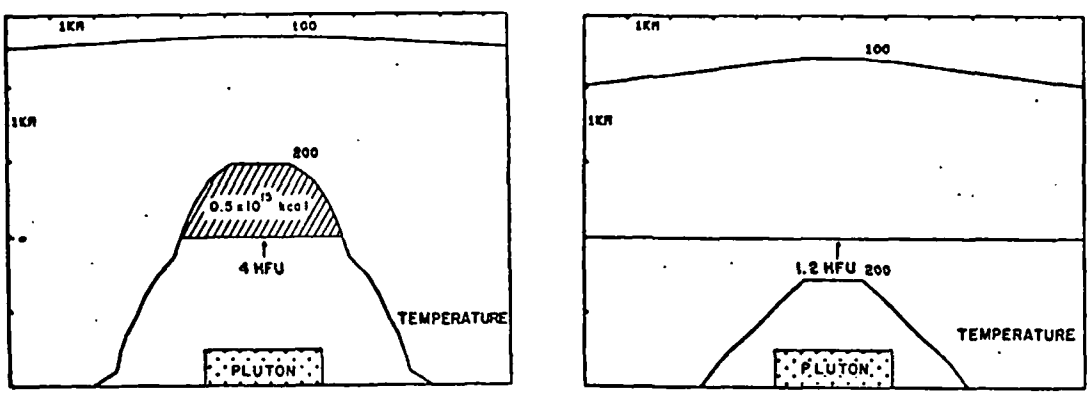

5.0×10^5 YEARS

8.0×10^5 YEARS

Figure 7

the largest energy content, and includes the maximum rock mass. Economically, this could be interpreted to be the largest tonnage of highest grade material at shallowest "mining" depths.

Through the cooling history of the system the thermal energy content of the prospective resource region is ∿ 55 cal/gr, but the mass of rock containing this concentration of energy varies from < 3 x 10^{10} tons at 10^5 years to a maximum of 7 x 10^{10} tons at 2.5 x 10^5 years, after which time the mass decreases exponentially to zero at ∿ 6.5 x 10^5 years, figure 8.

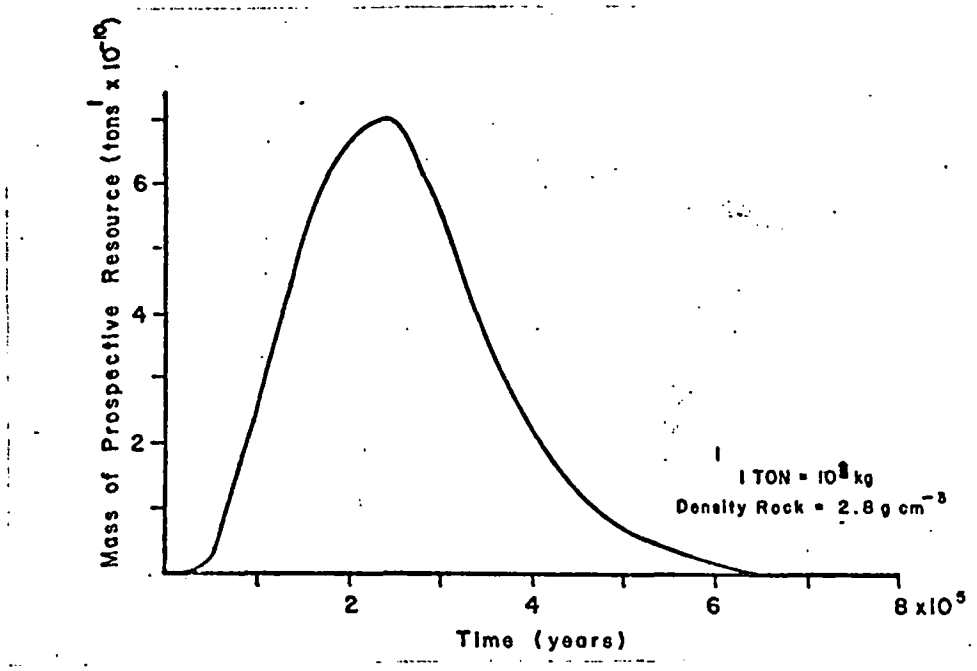

Figure 8

Similarly, the total heat content varies from a maximum of 6 x 10^{15} kcal at 2 x 10^5 years to less than 2 x 10^{15} kcal at 4 x 10^5 years, figure 9. Greater than 10^5 kcal of energy distributed over more than 1.5 x 10^{10} tons of rock, above 3 km depth, persists in the system for about 4 x 10^5 years, figures 8 and 9. The rate of energy input into the region by conduction and convection of energy from the heat source has a well-defined maximum at 10^5 years but averages about 4.5 x 10^2 kcal/sec over the similar elapsed time period of

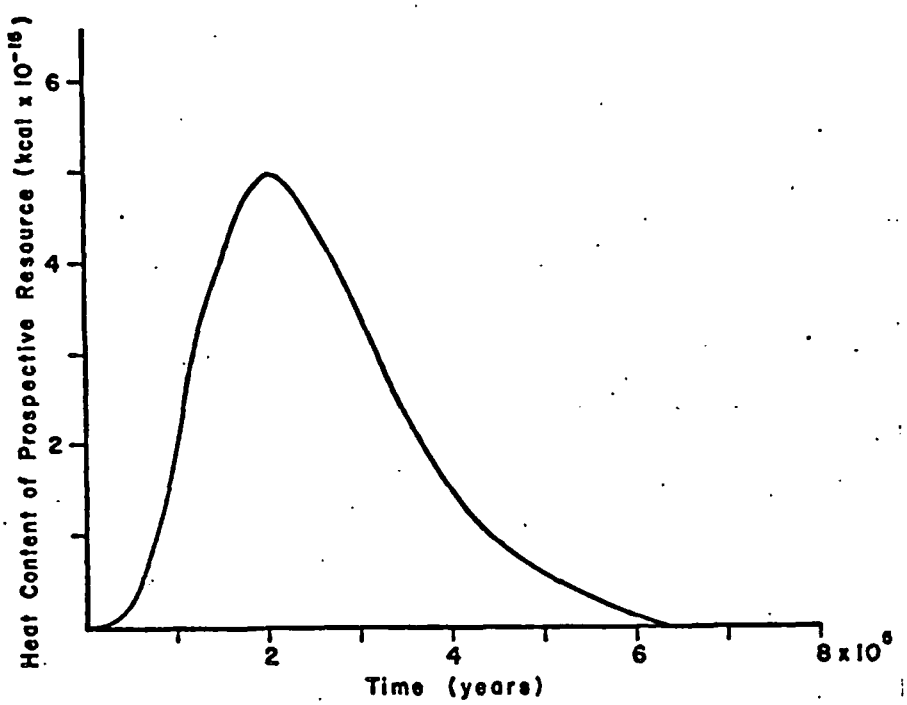

Figure 9

4 x 10^5 years, figure 10.

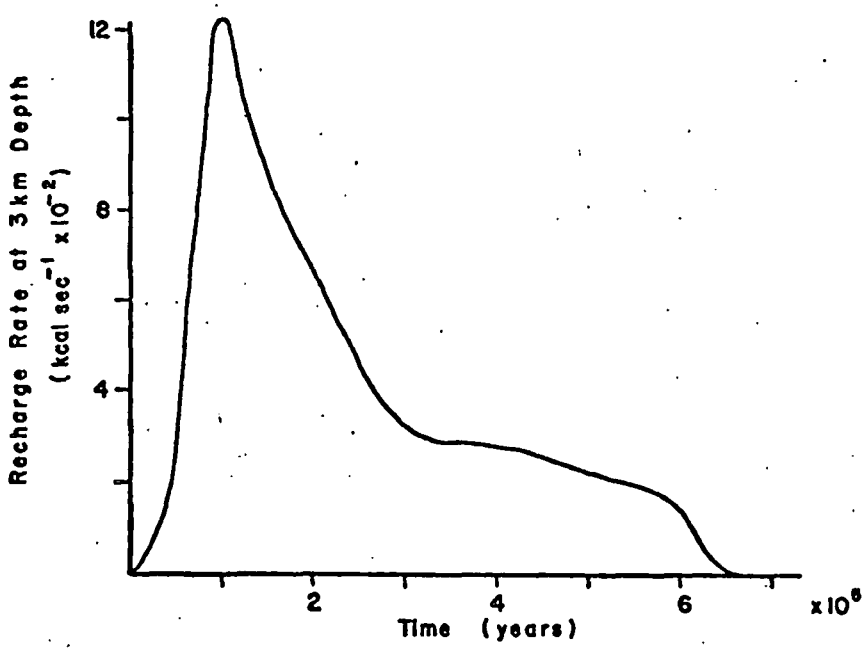

Figure 10

An an elapsed time of 3×10^5 years the total remaining resource is about one-third of the total resource available, or about 0.4 of the initial heat in the pluton, H_p^o, figure 11. Associated in time with the resource are the thermal gradient and temperature as depth functions, figure 11. The magnitude of the heat fluxes at shallow, down to $\sim$ .5 km, depths indicates the nonuniqueness of energy resource distribution and this parameter. Particularly note the conductive heat flux at 5×10^5 years is 13 HFU where the resource has been nearly dispersed.

Thermo-mechanical processes related to the dispersal of heat away from thermal perturbations result in thermal expansion of rocks. Non-uniform volume changes in the system cause displacements and thermal stresses. The magnitude and sense of these effects are analyzed for several different systems, and their implications to resource assessment are considered. It should be noted that only displacements and stresses resulting from dispersal of heat from the pluton are examined; effects of other potential displacement-stress sources, such as the buoyancy effect of the pluton, are not considered.

Thermal strains and stresses were estimated by the method of strain-suppression (Timoshenko and Goodier, 1951), with the aid of finite elements (Zienkiewicz, 1971). The system was subdivided into 100-200 triangular elements with nodal points at the corners of the triangles. Strains that result from a change in temperature, ΔT, are first computed from

$$(8) \quad \varepsilon_x = \frac{1}{3} \alpha_v \Delta T,$$

where α_v is the isobaric coefficient of thermal expansion, then converted to fictive forces and applied to the nodes of the element. Elements are loaded into a matrix, where each element is allowed to interact with its neighbors, and the nodal displacements are solved for these displacements and are then converted to stresses. The final stress in each

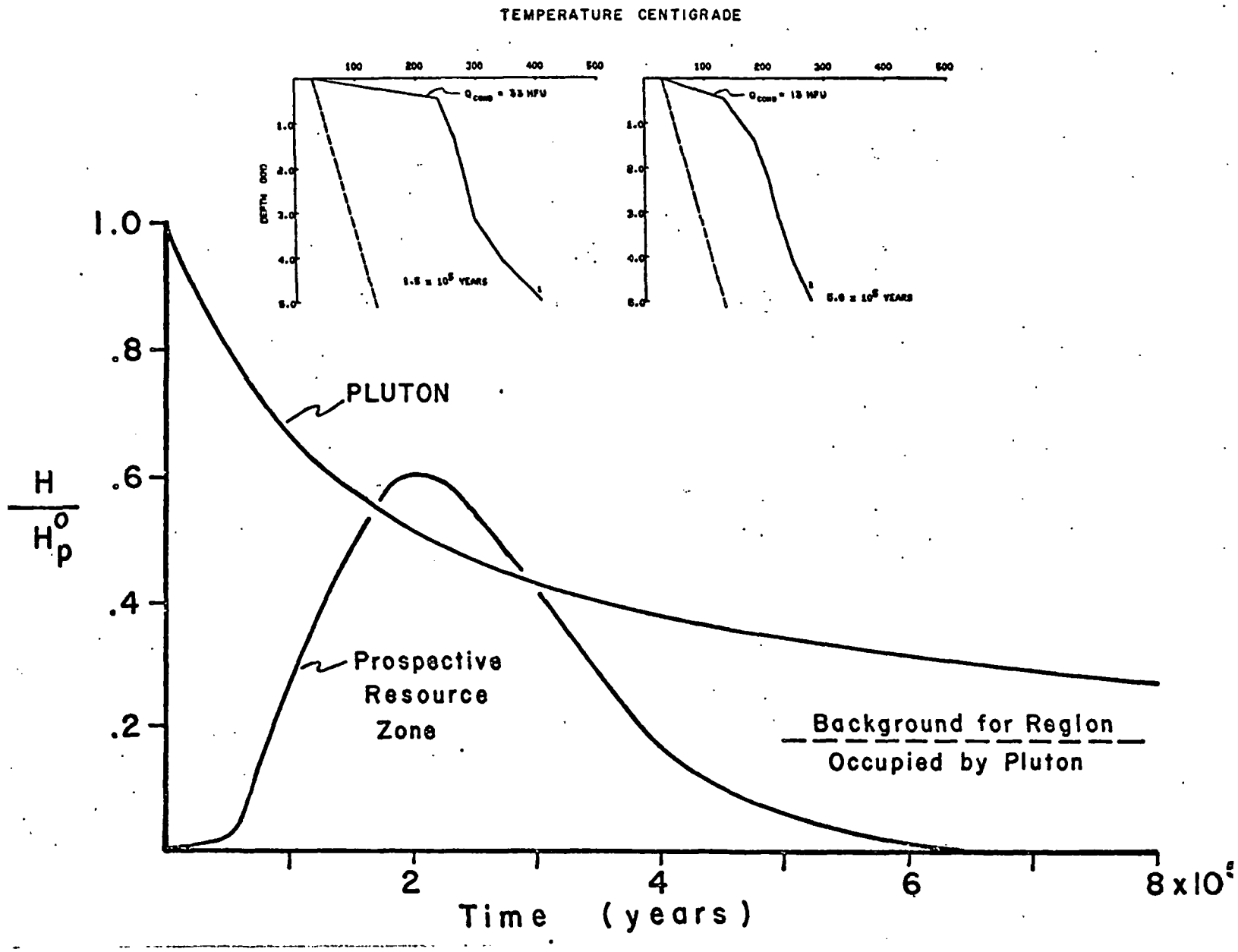
TEMPERATURE CENTIGRADE
100
200
300
400
500
DEPTH (km)
1.0
2.0
3.0
4.0
5.0
1.5 x 10^5 YEARS
5.0 x 10^5 YEARS
1.0
.8
.6
.4
.2
H / H_p^o
PLUTON
Prospective Resource Zone
Background for Region Occupied by Pluton
2
4
6
8 x 10^5
Time (years)

Figure 11

element is, then, the sum of those stresses, calculated from the interaction of all elements and the stress required to suppress the thermal strain, equation (8) in each element.

Elastic constants, as a function of temperature, for silica glass (Birch, 1966) and α_v microcline (Skinner, 1966), were used because of the lack of equation-of-state data on more geologically reasonable material. However, where data on rock-forming minerals are available, the constants are comparable to silica glass. Tensile stresses are taken as positive.

Systems

Three different systems were analyzed, P1 (conduction dominated) and P3 (convection dominated), figure 5. Displacement boundary conditions used were:

boundary	horizontal displacements	vertical displacements
left	fixed	free
top	free	free
right	fixed	fixed
bottom	free	fixed

For short elapsed times, i.e., Stages I-II, the general style of displacements is expansion in the host rocks and contraction within the pluton, but at longer elapsed times, Stage III, the host rock displacement pattern is one of progressive contraction. Consequently, displacements and rates of displacement that are functions of the pluton size, permeability, depth of emplacement, and host rock permeability occur.

Vertical displacements at the top boundary of P1, same system as 1, display a broad, gently sloping pattern which reflects the isothermal geometry for elapsed times less than about 3×10^5 years, figure 12. Maximum net vertical displacement at any time is less than one-half meter and is displaced from the symmetry point. The deflation of the surface directly over the pluton, with respect to points farther away, is a direct result of cooling and resultant contraction

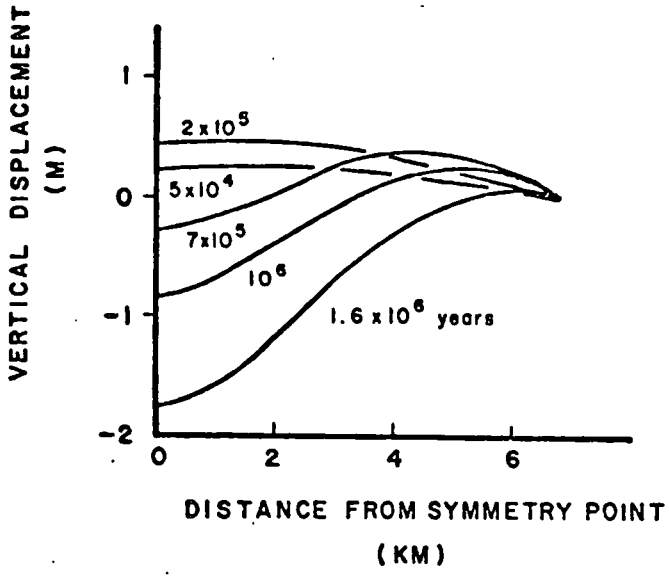

Figure 12

within the pluton and, at later times, contraction of host rocks around the pluton. As time progresses, the point of net vertical displacement moves farther away from the center of symmetry as deflation also moves progressively outward. For elapsed times greater than 10^6 years, the maximum deflation (up to about 2 m) is several times greater than the maximum net uplift.

The rate of vertical displacement, figure 13, shows a gradual decline from an initial rate of $\sim$ 5 μm/yr to -2, or -1 μm/yr at 7.5 x 10^5 years or 10^6 years, depending on location. Differences in these rates reflect simply the convex upward isotherm geometry and location of the contracting pluton. The slight increase in displacement rate after 10^6 years is probably a result of a decrease in the rate of cooling at the pluton and its immediate surroundings.

Surficial horizontal displacements are often an order of magnitude smaller than the vertical displacements. At early times the sense of horizontal displacement for all points is away from the center of symmetry; for later times, however, there is a progressive reversal of this sense. At all points this reversal precedes the reversal in vertical displacements by several tens of thousands of years.

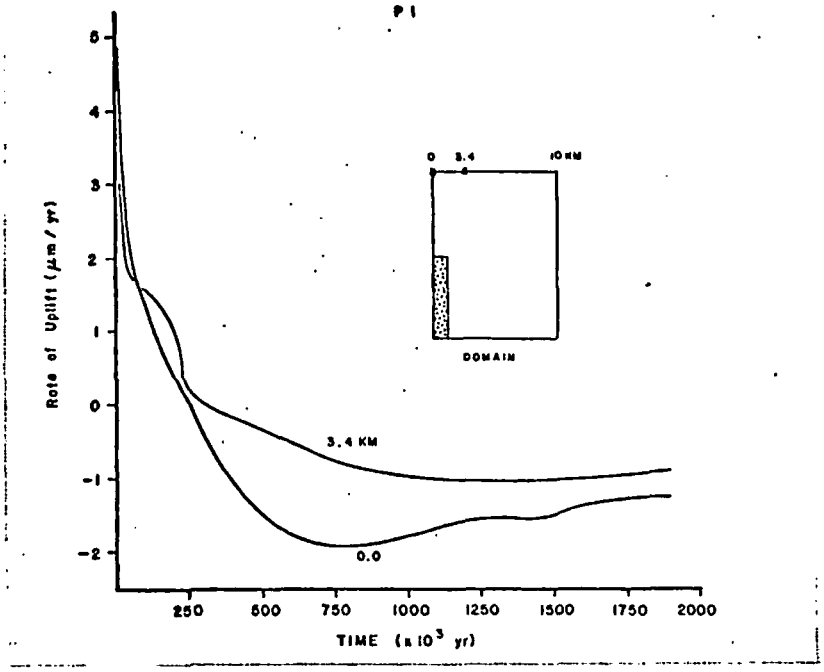

Figure 13

Vertical and horizontal displacements for P1 would be undetectable, since in 50 years elapsed time the maximum displacement would be 1/4 mm vertical displacement. Surficial displacement would, therefore, not be a useful guide for detecting hidden plutons that are cooling by conduction alone.

The surficial vertical displacements for P3 show an initially broad convex upward shape (2×10^4 years) that gradually changes to a more narrow geometry, with the maximum vertical uplift directly on the center of symmetry (10^5 years), figure 14. After 10^5 years this pattern again starts to broaden. Maximum net vertical displacement is about 6.5 m at 1.15×10^5 years. The greater net vertical displacement in P3 than in P1 is a direct result of the convective transfer of heat above the pluton toward the surface. Contraction with the P3 pluton does not vary significantly from the P1 case. For times greater than about 2×10^5 years, the central surface portion will begin to show the deflation as in P1 and, eventually, will show a negative net vertical displacement.

The rate of vertical displacement varies from -20 μm/yr

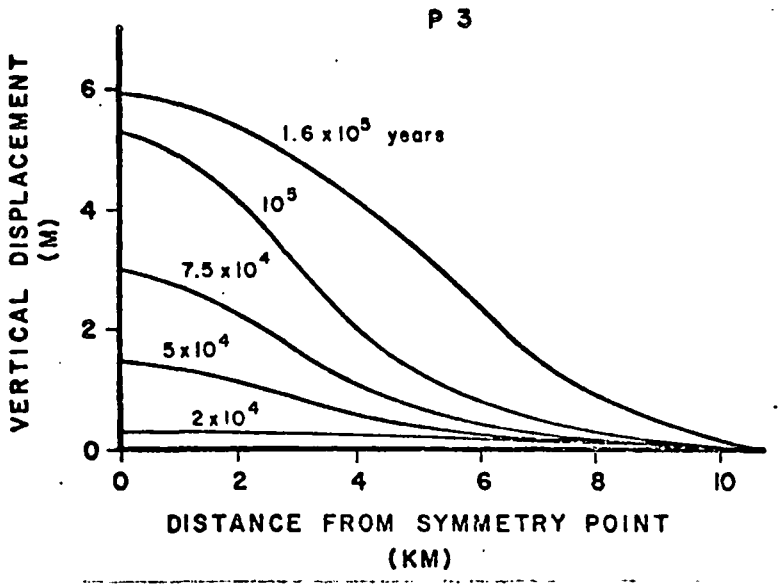

Figure 14

to about 105 μm/yr over the 2 x 10^5 years studied, figure 15.

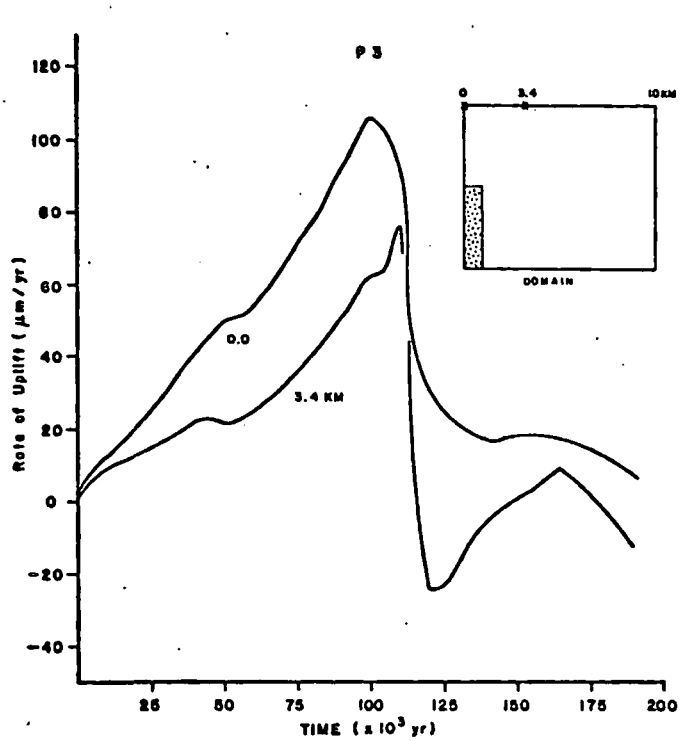

Figure 15

Even at 105 μm/yr the vertical displacement after 50 years would be only 5 1/4 mm, which, though measurable (the NBS first order standard deviation for leveling is 1 mm), may not be large enough to compensate for surficial processes such as erosion. As a comparison, Brown and Oliver, 1976, reported uplift rates of about 2 - 25 mm/yr for the eastern United States. These are 1 - 2 orders of magnitude larger than the maximum uplift rates for P3. So, for the convection dominated case, P3, the displacements do not seem to be a reasonable guide for exploration.

Stresses resulting from lithostatic load, tectonic forces, magma buoyancy, pore-fluid expansion by generation of a residual magmatic fluid or by differential expansion between pore fluid and rock, and simple temperature changes occur in pluton environments where a thermal stress is that stress generated by inhibition of free expansion or contraction as temperature changes non-uniformly in the domain.

The main process controlling the magnitude and direction of the thermal stresses is the initial concentration within the pluton and expansion in the host rocks. As the pluton continues to cool, the host rocks progressively away from the pluton also contract toward the pluton. The contraction within the P1 or P3 plutons almost immediately causes one of the principal stresses to be tensional, and, as time continues, the magnitudes increase to over 2 kb. It seems likely that this tensional stress will result in fracturing, since stress due to the lithostatic load varies from about -1.2 kb at the top of the pluton to about -2.5 kb at the bottom of the domain. Furthermore, the direction of fracturing, as shown by the directions of the least principal stress in figures 16 and 17, is very similar to what is usually called unloading fractures, that is, the fracturing is nearly horizontal toward the center of the pluton and gradually turns toward the vertical at the flanks.

A second area of high tensile stress develops near the

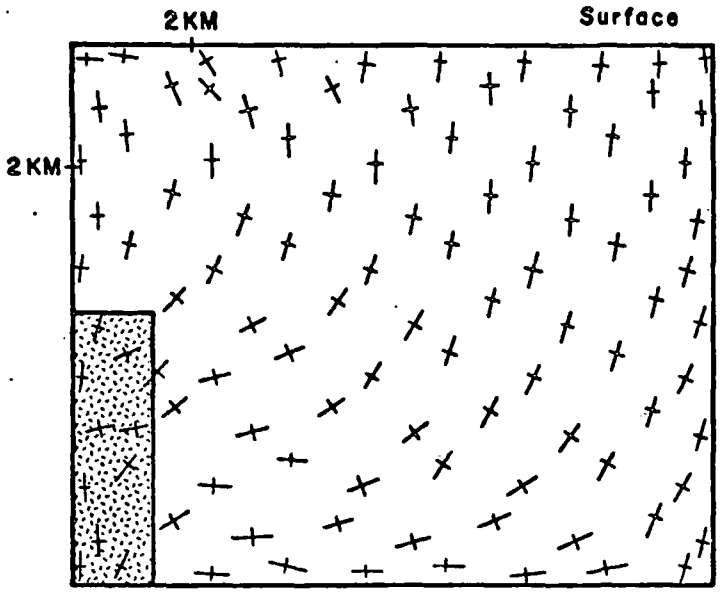

Principle Stress Directions for P3 at 10^5 yr
(longest lines are maximum stress)

Figure 16

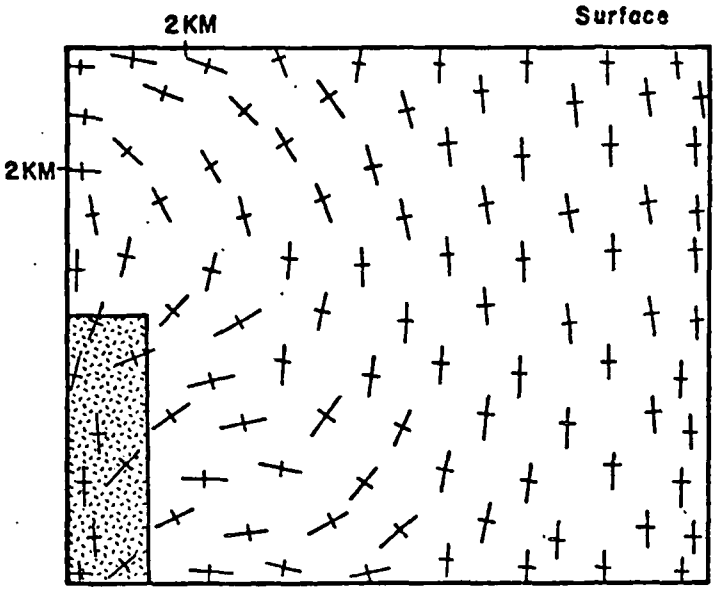

Principle Stress Directions for P 3 at 5×10^4 yr
(longest lines are maximum stress)

Figure 17

surface directly over the P3 pluton. The magnitude of this reaches a maximum of about 1 kb several tens of thousands of years before vertical subsidence begins. The magnitude and direction of this stress, figures 16 and 17, are controlled by the horizontal displacements and upper boundary condition. The free surface at the upper boundary has the affect of suppressing the vertical stress, since in free thermal expansion no stresses develop. Horizontal displacements are suppressed somewhat, however, by the interaction of adjacent elements. Therefore, for early elapsed times when there are significant positive horizontal, as well as vertical displacements, a horizontal maximum principal stress develops. When the sense of the horizontal displacements reverse themselves, the magnitudes of the principal stresses begin to approach each other. The 1 kb magnitude of the maximum principal stress strongly suggests that vertical tension fractures will develop in the near-surface environment directly over the pluton. Furthermore, the anomalous nature of the magnitude and the direction of this stress should be detectable by in-situ stress measurements and should be extremely diagnostic of a hidden hot pluton environment where convection plays a significant role in heat transfer. The P1 environment does not display this near-surface stress anomaly since the horizontal displacements are not large enough to induce a significant tensile stress.

Surficial displacements due to the cooling of plutons will not serve as useful exploration tools for hidden geothermal sources. However, the near-surface stress field, as modified by the development of large horizontal, thermally-induced tensile stresses, should be extremely diagnostic of a buried thermal reservoir. In-situ stress determinations, therefore, should serve as useful exploration tools. It is also apparent that arc tension fractures will develop late in the pluton's cooling history, due to thermal contraction. These types of fractures are observed in nature but heretofore have been attributed to unloading.

In-situ stresses affect the orientation, abundance, and continuity of fractures which develop naturally or are induced by hydraulic fracturing around well bores. The process of stimulating and generating reservoirs by extensive hydraulic fracturing of low permeability rocks in pluton environments requires knowledge of the in-situ stresses. The stress field which results from differential thermal expansion and lithostatic load can be used to predict directions of fracturing, and value of pore-fluid pressure required to induce hydrualic fracturing can be estimated for P3, figures 16 and 17, when the thermal and lithostatic stress directions coincide. This is the case, or nearly so, for the areas within the hypothetical reservoir zone of P3, figure 7.

The principal thermal stresses in the reservoir zone of P3 at 5×10^4 years after emplacement (Stage I) are horizontal (least-compressive) and vertical (maximum-tension). The maximum principal thermal stress has a value of about 50 bars, and the least principal stress has a value of about -250 bars. Average vertical stress due to the lithostatic load in this depth range is about -625 bars. Therefore, unless horizontal or lithostatic stress greater than -325 bars exists, any hydraulic fractures will be horizontal, and a pore pressure of $\sim$ 575 bars would be required to induce hydraulic fractures.

Directions of the principal stresses, in the reservoir zone, for times intermediate to Stages I and II, 10^5 years, figure 17, are nearly the same as for Stage I; the maximum principal stress varies little from the vertical. Furthermore, the vertical thermal stress has increased to about 170 bars throughout and the horizontal thermal stress varies from about -425 bars at the bottom of the economic zone to about -200 bars at the top. There seems to be little significant horizontal variation in either principal stress. Vertical lithostatic stress in this region varies from about -275 bars to -625 bars. Therefore, directions of induced fracturing would almost certainly be horizontal since horizontal stresses

of 100 bars near the top of the zone and -45 bars near the bottom of the zone would be required to reverse this orientation. Fluid pressures between -100 bars (near the top of the reservoir zone) and -455 bars (near the bottom) would be required to induce hydraulic fracturing at this stage.

The orientations of fracturing and pore fluid pressure required to induce fracturing in the reservoir zone directly above the pluton at Stage II are similar to the intermediate stage. However, Stage II covers a wider lateral area, and, in general, the maximum principal thermal stress decreases (actually becomes compressive) while the horizontal principal stress becomes less negative so that the stress differences are similar to those in Stage I. Therefore, a higher pore-fluid pressure (between about -250 to -600 bars) would be required to induce horizontal fractures in the areas of the reservoir zone in Stage II that are farther away from the pluton.

Migration of thermal energy away from the source, regardless of permeability values, causes pore fluid expansion and concomitant decrease in effective pressures, P_e, to a value which causes the rock to fracture. This process is effective for fluids contained in residual porosity and interconnected porosity, if in the latter case the rate of heating is rapid relative to the flow rate of fluid from the heated pores. For fluid in an isolated pore the differential pressure change at constant volume is

$$(9) \quad dP_f = \frac{\alpha}{\beta} dT,$$

where α is the isobaric coefficient of thermal expansion, and β is the isothermal compressibility of the fluid. Then the effective confining pressure on the pore is

$$(1) \quad P_e = P_\ell - P_f,$$

where P_ℓ is the confining lithostatic pressure on the pore.

When $P_e \rightarrow 0$, rock failure is predicted to occur since the tensile strength of rocks is nearly zero. Although the manner in which fractures propagate and their final dimensions are not predicted, an increase in interconnected porosity and an energy release in the form of microearthquakes seems inevitable. The propagation of a $P_e = 0$ isobar away from a pluton which cools by conductive heat transport illustrates the extent of this effect.

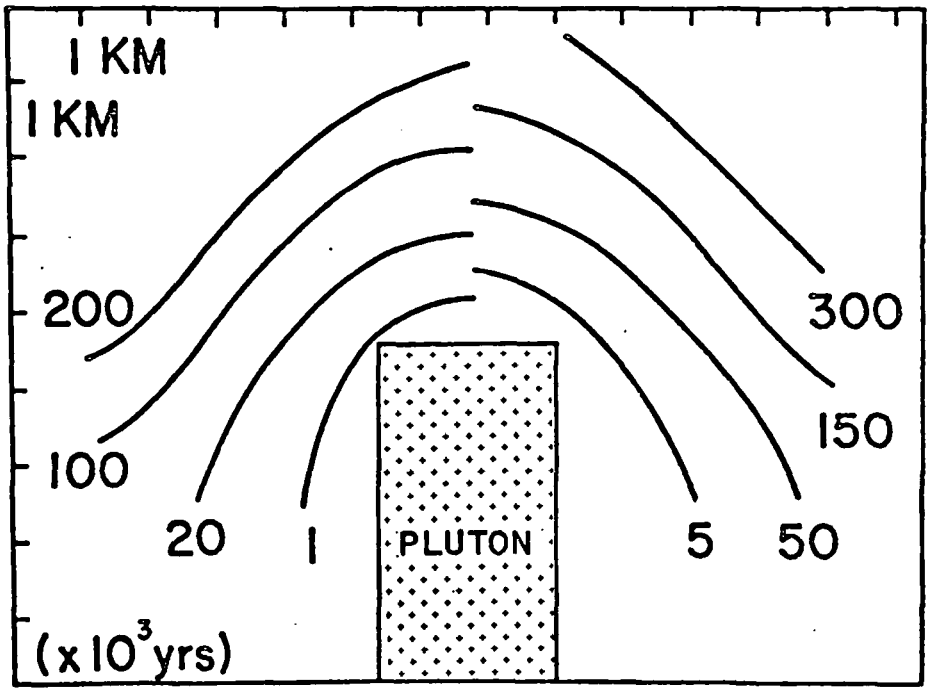

Figure 18

Assuming a distribution of fluid-filled isolated pores in the host rocks, the frequency of microearthquakes associated with rock failure at $P_e = 0$ can be computed. Although the frequency of events is greatest during the initial cooling period, the majority of these events occur <u>after</u> the causative pluton has cooled to below its solidus temperature, figure 19. For this particular system, on the order of 20 - 60 events/day were predicted. The distribution of the events as a function of depth and time is illustrated in figure 20.

As a consequence of thermal expansion of pore fluids in residual pores, generation of zero effective pressure, and

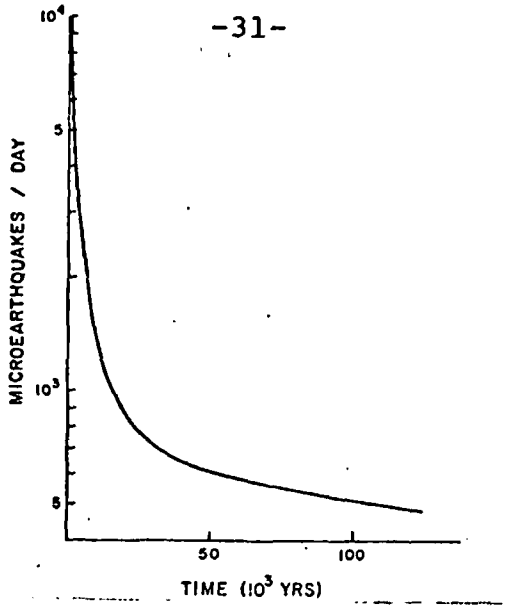

Figure 19

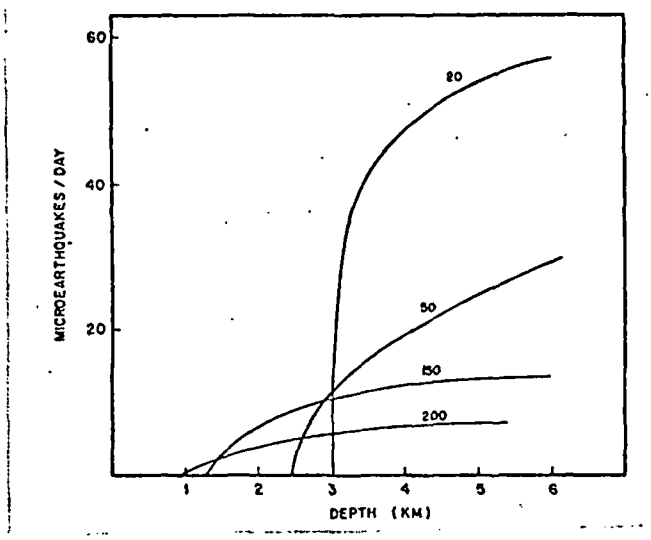

Figure 20

rock failure by fracture, the interconnected porosity of the rock mass will undoubtedly be increased. Depending on the geometry and continuity of these newly interconnected pores, bulk rock permeability and electrical porosity may also increase.

Increase in interconnected porosity and decrease in fluid resistivity with increasing temperature, figure 21, results in the formation of regions in which the intrinsic electrical resistivity is anomalously low. Intrinsic electrical resistivity, ρ_{rock}, can be related to porosity and fluid resistivity, ρ_f, by Archie's function: $\rho_{rock} = \hat{k}\rho_f\phi^{-n}$, where n is

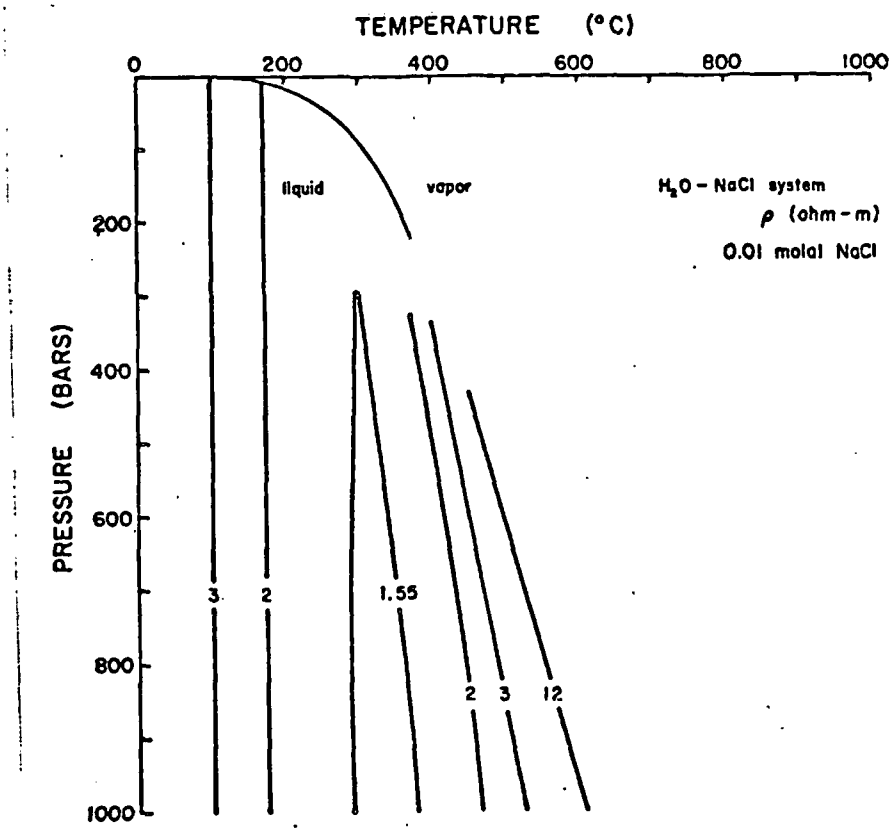

Figure 21

$\sim$ 2 for fractured media, and ϕ is effective electrical porosity. The low-magnitude anomaly is primarily the result of porosity changes since intrinsic resistivity is probably related to $1/\phi^2$, figure 22, as suggested by Archie's function,

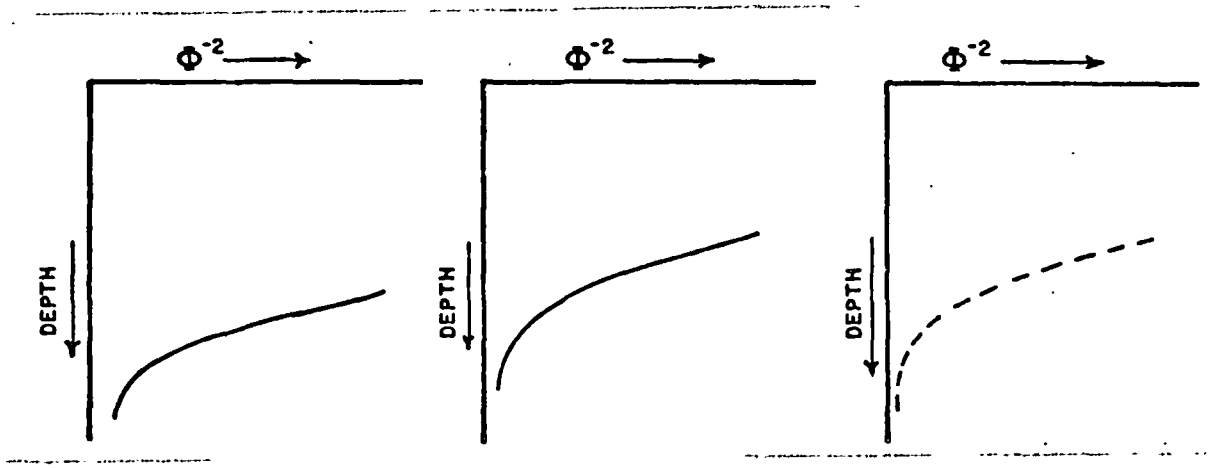

Figure 22

and is probably not detectable by present electrical resistivity measurement methods (Moskowitz and Norton, 1978). The exponential factor on ϕ is poorly defined for fractured igneous rocks, and studies by Brace (1971) actually suggest that at low confining pressures the factor is closer to 1.5 than to 2.

The ϕ^{-2} versus depth plots with respect to time are proportional to the variation in bulk rock resistivity, as a result of porosity changes. Porosity values are not well defined once the system has developed to maximum thermal effects near the surface, because mineral fluid reactions will tend to fill pores, and decreasing pore fluid pressure will allow the pores to collapse.

Note that we are assuming only fluid resistivity and porosity effects on intrinsic resistivity and that the time and space variation in mass abundance of conductive minerals deposited by the circulating fluids is not considered. The effect of fluid composition on the bulk rock resistivity is much larger than temperature or pressure variations, but is less than the effect of porosity variations.

Salinity-porosity affects which result in low intrinsic resistivities are not unique for hydrothermal systems, however. As can be seen in figure 23, metal-sulfide deposits and high porosity sedimentary basins containing saline fluids are also characterized by low intrinsic resistivity values. This point is further substantiated by the use of electrical methods to prospect for metal sulfide deposits and saline fluids.

Thermal anomalies in relatively permeable host rocks might develop broad regions of abnormally low conductive heat flux around the margins of the system, coincident with the zones of downward fluid circulation, figure 24. As can be seen in the figure, circulating fluid convects near-surface low energy fluids downward and depresses the isotherms below the regional values. These regions of abnormally low heat flux could be useful in outlining the regions of upward fluid

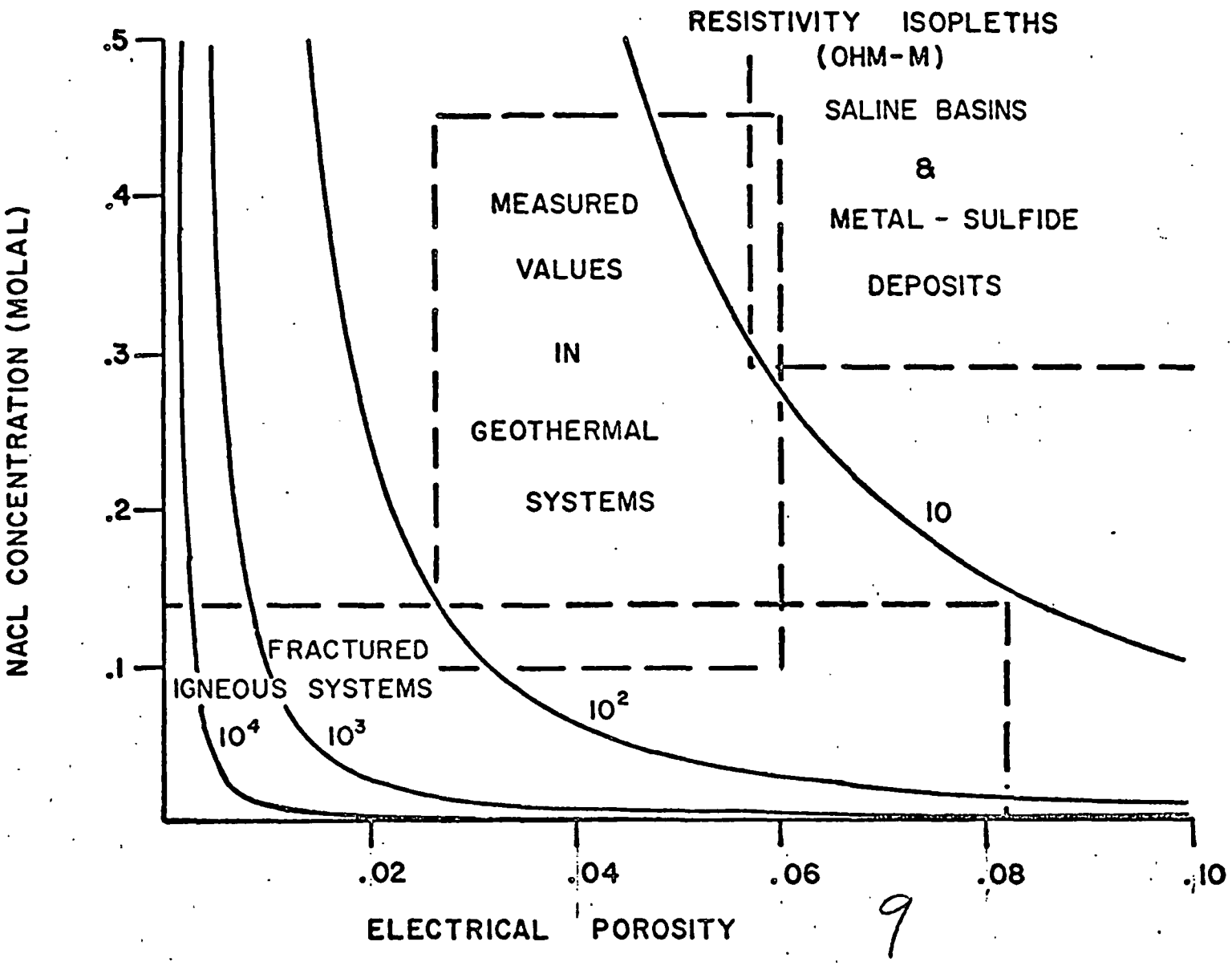
RESISTIVITY ISOPLETHS
(OHM-M)
SALINE BASINS
&
METAL - SULFIDE
DEPOSITS
MEASURED
VALUES
IN
GEOTHERMAL
SYSTEMS
FRACTURED
IGNEOUS SYSTEMS
10⁴
10³
10²
10
.5
.4
.3
.2
.1
NACL CONCENTRATION (MOLAL)
.02
.04
.06
.08
.10
ELECTRICAL POROSITY

Figure 23

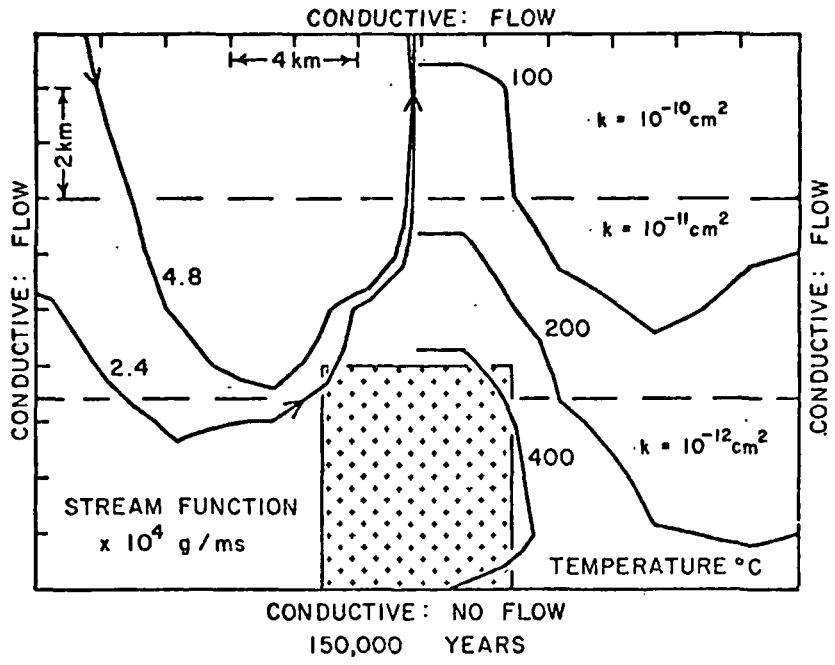

Figure 24

circulation, obviously the regions of greatest thermal energy potential, e.g., high energy concentration, large mass, and shallow depths.

Geologic Reality

An important conclusion of this study is to reemphasize the nonuniqueness of predictions regarding the presence of geothermal resources. In order to effectively detect subsurface resources, existing exploration methods must be significantly improved. Furthermore, because of the intrinsic properties of rocks in the region around cooling plutons, deep drill holes may not adequately define these resources. These conclusions are based on a few very simple geological facts; the consequence of these facts is realized in the numerical models discussed above.

The most important parameter in defining the nature of heat transport in the subsurface, as indicated by the numerical studies, is bulk rock permeability. Geologic observations confirm the significance of this parameter, since host rocks and igneous rocks are, in general, relatively permeable in the upper crust. This observation is qualitatively supported by the fact that eroded equivalents to the system modeled above show evidence that large amounts of fluid have circulated through systematically developed fractures in these rocks. This evidence is in the form of hydrothermal alteration minerals, gains and losses of components from the rocks, shifts in hydrogen and oxygen isotope values, and composition of fluid inclusions. Many plutons and adjacent host rocks appear to have had permeabilities $> 10^{14}$ cm^2 during some stage of their formation. The systematic contribution of continuous fractures in some pluton environments suggests much larger permeabilities, Villas and Norton, 1977. Numerous igneous plutons appear to have had relatively low permeabilities, but the surrounding host rocks usually show evidence that fluid circulation was significant.

Magma intrusion into the upper crust, thermal energy transport away from the crystallizing body, concomitant volume increases in the magma+solid pluton, and temperature increases in the host rocks all result in significant changes in the

stress conditions, which often result in thorough fracturing of the rocks. Although the physics of this entire process is not well understood, it is clear that shallow igneous systems will contain permeable rocks.

The regions of volcanic activity contain plutons emplaced over a time span of a few million years, and each pluton may have a thermal life on the order of a few hundred thousand years. As we noted in the numerical studies, this transient feature of the thermal sources must be considered in evaluating resources.

The pragmatic question is: How can we increase the confidence level of predictions based on surface or shallow drill hole information? The following is a synthesis of data utilizations and limitations concerned with this question.

1. Temperature

   Thermal gradient data are useful if the drill hole conditions where they are collected are thoroughly documented. In particular, those data collected above the groundwater table can be very misleading. Projection of thermal gradient data requires independent information on subsurface conditions, e.g., permeability and thermal conductivity.

   The nonlinearity of thermal gradients is a function of bulk rock permeability; coupled with paleo-temperatures, this information could potentially be used to define the bulk permeability of the system.

2. Conductive Heat Flux

   Conductive heat flux relates directly to the thermal gradient comments. Those fluxes estimated from temperatures measured above the groundwater table should correlate with numerical models which have conductive and impermeable top boundary conditions, whereas those measured in the vicinity of

springs should correlate with conductive and permeable boundary conditions.

Regions of downward fluid circulation around the pluton should be detectable as regions of abnormally low conductive heat flux. These regions define the outer limits of the high thermal energy portion of the system.

The magnitude and width of the conductive thermal anomaly can be used to define the depth and width of the thermal source only in a steady state system in which there is no convective heat transport. However, other information in detailed thermal surveys, e.g., low amplitude noise, may be useful in defining these parameters in a convection dominated system.

3. Convective Heat Flux

This variable is a direct measure of system permeability and is probably not measurable because of the low mass fluxes, but it does deserve consideration.

4. Electrical Resistivity

Electrical resistivities on the order of 500 Ω-m or less cannot be attributed to simple temperature increases at depth. These values clearly require abnormally large electrical porosities, fluid salinities, and/or conductive minerals. The coupled temperature and porosity increases in the subsurface can account for a 2x decrease in intrinsic resistivities, and salinity can account for a 10^2 decrease at an electrical porosity of 0.1.

Fluid circulation in pluton environments always results in the formation of hydrothermal minerals, some of which are conductive. Furthermore, the metal-sulfides tend to deposit in regions above the top of the pluton.

5. Microearthquakes and Tilts

Magma emplacement and magma crystallization generate seismic noise for the first few 10^4 years, or, in general, < 10% of the pluton's total duration. Thereafter, temperature increases in the surrounding host rocks appear to be the principal process by which seismic noise is generated. Detailed mapping of the seismic noise would provide depth information on the location of the zero effective pressure front and could possibly provide an indirect measure of the elapsed time of the system.

Tilts associated with thermal expansion of the rocks could be as large as a fraction of a cm/yr.

6. In-situ Stress

Thermally-induced stress patterns vary considerably in time and space and might affect the design of subsurface reservoirs which require hydraulic fracturing.

7. Chemistry

Bulk chemistry and stable light isotope concentrations, as well as temperature and electrical resistivity of springs and borehole fluids, provide a data base which permits estimation of subsurface rock compositions and temperature, cf. Norton and Panichi, 1977, and mass abundance of mineral phases in surface and subsurface rocks, Villas and Norton, 1977.

A First Approximation of Real Systems

The exploration for geothermal resources has resulted in successes, surprises, and many unanswered questions. This section attempts to apply some of the insight into geothermal systems, obtained through the numerical studies, to natural systems. Data from several systems has been reviewed; the results are presented below.

Those geothermal systems which represent the "A" (conduction dominated) type have been identified only as subsystems within the "B" or "C" type. We do not know of a thermal resource related to an igneous pluton in which heat transport throughout the system is by pure conduction. The "C" type are exemplified by systems from which energy is currently being produced. "B" type systems include those that may contain reservoirs of the "C" type, but the latter have not been detected.

The most interesting consideration is the time stage to which various systems can be assigned. Stage I is mostly speculation since the only evidence would be found through remote measurements of magmatic activity at several kilometer depths. Seismic zones might provide examples of this stage, such as the Intermountain Seismic Belt defined by Smith et al., 1974, along which "swarms" of seismic activity have been noted, and an incipient spreading of the continental crust has been suggested. A few occurrences of very young basalt cinder cones and flows, and some thermal activity, are present along this zone. A second example is found along the extension of the volcanic time trend in the San Francisco Peak region.

Stage II systems include Yellowstone, Geyser, Wairakei, Larderello, and possibly Coso and Long Valley.

Stage III systems are typified at the extreme by sulfide mineral deposits. These systems have moderate thermal anomalies resulting from oxidation of sulfides and anomalous concentrations of radiogenic sources (^{238}U, ^{232}Th, ^{40}K), electrical resistivity lows caused by metal sulfides, and thoroughly

altered rocks. The Marysville, Montana, site is clearly another example of Stage III systems, cf. McSpadden, 1975.

Another style of "thermal" system which is very common in the Basin and Range Province is depicted by the intermontane basins, an example being Safford Valley, Arizona. Norton and Gerlach, 1975. Very porous sediments fill a basin which is $\sim$ 1.5 km deep, saline pore fluids and evaporite-bearing formations are present, and the fluid circulation path of groundwater is from the surrounding mountains, which rise to 2 km above the valley, as well as from the Gila River, which flows through the valley. There are thermal springs which flow from the basin margin faults and scattered occurrences of "young" looking basalts which intrude the sediments. The valley is characterized by low electrical resistivity and anomalous heat flow. However, the entire "thermal" system could be the result of forced fluid convection through the anhydrite-bearing rocks, hydration of anhydrite to gypsum, and associated heat of reaction, or a significant volume of basalt may underlie the valley.

III

Second Objective

Application of Transport Theory to an Analysis of the Coso Geothermal System, Inyo Co., California

This chapter exemplifies the summary of observational and geophysical data into a conceptual geological cross-section which includes a hypothetical thermal energy source, figure 1, Section I (7). These data are from the Coso region, figure 1, Section I (2), on which resource evaluation and data collection were initiated several years ago, figure 1, Section I (3)(4). Data and concepts related to the formation of geothermal energy resources were synthesized from the literature and interpreted in the context of heat and mass transport theory. The geologic cross-section is consistent with available data, and interpretive features of the section are believed to be permissive. The remainder of this chapter summarizes steps (5) - (11) on figure 1, Section I, and presents the results of (8) - (11).

Data on the Coso System

Rocks

The Coso Range, figure 1, is underlain by Mesozoic granitic and metamorphic rocks similar to those found to the west in the Sierra Nevada (Schultz, 1937; Fraser and others, 1943; Austin and Pringle, 1970; Koenig and others, 1972; Babcock, 1975; Babcock and Wise, 1973; Duffield, 1975; Bacon and Duffield, 1976; Duffield and others, 1976). These crystalline rocks are mostly covered by a thin veneer of Cenozoic volcanic and sedimentary rocks, which includes basalt and dacite tuff flows, basaltic cinder cones, and rhyolitic obsidian domes. Alluvium filled graben-like basins occur on the flanks, as evidenced by geophysical data which indicate the sediments may approach thicknesses up to 1.9 km (Zbur, 1964).

Structures

Duffield (1975) has mapped an oval-shaped zone of ring faults which defines a caldera-like crater measuring 40 km east to west and 45 km north to south and which contains most of the Coso Range and a portion of the Sierra Nevada. The youngest volcanic rocks and fumaroles occur in an 18 by 10 km rectangular structural and topographic ridge near the center of the ring structure. Much of the Coso Range is cut by a reticulate pattern of steeply dipping faults, and large areas of rock are thoroughly shattered by fractures a meter or less apart (Combs, 1975; Combs, 1976a).

Age of the System

The oldest dated volcanic rocks in the Coso area are 3.24 ± 0.1 million year old basalt flows (Lanphere and others, 1975) and 2.2 million year old dacite flows and tuffs (Everden and others, 1964). The ages of many of the younger volcanic rocks have been determined by Lanphere and others (1975) and are summarized in figure 2, 10^6 years, and table 1.

The anomalous energy content in the Coso system today

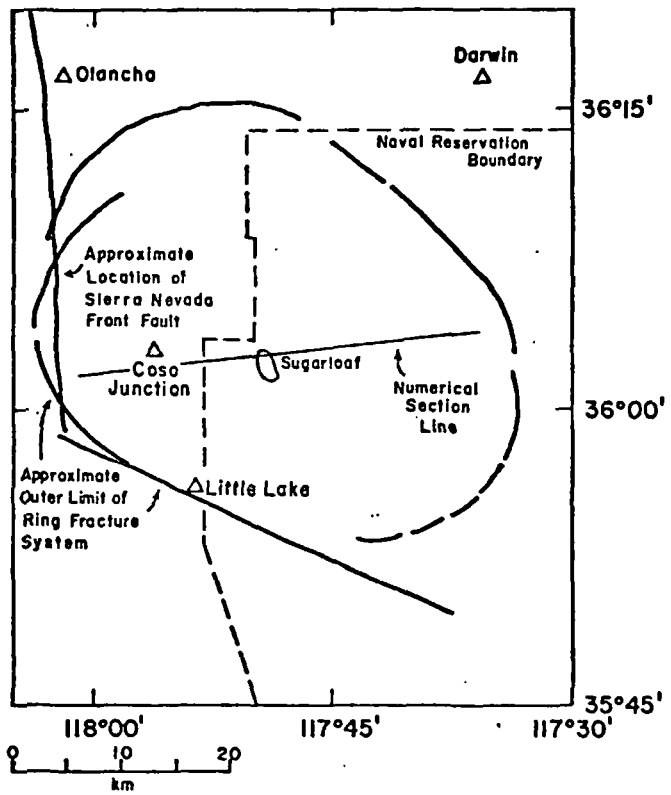

Figure 1

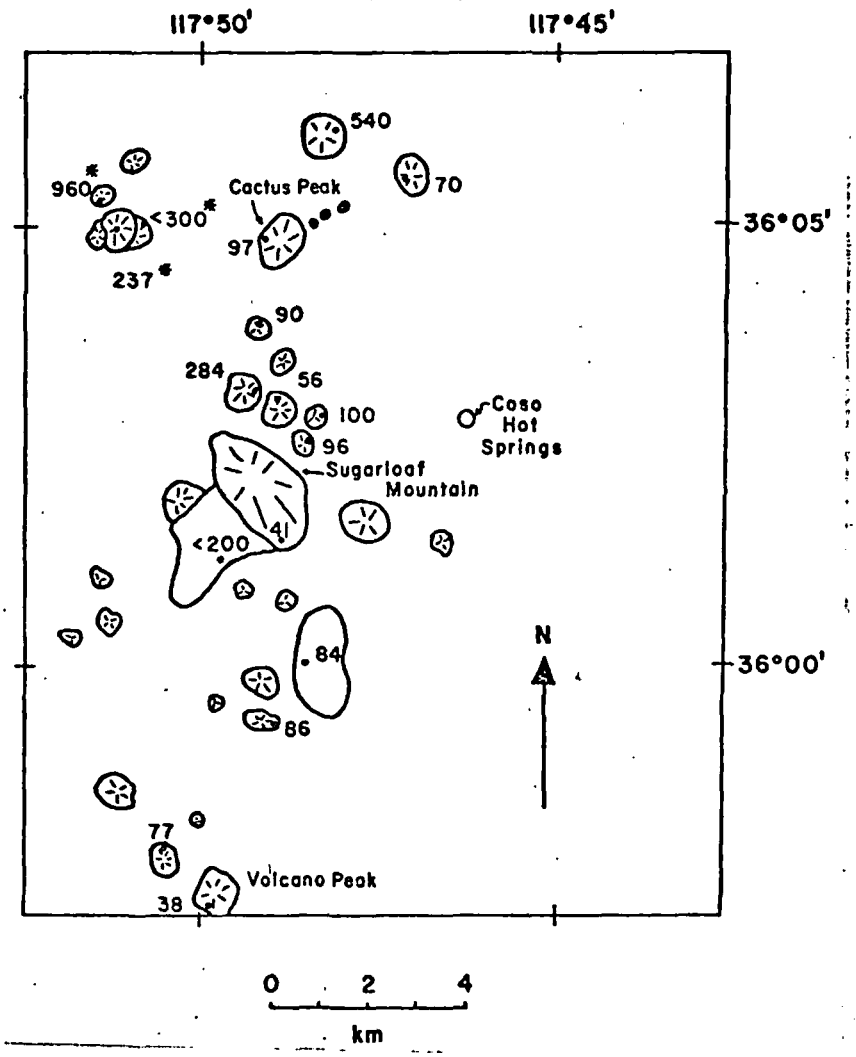

Figure 2

appears to be directly associated with an intrusive event on the order of 10^5 years. Even though a wide range in igneous rock ages has been recorded, most (10) of the radiometric dates are less than 10^5 years b.p. Since plutons of size consistent with the geophysical anomalies and volume of extrusion observed at Coso completely solidify in approximately 10^5 years, we have excluded the 2.37×10^5 and 5.40×10^5 year dates because they are derived from a pluton which is unrelated to the pluton responsible for the $< 10^5$ year volcanic activity and present geothermal activity. These two dates are probably the result of either small earlier intrusions or contamination with older rock. The magma(s) which produced the basalt flows

Table 1

K-Ar Age Dates at Coso (Lanphere and others, 1975)

Age (10^3 yr)	Rock Type	Comments
38 ± 32	basalt flow	ignored
41 ± 21	obsidian	
56 ± 16	obsidian	
70 ± 30	obsidian	
77 ± 8	sanadine	
84 ± 36	obsidian	
86 ± 24	obsidian	
90 ± 25	obsidian	
96 ± 70	obsidian	
97 ± 32	obsidian	
237 ± 27	obsidian	basaltic xenoliths
284 ± 34	obsidian	
540 ± 230	obsidian	
960 ± 190	obsidian	basaltic xenoliths
3240 ± 100	basalt flow	ignored
< 100	obsidian	
< 200	obsidian	
< 300	obsidian	basaltic xenoliths

were assumed to have not contributed significantly to the thermal energy content of the system. This is consistent with the observation that most basalt flows and volcanos are fed by thin sheets or pipes from the lower crust or upper mantle (Smith and Shaw, 1973). The subsurface magmas which produced the 2.2 million year dacite flows and tuffs were not considered sources since any anomalous energy associated with such a pluton has surely been dissipated. Of the sixteen rhyolites dated by Lanphere and others (1975), three are described as comtaminated with basalt fragments and have, therefore, been excluded.

Heat Flow

A region of anomalously high heat flow centered in the vicinity of Devil's Kitchen and Sugarloaf Mountain, which is roughly elliptical and measures approximately 20 km NE-SW and 10 km NW-SE, is defined by heat flow measurements from twenty-seven heat flow wells, figure 3, (Combs, 1975; Combs, 1976b). The maximum measured heat flow is 18 μcal cm^{-1} sec^{-1} (HFU), and a region of at least 20 km^2 is characterized by heat flows of greater than 10 HFU.

Variation of heat flow with distance along the numerical simulation sections (section line in figure 3) is needed for comparison with values predicted by the numerical simulations and is shown in figure 4. Along this section line the width of the heat flow anomaly is 16 km for > 3 HFU, 8 km for > 5 HFU, and 5 km for > HFU.

Seismicity

Microseismic surveys have found variable, microearthquake activity in the Coso ring structure, from a few to over 100 events per day (Combs, 1975; Combs and Rotstein, 1976; Teledyne Geotech, 1972). Three separate regions of high microearthquake activity occur in the ring structure (Teledyne Geotech, 1972); two of these are associated with the fumarolic areas at Coso Hot Springs and Devil's Kitchen, and the third is centered

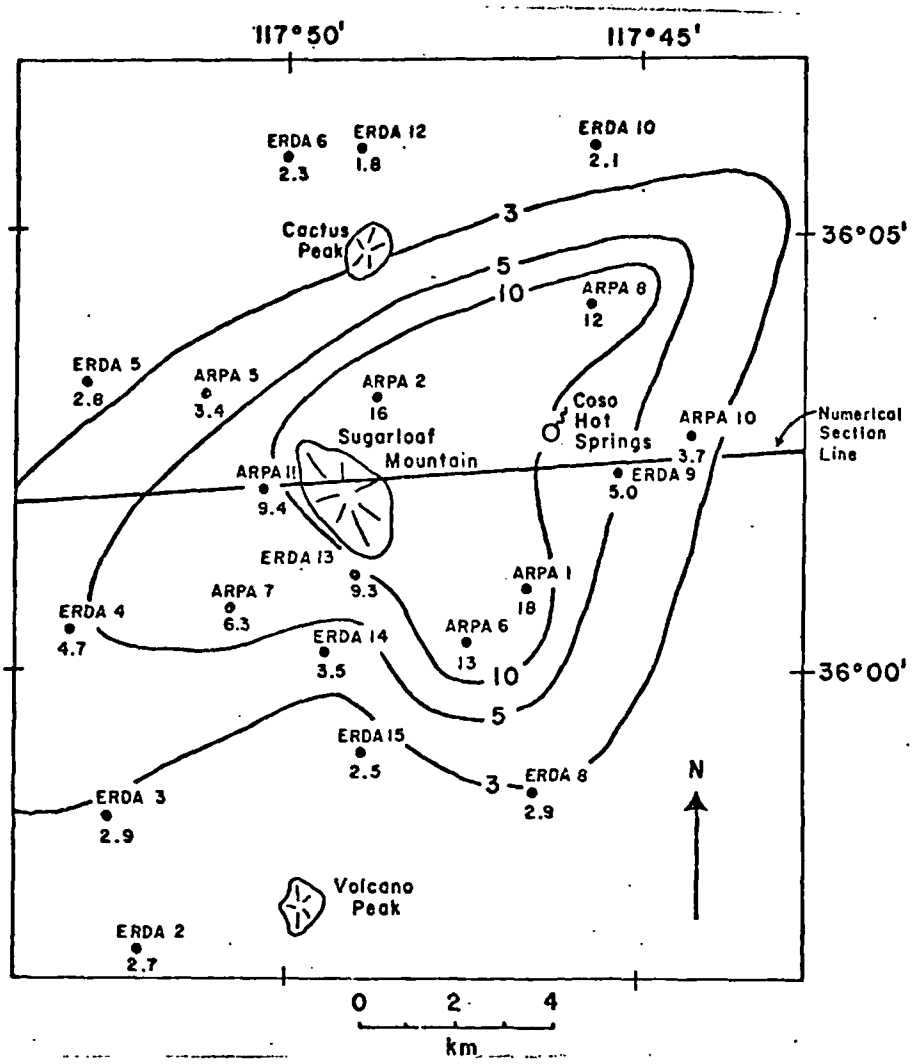

Figure 3

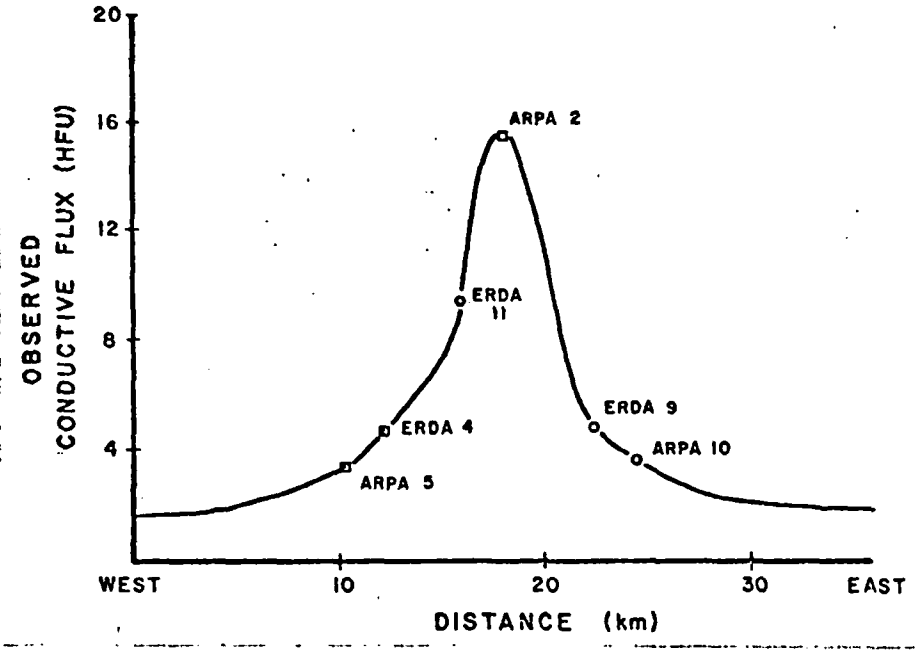

Figure 4

around Cactus Peak and is not associated with any present-day fumarolic activity.

Epicenters of 78 microearthquakes (Combs, 1975; Combs and Rotstein, 1976) are scattered throughout the Coso ring structure but show a clustering about Coso Hot Springs and Cactus Peak, figure 5. Seismic sources at Coso Hot Springs tend to be shallow (< 3 km) while those at Cactus Peak tend to be deep (> 6 km). A ring of intermediate depth hypocenters (3 - 6 km) circumscribes the cluster of deep hypocenters at Cactus Peak.

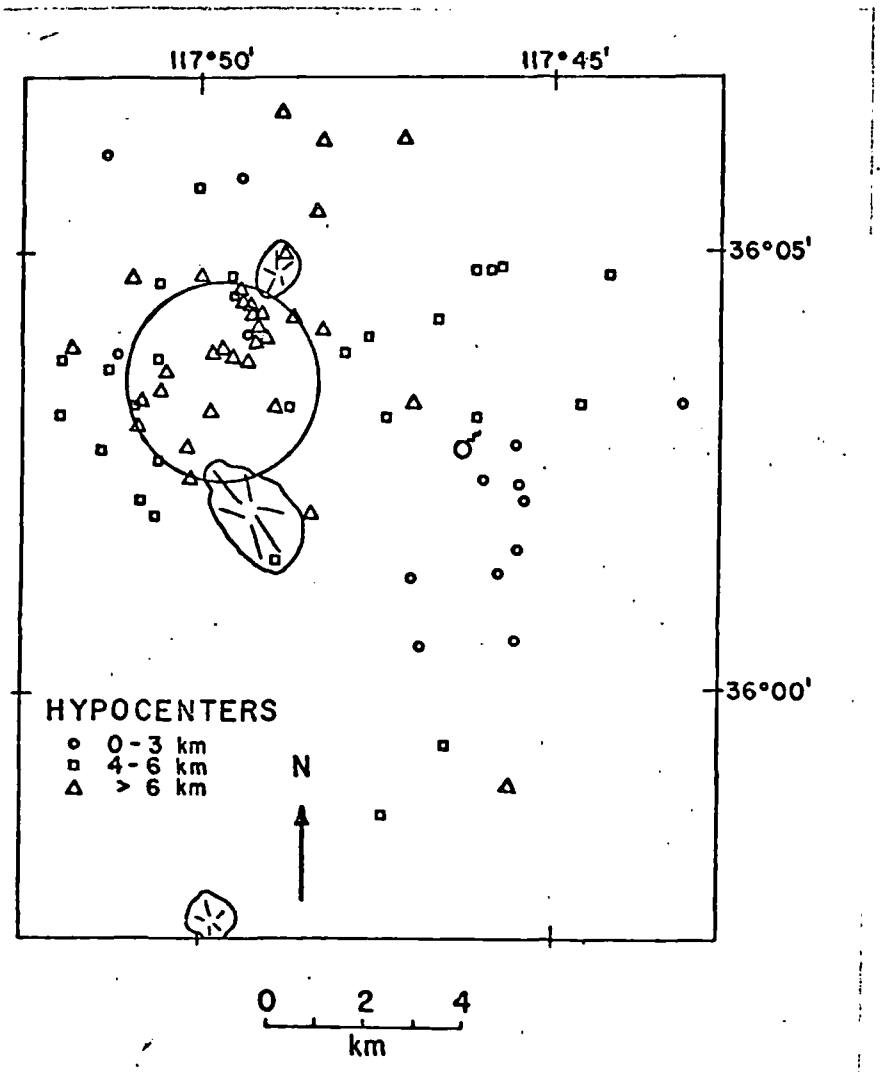

Figure 5

Seismic p-wave velocities are nearly constant at 4.75 km sec^{-1} to a depth of 5 km (Combs and Rotstein, 1976; Zbur, 1973). This 5 km thick layer overlays a half space with a p-wave velocity of 6 km sec^{-1}. Analysis of the relative p- and s-wave velocities for a number of wave paths indicate a region of low Poisson's ratio underlies the Sugarloaf Mountain-Devil's Kitchen area, suggesting that this region may contain in-situ steam or may be devoid of pore fluids (Combs and Rotstein, 1976). However, similarities between the densities and compressibilities of steam and supercritical fluid indicate that supercritical pore fluids and/or changes in the abundance of continuous fractures are other possible sources of low Poisson's ratios.

Resistivity

The crystalline granitic and metamorphic rocks in the Coso region have resistivities of 200 ohm-m, figure 6, or more whereas the rocks in the vicinity of the surface manifestations of hydrothermal activity have resistivities of 50 ohm-m or less (Furgerson, 1973).

Approximation of the Coso System by Numerical Models

Descriptive data on the Coso system have been summarized into a hypothetical two-dimensional geologic cross-section, figure 7, which includes both directly measured data and relationships inferred from the literature and our own interpretations. This section will be used to represent the (1) initial conditions 10^5 years b.p., at which time an igneous pluton was evidently emplaced into the system, (2) present conditions, and (3) conditions predicted on the basis of our analysis.

Orientation

The orientation of our cross-section, figure 3, was chosen so as to pass directly over a hypothetical pluton beneath the dome field and through or near the maximum density of data of geographic and drill and to coincide with the heat

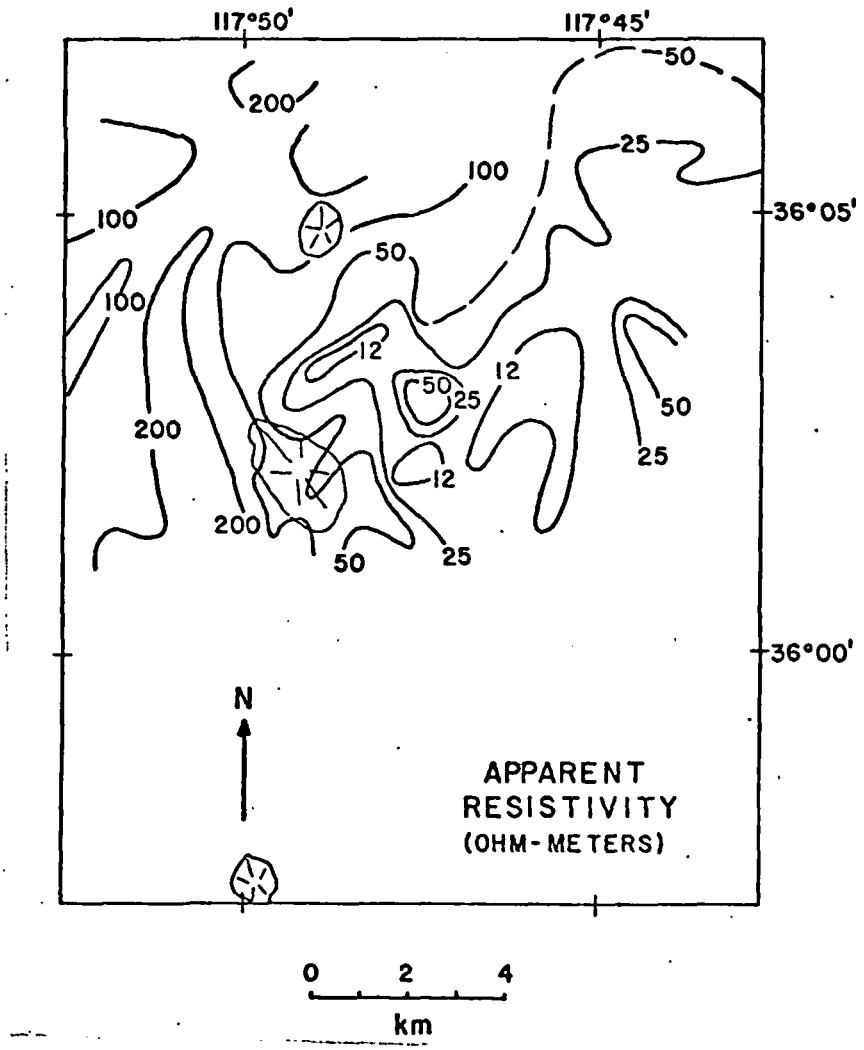

Figure 6

flow, microseismic activity, and resistivity anomalies, as well as include a significant portion of the ring structure. The section trends S84W from the benchmark on Louisiana Butte, is 36 km long, is centered 100 m east of Sugarloaf Mountain, and passes just south of Coso Hot Springs, just north of Devil's Kitchen, and through Sugarloaf Mountain. The ends of the section correspond roughly to the location of the ring faults reported by Duffield (1975). Heat flow holes 9 and 11 (Combs, 1976b) and the proposed sites of drill holes 1, 2, and 4 (Combs, 1976a) are all within a few hundred meters of the section line.

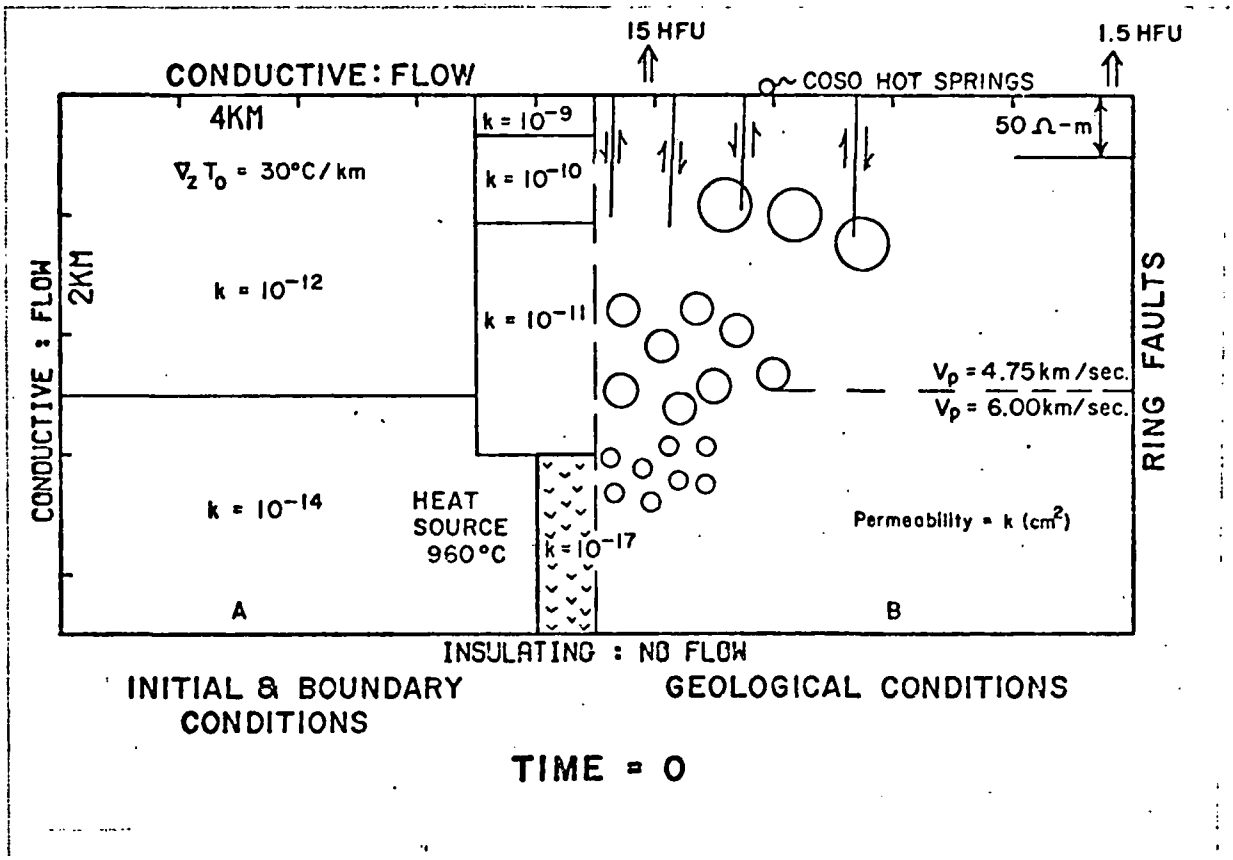

Figure 7

Pluton

The thermal energy source is considered to be a simple pluton whose size was defined on the basis of hypocenters for > 6 km deep microearthquakes and geological inference and whose initial temperature of 920°C is consistent with experimental, petrologic data on granitic rocks. Although there is some evidence for more than one source magma (Bacon and Duffield, 1976), the cluster of > 6 km deep microearthquake epicenters which occurs near Cactus Peak, figure 5, can be interpreted to be the result of tectonic activity and heating of host rocks (Knapp and Knight, 1977), associated with a pluton at depth. The pluton's 4 km width is defined by the diameter of a circle which circumscribes most of the > 6 km deep hypocenters but which excludes most of the shallower hypocenters. The depth to the top of the pluton is uncertain, but, again, from the hypocenters, a depth of 5 or

6 km seems reasonable.

Permeability

Definition of initial rock permeabilities is the most uncertain step in the construction of the numerical cross-sections, for very little is known about the permeability of crystalline rocks. In the models presented here we assume that the permeability is isotropic and that the permeability of several kilometer square blocks of rocks can be represented by a single average permeability that is constant with respect to time.

The data that were used to define initial relative permeabilities are:

1. The increase in p-wave velocity from 4.75 to 6.00 km sec^{-1} at 5 km depth (Combs and Rotstein, 1976), which we have associated with a decrease in fracture frequency and aperture and, hence, a decrease in permeability.
2. The abundance of continuous fractures over large areas is greater than 1 fracture/meter, particularly in the central part of the volcanic field (Combs, 1976a).
3. Low resistivity values in the center portion of the Coso ring structure (Furgerson, 1973) also suggest continuous fractures and a near-surface (1 km deep) zone of high permeability.
4. Limited data on the correlation of fracture frequency with permeability (Snow, 1968; Villas and Norton, 1978; and Brace, 1977).
5. The observation that transition from conduction-dominated to convection-dominated heat transport in fractured media occurs at a permeability of $\sim 10^{-14}$ cm^2 (Norton and Knight, 1977).

6. The permeabilities of producing geothermal reservoirs on the order of 10^{-10} cm^2.
7. Limited data on permeability of igneous rocks.

Since the observed surface heat fluxes at Coso indicate the system is probably dominated by convective heat transport (Combs, 1976b) and because there is only minor surface geothermal activity at Coso, we believe that the bulk permeability of most of the geothermal systems is between 10^{-14} cm^2 and 10^{-9} cm^2. Permeabilities assigned to the numerical section are consistent with these facts and with the relative permeabilities outlined above, figures 8 and 9.

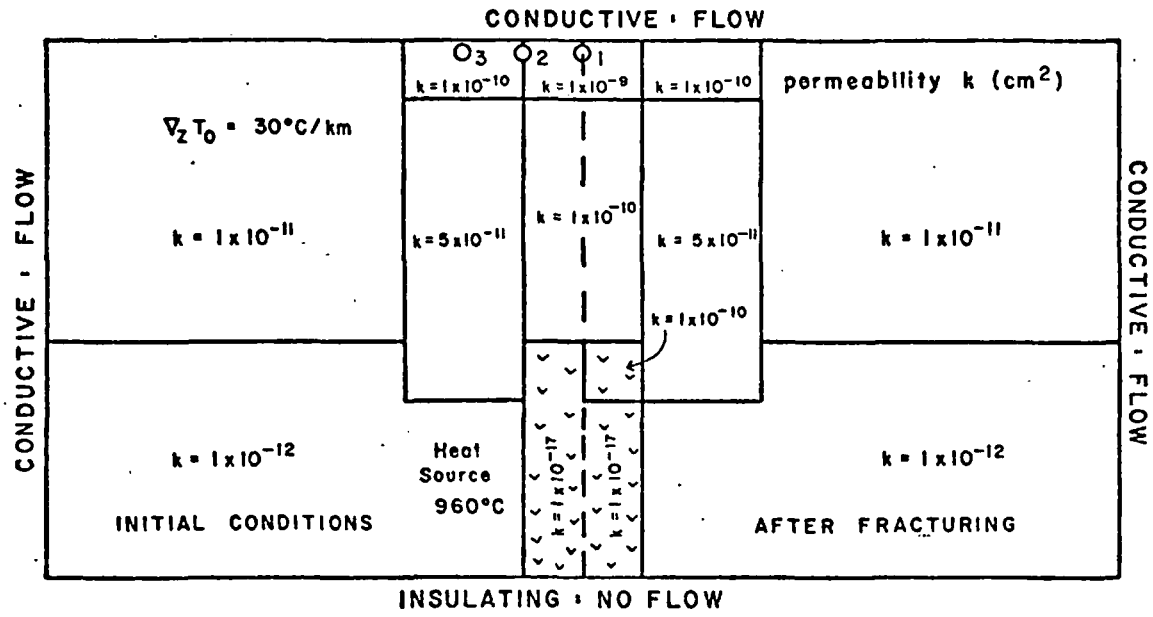

Figure 8

The permeability of most hot plutons is apparently large enough to significantly affect the transport of thermal energy away from the pluton. This is evident in both eroded igneous systems where large chemical gains and losses are evident in the rocks adjacent to continuous fracture sets and in numerical studies of fractured hot plutons (Norton and Knight, 1977). Since the actual fracturing temperature of plutons is unknown,

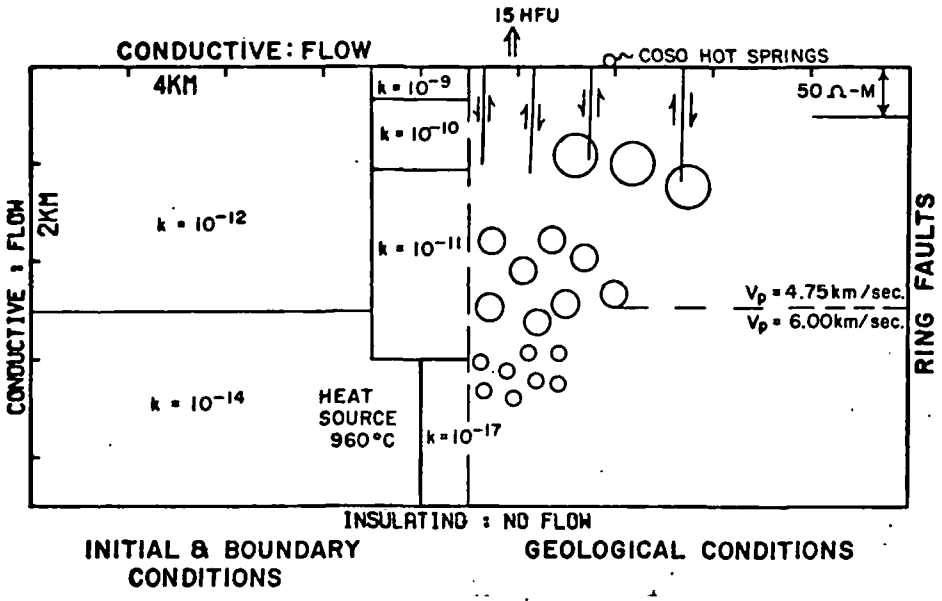

Figure 9

we have varied this parameter to examine its importance to systems like Coso.

Our cross-section is similar to the hypothetical cross-section, figure 10, constructed independently by Combs (1976a).

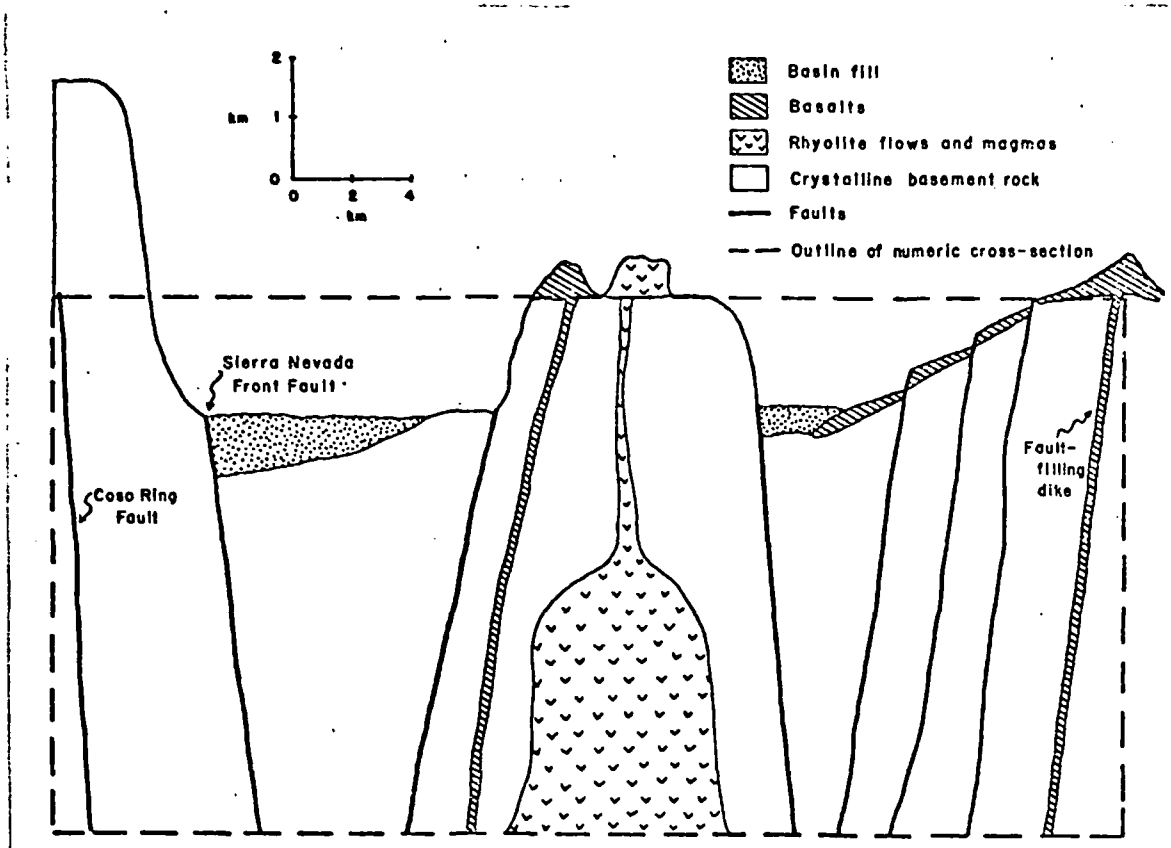

Figure 10

The two sections differ primarily in that we have not allowed for topography. This difference only slightly affects the numerical simulation, for the hydrothermal system is confined largely to the region below the central volcanic field.

Initial Conditions

Hypothetical initial conditions have been defined at 10^5 years before present, using the above data as a guide, figures 8 and 9. The background geothermal gradient of $30^{\circ}C\ km^{-1}$, for a rock conductivity of 5×10^{-3} cal cm sec^{-1} $^{\circ}C$, is equivalent to 1.5 mcal cm^{-1} sec^{-1} (1.5 HFU), slightly less than the minimum measured heat flux of 1.8 HFU at Coso (Combs, 1976b).

Numerical boundary conditions, figure 8, were set to be consistent with the conditions at Coso. The bottom is made insulating and impermeable to flow, consistent with an expected closing of flow channels in the lower crust due to overburden pressure. The sides and top are conductive and below the surface, which is consistent with the observed water table (Combs, 1976a). Fluid recharge or discharge occurs at the side and top boundaries as a result of thermally induced fluid potentials.

In each simulation the numerical domain was discretized into either 144 or 400 distinct points. The governing differential equations (Norton and Knight, 1977) were solved by standard ADI methods (Peaceman and Rachford, 1955). Error analysis indicates that the computed values have no more than a 10 percent error in the first derivatives, with respect to time and distance.

Fluid Properties

The enthalpy, density, heat capacity, and coefficient of isobaric expansion for the fluid in the numeric simulations have been computed with the equations of Keenan and others (1969), programmed and provided to us by Helgeson (Helgeson and Kirkham, 1974). The viscosity of the fluid was computed with the equations of Bruges, Latto, and Ray (1966). We have

assumed that in-situ fluid properties are approximated by the analogous phases in the H_2O system.

Bulk Rock Properties

A constant bulk rock (rock plus pore fluid) thermal conductivity of 5 mcal cm^{-1} sec^{-1} K^{-1} and volumetric heat capacity of 1 cal cm^{-3} were used for all rocks in the numerical cross-sections. The conductivity is slightly less than the mean measured value of 5.3 ± 0.8 mcal cm^{-1} sec^{-1} $^{o}C^{-1}$ (Combs, 1975).

Analysis

A series of seven systems was simulated in order to analyze various characteristics of the Coso system. This series examined the sensitivity of the numerical prodictions to variations in permeability and pluton geometry. The series included (1) an impermeable system where the permeability is 10^{-20} cm^2 throughout the domain, which illustrates the characteristics of a system analogous to the Coso system but in which heat transfer occurs only by conduction, (2) two systems with permeability, as shown in figure 8 (lower permeability), in which the pluton geometry was varied, and (3) four systems with permeability as shown in figure 9 (higher permeability), in which the pluton geometry was varied; in three of these systems the effect of pluton fracturing was examined, figure 9, table 2.

Conductive heat fluxes were computed at 100 m depth below the surface for positions over the pluton's center, its edge, and 2 km to the side. These points (labeled 1, 2, and 3, respectively in figures) are spaced at 2 km intervals and correspond roughly in position to heat flow holes ARPA2, ERDA11, and ERDA9 (Combs, 1976b). The measured fluxes in these holes are 16, 9.4, and 5.0 HFU, respectively.

Table 2

Simulation Characteristics

Name	Initial Pluton Temperature (^{o}C)	Anomalous Heat in Pluton (kcal)	Pluton Width (km)	Pluton Height (km)	Depth to Pluton Top (km)	Fracture Temperature (^{o}C)	Permeability (Lower=fig.7) (Higher=fig.8)	Time to Develop ∿ 16 HFU Anomaly (1000 yrs)
COSO6	960°C	9×10^{15}	4	4	5	---	10^{-20} cm^2	---
COSO2	960°C	9×10^{15}	4	4	5	960°C	HIGHER	25
COSO8	960°C	9×10^{15}	4	4	5	700°C	HIGHER	45
COSO7	960°C	9×10^{15}	4	4	5	---	HIGHER	60
COSO10	960°C	9×10^{15}	4	4	5	700°C	LOWER	180
COSO1	960°C	6×10^{15}	4	3	6	---	LOWER	> 150
COSO9	960°C	6×10^{15}	4	3	6	---	HIGHER	80

Systems Dominated by Conductive Heat Transfer

Host rock temperature changes in the conductive Coso simulation (COSO6) are characterized by upward displacement of isotherms concentrically about the heat source, figure 11. The isotherm perturbations have a height:width ratio $\leq$ 0.5. Temperature and magnitude of the temperature gradient decrease monotonically along lines connecting the pluton and the surface. Thus, the height of isotherm displacement decreases for each successively lower isotherm. In COSO6 the maximum upward displacement of the 200°C isotherm is 3 km while that for the 100°C isotherm is 1 km, figure 11b.

The entire magma in COSO6 cooled below its solidus (700°C) in 1.2×10^5 years. However, temperatures in the host rocks continue to increase until 5×10^5 years, after which temperatures near the host rock-pluton contact decrease, and temperature in more distant rocks, > 5 km from the contact, continues to increase.

The shapes of the isotherms, figure 11, and conductive heat flux profiles, figure 12, reflect the beginning of cooling of the inner host rocks. While temperature is increasing (time < 5×10^5), the ratio of height to width of isotherm perturbation remains approximately 0.5, and the maxima in isotherm and heat flux curves are sharply defined. After the inner host rocks start to cool (time > 5×10^5 years), the ratio of height to width of isotherm perturbation steadily decreases, and the maxima in the isotherms and heat flux become progressively broader and less sharply defined.

The predicted heat flux directly above the pluton center in COSO6 (point 1) does not rise above 2 HFU until 10^5 years after initial conditions, figure 12. A maximum heat flux, 3.8 HFU, occurs at 4×10^5 years, roughly coincident in time with the transition from heating to cooling of the innermost host rocks. The maximum predicted heat fluxes and their times at points 2 and 3 are 3.2 HFU at 5.4×10^5 years and 2.5 HFU at 5.2×10^5 years, respectively. These values are much

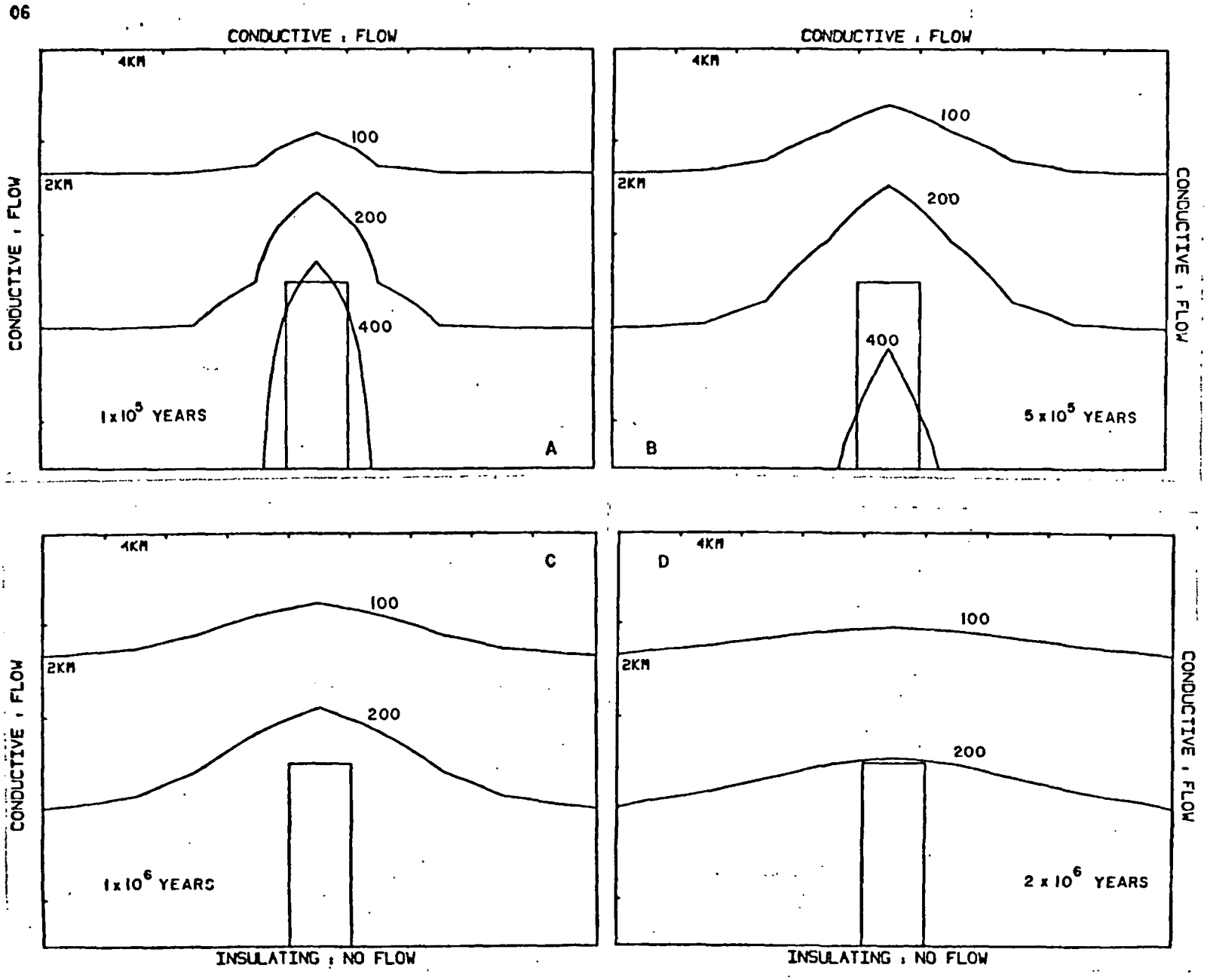
06
CONDUCTIVE ; FLOW
4KM
100
2KM
200
400
1x10^5 YEARS
A
CONDUCTIVE ; FLOW
4KM
100
2KM
200
400
5x10^5 YEARS
B
CONDUCTIVE ; FLOW
4KM
C
100
2KM
200
1x10^6 YEARS
INSULATING ; NO FLOW
4KM
D
100
2KM
200
2x10^6 YEARS
INSULATING ; NO FLOW
CONDUCTIVE ; FLOW

Figure 11

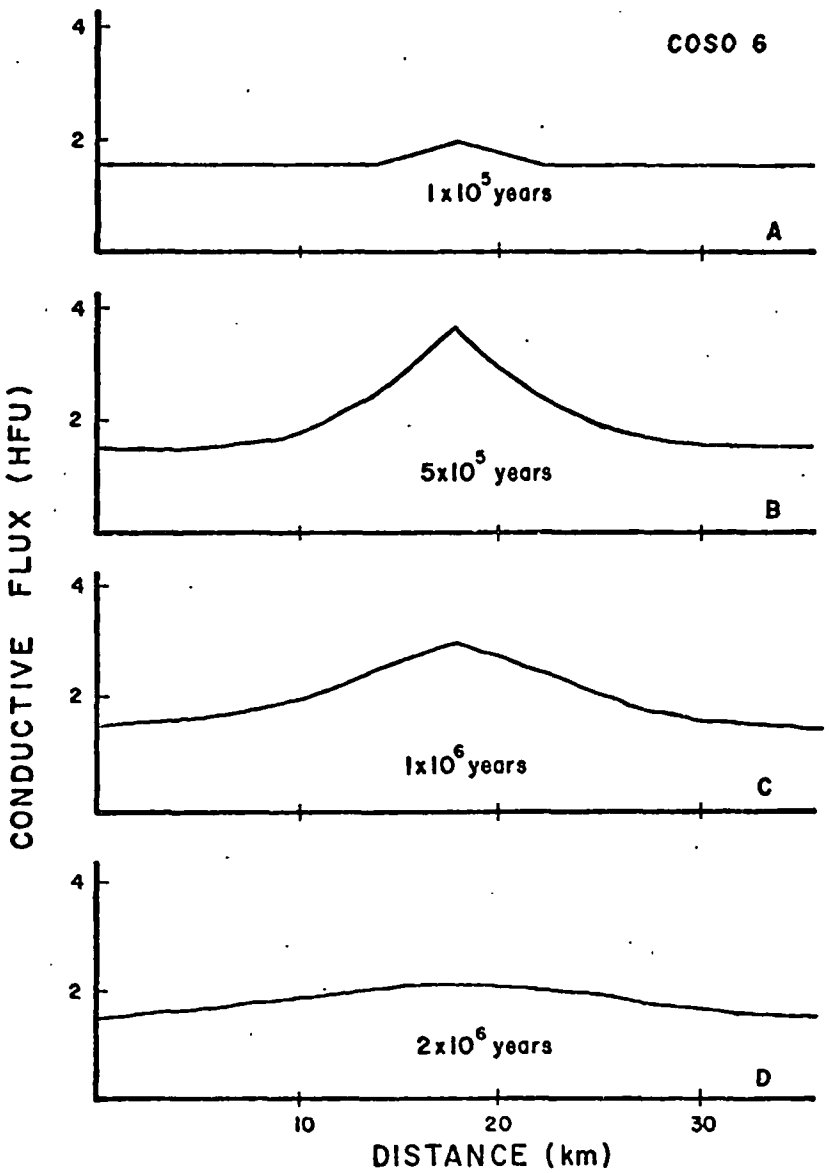
COSO 6
4
2
1x10^5 years
A
4
2
5x10^5 years
B
4
2
1x10^6 years
C
4
2
2x10^6 years
D
CONDUCTIVE FLUX (HFU)
10
20
30
DISTANCE (km)

Figure 12

smaller than the measured values at comparable heat flow holes (16, 9.2, and 5 HFU) and occur long after the inferred age of the Coso system, 10^5 years. Clearly, the Coso system is not the result of a single pluton cooling by conductive heat transport through impermeable rocks.

Systems Dominated by Convective Heat Transport

Thermal energy redistribution and heat flux profiles are much different in permeable Coso-type systems than in the impermeable, conductive system. Perturbations in the density of pore fluid contained in host rocks near a magma cause fluid flow early in the life of a permeable system. Fluid circulation and large convective heat flux produce several unique characteristics in these systems. The style of fluid flow is for heated fluids to move upward from the heat source and to be replaced by cooler fluid derived farther from the flanks of the heat source. As a result, the rocks above the pluton are heated at a greater rate, while the rocks to the flanks of the pluton are heated at a smaller rate than in the conductive case (Norton and Knight, 1977). The pluton cooling rate is not affected appreciably by fluid convection for impermeable plutons; however, for pluton permeabilities larger than 10^{-14} cm^2 significant amounts of fluid penetrate directly into the pluton and transport the anomalous heat upward into the host rocks within a few thousand years.

The amplitude, figure 13, of isotherm perturbations in the convective Coso system tends to be at least a factor of 2 greater than in the conductive system. As the convection system develops, the amplitude, but not the wavelength of temperature perturbations, increases as long as the temperature in the host rocks above the pluton increases. In these systems the temperature does not decrease monotonically from the pluton to the surface, and, therefore, the magnitude of the temperature gradient is a function of depth. At the time of maximum upward displacement of isotherms, figure 13d, the

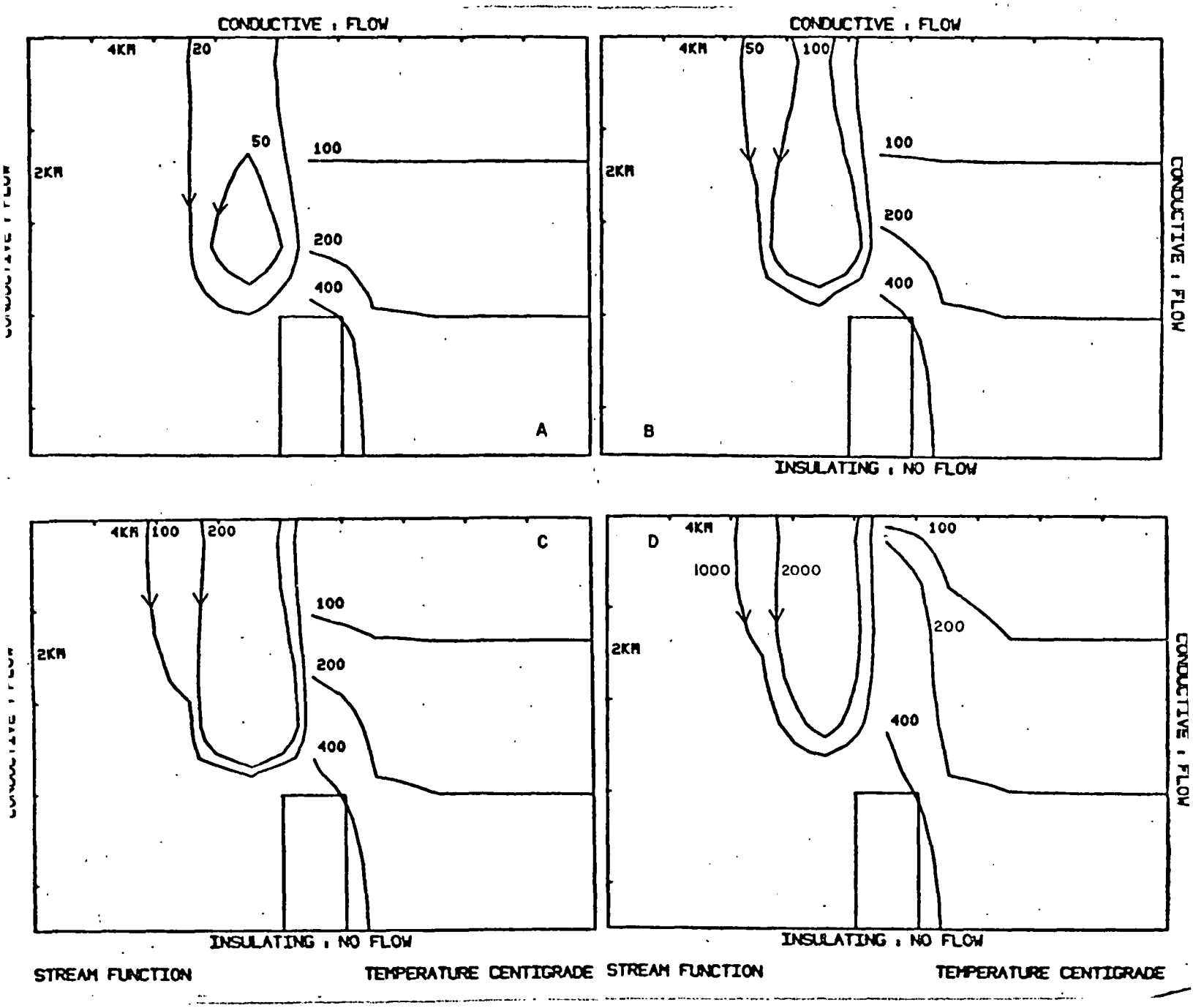
CONDUCTIVE : FLOW
4KM
20
50
100
2KM
200
400
A
CONDUCTIVE : FLOW
4KM
50
100
100
2KM
200
400
B
CONDUCTIVE : FLOW
INSULATING : NO FLOW
4KM
100
200
C
100
2KM
200
400
INSULATING : NO FLOW
D
4KM
100
1000
2000
200
2KM
400
CONDUCTIVE : FLOW
INSULATING : NO FLOW
STREAM FUNCTION
TEMPERATURE CENTIGRADE
STREAM FUNCTION
TEMPERATURE CENTIGRADE

Figure 13

temperature gradient directly above the pluton is large near the surface, 500°C km^{-1}, and persists for 2.5 km downward to the 200 or 250°C isotherm. Below this depth, for 4 to 5 km, the magnitude of the temperature gradient decreases sharply to $\sim$ 30°C km^{-1}, and the temperature slowly increases from 250 to 400°C. Below the 400°C isotherm, at about 5 km depth, the magnitude of the temperature gradient increases and is maintained at a large value downward to the pluton.

The large near-surface temperature gradients and the region of relatively lower temperature gradient which develop between 1 and 4 to 5 km depth are a consequence of fluid transport properties. Physical properties of the fluid between 275 and 375°C tend to maximize upward advection of energy (Norton and Knight, 1977). Rocks above the pluton become heated until fluid transport is maximized, at which time all heat added from below is rapidly transported upward through the 250 - 400°C region, extending the height of the zone and compressing the 250°C and lower temperature isotherms against the surface, figure 13. This process continues until upward migration of the isotherms causes boiling, further upward migration of isotherms stops, and near-surface temperature gradients become constant.

Fluid flow in the convective systems is represented in the left halves of the four drawings in figure 13 by streamlines. The streamlines represent the instantaneous direction of fluid flow everywhere in the numerical cross-section. Fluid velocity at every point has a magnitude equal to the gradient of the streamfunction at that point and is directed along the streamfunction contour.

The height of the 275 - 375°C region is dependent upon the fluid velocity, since hydrothermal fluids have maximum transport capabilities in this temperature range. As the height of the region changes through each of the drawings in figure 13, 1 km to 1.4 km to 1.8 km to 41. km, the velocity changes from 1 to 1.3 to 1.7 to 26.7 times the velocity of the earliest time.

The major portion of the fluid flow and the largest fluid velocity occur in the central fracture zone of the numerical cross-sections (compare figure 13 to figure 9). The style of flow is downward along the outer edge and side of the fracture zone. It should be noted that the width of the central fracture zone affects the width of the 250 - 400°C temperature zone above the pluton and, consequently, affects the width of the observed near-surface conductive heat fluxes.

The development of the near-surface conductive heat fluxes in the convective system as a function of time for points 1, 2, and 3, figure 9, is depicted schematically in figure 14. This

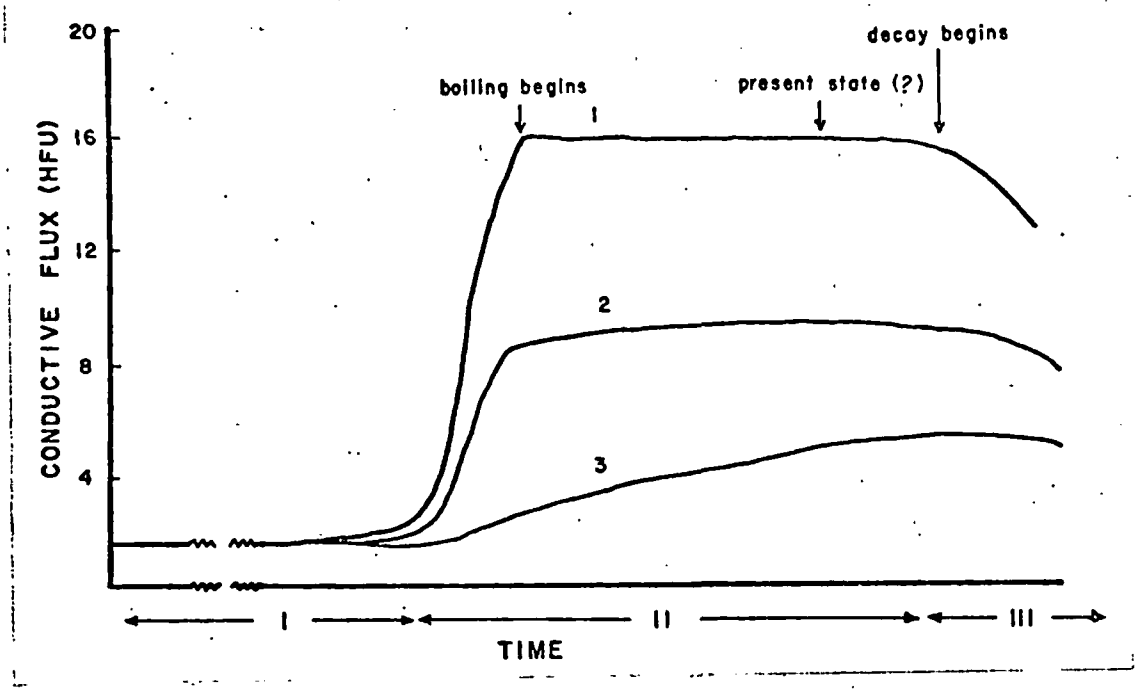

Figure 14

development can be broken into stages, figure 15: (I) concealed, (II) maximum development of circulation accompanied by boiling, and (III) decay of system. During the concealed stage, which may last from 10^4 to 10^5 years, there will be no expression of the subsurface geothermal system in the near-surface conductive heat fluxes. During the developing stage the temperatures in the upper several kilometers of rocks above the pluton rise rapidly as the region of 250 - 400°C

temperatures grows in height, and the < 250°C isotherms are displaced to the surface. During this time, which may last from 10^4 to 4 x 10^4 years, profiles of near-surface conductive heat flux will show a sharp, narrow maximum which will not extend much beyond the projection of the pluton's sides. The maximum heat flux development is coeval with boiling in the subsurface. The heat fluxes at points directly above the pluton are constant as boiling causes the near-surface temperature to remain constant. As heat is conducted away from the rocks directly above the pluton, the observed heat fluxes at point 3 and beyond rise. Profiles of conductive heat flux continue to show well-defined maxima over the pluton center, but the width of the anomaly increases with time.

Comparison of Systems

In order to limit the possible physical attributes of the Coso geothermal system, six permeable systems (Table 2) were analyzed. In each case the near-surface conductive heat fluxes were computed and then compared to the observed heat fluxes at comparable positions in the natural system. The object was to obtain the present-day observed heat fluxes at a model system age of 10^5 years, the hypothetical real system age. In some of the simulations, numerical difficulties caused by boiling were encountered. These cases could not be run to 10^5 years; so, with the aid of the idealised curves of figure 14, conductive heat fluxes at 10^5 years were estimated.

The time required to achieve a 16 HFU or larger conductive heat flux was greater than 1.5 x 10^5 years for the two lower permeability simulations (COSO1 and COSO10, Table 2), even though COSO10 had a 5 km deep pluton which fractured at 700°C. The heat flux directly above the pluton in simulation COSO10 did not exceed 2 HFU until 8 x 10^4 years and did not exceed 4 HFU until 1.6 x 10^5 years. Having achieved a 4 HFU, the heat flux rose rapidly to 18 HFU at 1.8 x 10^5 years, where it became fixed as the system began

to boil. The heat fluxes at points 2 and 3 (figure 8) at 1.8×10^5 years were 10 and 3.1 HFU, respectively. Predicted conductive heat flux for run COSO1 did not exceed 2 HFU until 1.4×10^5 years, and the run was abandoned shortly afterward.

Three systems having high permeability host rocks and 5 km deep plutons were analyzed to ascertain the effect of pluton fracturing. At the "fracturing temperature," fluid was allowed to flow through the upper 1 km of the pluton. Fluid was allowed into the pluton through the computation, COSO2, when the pluton temperature was less than 700°C, COSO8, and not at all, COSO7. The "fracturing temperature" greatly influenced the time of high near-surface heat flux development and the rate of pluton solidification but did not appreciably affect the style of heat flux development.

The primary affect of "fracturing temperature" on development of near-surface conductive heat fluxes is to decrease the time required to develop a boiling system and the maximum heat flux, figure 15. Simulation of COSO2 represents the minimum possible time required to develop an ∿ 16 HFU system

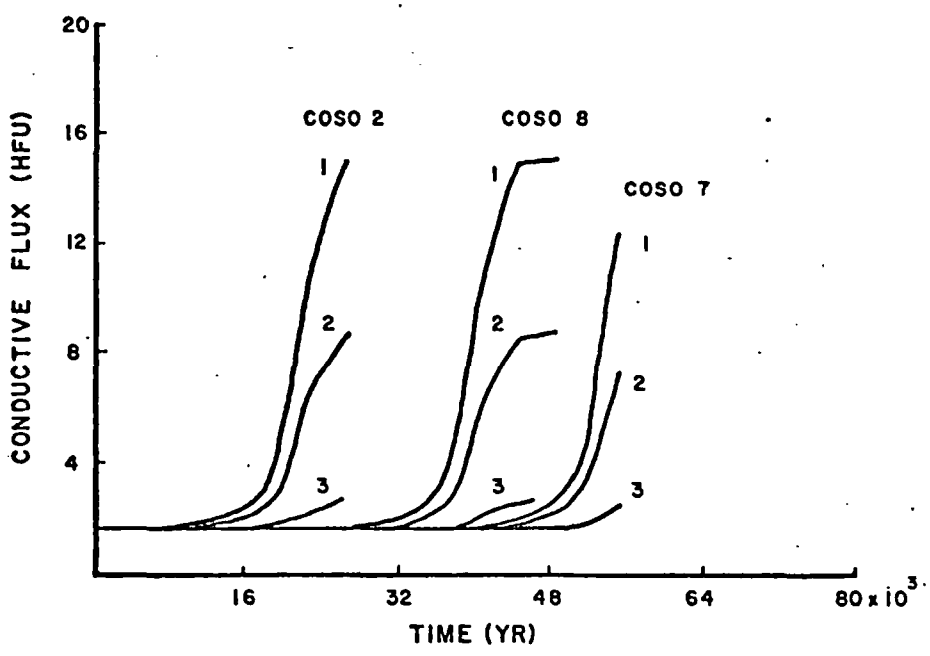

Figure 15

(2.5 x 10^4 years); given the assumptions used in these simulations, simulation COSO7 represents the maximum development time (6.0 x 10^4 years), and COSO8 is intermediate. Apparently, the effect of "fracturing temperature" is most pronounced at elevated temperatures, and it decreases at an increasing rate as the "fracturing temperature" decreases. The effect of changing "fracturing temperature" from 960 to 700°C is to delay development of the maximum heat flux for 2 x 10^4 years, while eliminating fracturing altogether delays development only another 1.5 x 10^4 years.

The "fracturing temperature" greatly affects the rate at which the height of the molten portion of the pluton (temperature > 700°C) decreases with time. Plutons, both 5 and 6 km deep, which do not fracture, solidify as in pure conduction systems, at a nearly linear rate of 17 m $year^{-1}$, figure 16.

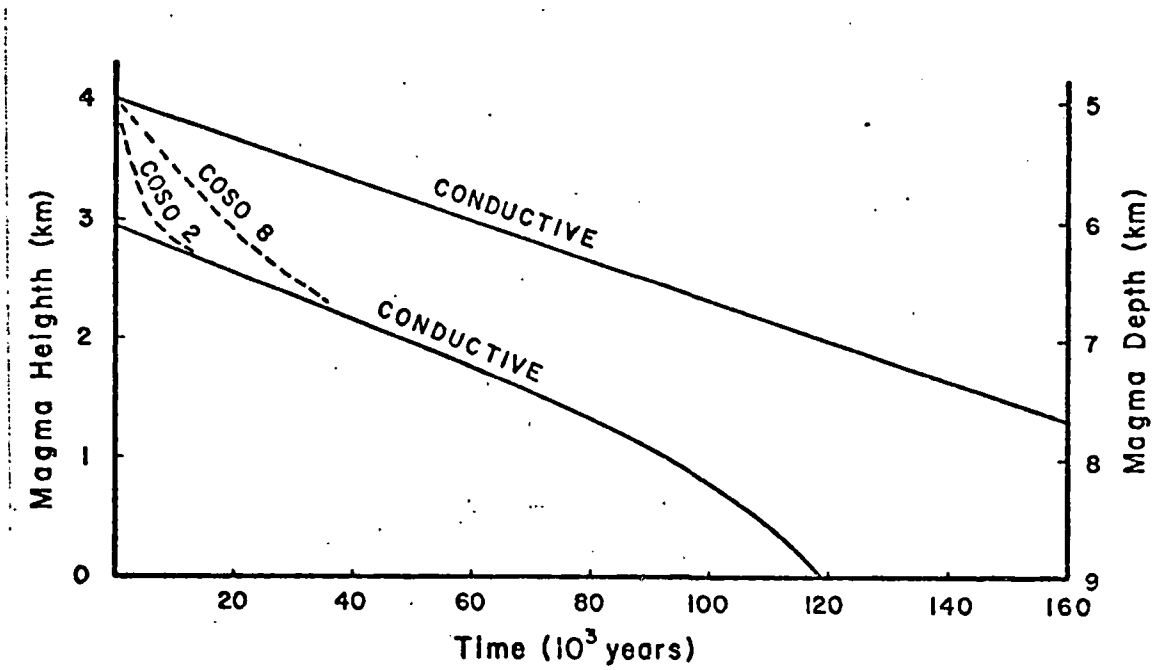

Figure 16

The effect of fracturing the upper 1 km of 5 km deep plutons is to greatly accelerate the cooling rate of the pluton. After the upper 1 km of the pluton has fractured, its temperature decreases quickly.

A single simulation, COSO9, was run with the higher permeability section and a 6 km deep pluton. The time required for development of maximum heat flux in this run was 8×10^4 years. At this time the heat fluxes are approximately 16, 9, and 3 HFU at points 1, 2, and 3, respectively. We estimate that the predicted heat fluxes would have converged upon the observed heat fluxes at approximately 10^5 years, our initial goal.

The anomalous energy represented by the pluton at Coso is probably 10^{15} to 10^{16} kcal, which is on the order of the U.S. annual energy consumption. Of this amount, the simulations predict that 31% has been removed from the pluton into the host rocks. The energy in host rocks above the pluton's center at 1, 3, and 5 km depth is 65, 92, and 108 cal g^{-1}, respectively, figure 17, compared to a background (geothermal gradient = $30^{\circ}C\ km^{-1}$) of 8, 24, and 40 cal g^{-1}. Thus, 57, 58, and 68 cal g^{-1} of anomalous energy are available at these points.

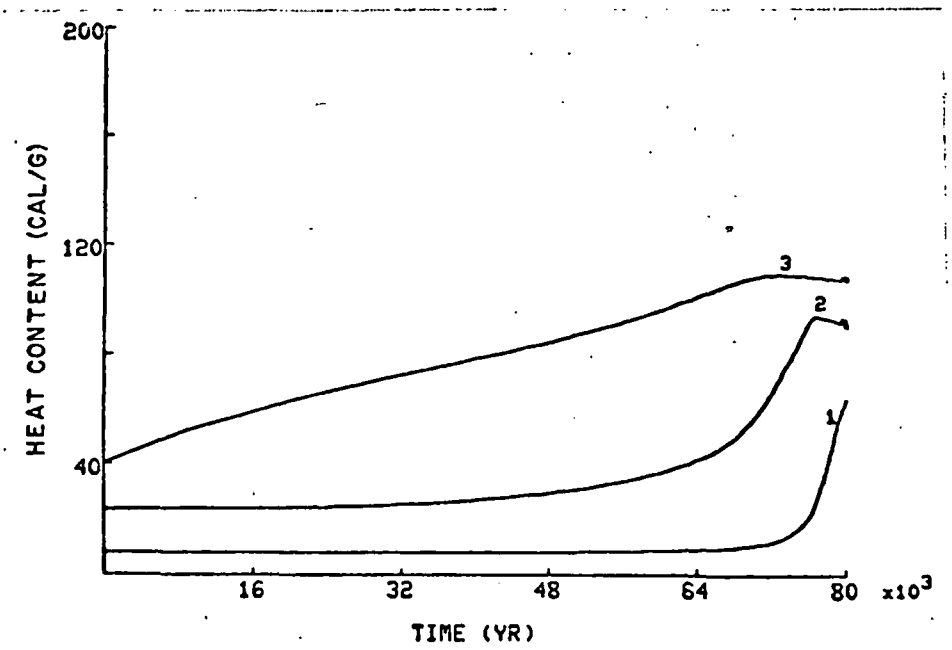

Figure 17

The low electrical resistivities measured at Coso (Furgerson, 1973) have been interpreted as indicating high temperature rocks at shallow depth. Given the temperature and pressures predicted by our simulations, rock and fluid conductivity, and rock porosities, one can compute in-situ bulk rock resistivities with Archie's function (Archie, 1942; Brace and others, 1965; Moskowitz and Norton, in press). Our computations, using 3% porosity and 0.1 molal NaCl solutions, show that temperature alone can not be responsible for the measured resistivities at Coso, figure 18. In fact, the lowest measured resistivities are on the order of the resistivities of pure concentrated NaCl brines. The measured resistivities apparently result from either a few weight percent conductive alteration minerals (pyrite or clay minerals) or from anomalously saline pore fluids and high porosities which are not apparent at the surface.

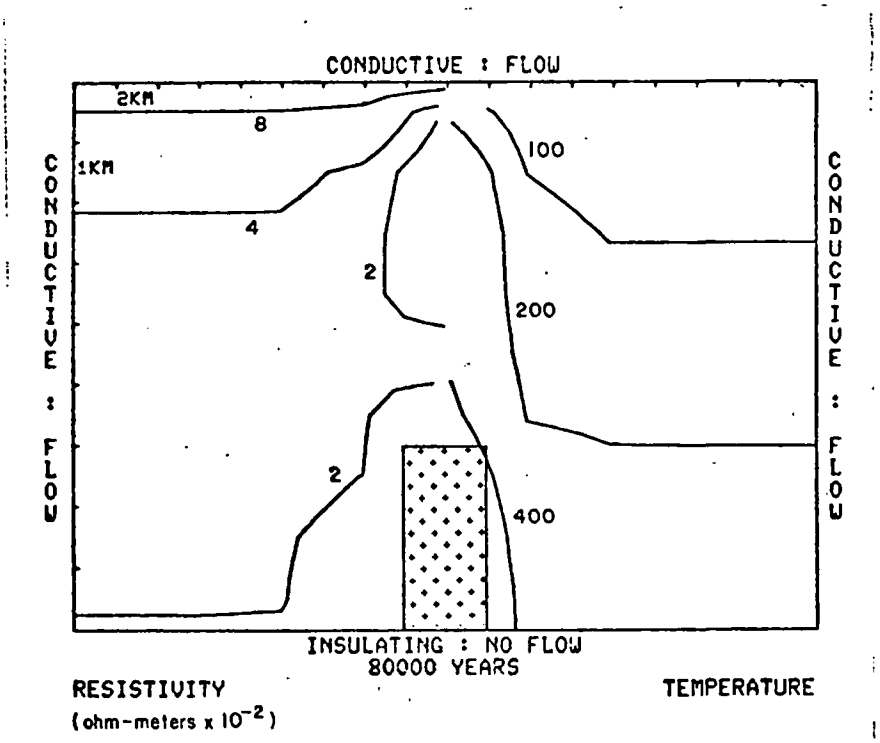

Figure 18

These results suggest that the present-day Coso geothermal system is the result of a single 10^5 year old, approximately 4 km wide pluton at approximately 6 km initial depth. The permeability in the Coso region is likely to be much as shown in figure 8. It is possible that the pluton was initially shallower than 6 km. If so, the permeability was probably intermediate, between that shown in figures 8 and 9. These conclusions are consistent with the data available, but may not be unique because of the data limitations and the assumptions involved in constructing the cross-sections.

Given that simulated system COSO9 is a reasonable analog of the Coso geothermal system, a number of predictions can be made:

1. The temperatures and fluid flow patterns in the present Coso system are similar to those in figure 14d.
2. The molten portion of the pluton (temperature > 700°C) would occur at 8 km or more below the surface.
3. Most of the Coso system is characterized by permeabilities which are too small for direct production of commercial geothermal steam, but large enough to significantly affect the distribution of thermal energy in the subsurface.
4. A two-phase liquid-vapor system occurs within 1 km of the surface.
5. Temperature gradients as high as 500°C km^{-1} exist within 0.5 km of the surface but do not continue below 0.5 km.
6. An average grade of 90×10^4 kcal Mg^{-1} of geothermal energy occurs in fractured rocks and pore fluids in 7×10^{10} Mg of rock above 2 km depth in the system today.

Conclusions

This analysis indicates that the observed conductive heat fluxes at Coso are consistent with a hydrothermal system produced by a single 4 km wide, 6 km deep, low permeability pluton emplaced 10^5 years ago into host rocks with bulk permeabilities similar to those in figure 8. These bulk permeabilities are either marginal or too low for commercial energy production, except along local fracture zones. The analysis predicts that the pluton has now crystallized to a depth of 8 km. Subsurface temperature and fluid flow in the Coso system are probably much as shown in figure 14d. Geothermal gradients of 500°C km^{-1} and steam are present in the upper 0.5 km of rock above the pluton's center, but this large gradient does not continue below 0.5 km. The subsurface environment at depths between 0.5 to 5 km is characterized by a geothermal gradient of approximately 30°C km^{-1}, temperatures between 250 and 400°C, and energy concentrations on the order of 90 cal/gr. Subsurface testing of the Coso system is clearly warranted, figure 1 (11). However, other interpretations of the results of this study are possible, and the best location for drill sites or other surface surveys may be in doubt. Since the hypothetical model may have some non-uniqueness, other hypotheses regarding pluton features (size, shape, initial emplacement, temperature, and age) and permeability distribution might be examined. Refinement of the analysis requires more data relevant to the energy transport process, but exploration of other hypotheses can be completed, hence the options in figure 1 (14).

IV

Recommendations for Future Studies

Certain types of data are critical to the assessment of the nation's geothermal energy resources. Methods for collecting these data will have to be developed or, in some instances, improved, and interpretation of the data in the context of the processes which concentrate thermal energy in near-surface regions is essential. As a consequence of our analysis of geothermal systems, the following types of studies should be encouraged.

Data	Direct or Indirect Measurements
Size, Depth of Thermal Source	-microearthquake hypocenters
	-p-wave velocities
	-tilt meter surveys
	-previous volcanic history
	-petrologic type of igneous rocks
Rock Permeabilities	-fracture abundance on surface and in drill core
	-microearthquake energy release and hypocenters
	-electrical resistivity
	-p-wave velocities
	-pressure tests in drill holes
	-subsurface rock units
	-chemical gains and losses
Surface Heat Flux	-conductive fluxes
	-convective fluxes
	-radioactive sources in bedrock
	-regional and local surveys to define inflow and outflow zones
	-non-igneous heat sources (evaporite beds)
Thermal History	-age dates of volcanic and igneous rocks
	-presence and characteristics of altered rocks

Data	Direct or Indirect Measurements
Fluid Distribution	-bulk chemistry and electrical resistivity of spring and bore fluids
	-reconstruct chemical reaction path of fluids
	-stable light isotopes
	-mass abundance of alteration mineral phases in surface and core samples
Resource Recoverability	-in-situ stresses

References

Archie, G. E., 1942, The electrical resistivity log as an aid in determining some reservoir characteristics: Trans. AIME, Petrol. Br., v. 146, p. 54-62.

Austin, Carl F., and Pringle, J. Kenneth, 1970, Geologic investigations at the Coso thermal area: Naval Weapons Center Tech. Pub. 4878, 40 p.

Babcock, James W., 1975, Volcanic rocks in the Coso Mountains, California: Geol. Soc. America, Absts. with Progs., v. 5, p. 6.

Babcock, James W., and Wise, William S., 1973, Petrology of contemporaneous Quaternary basalt and rhyolite in the Coso Mountains, California: Geol. Soc. America, Absts. with Progs., v. 5, p. 6.

Bacon, Charles R., and Duffield, Wendell A., 1976, Phenocryst mineralogy of Pleistocene rhyolites and heat content of the Coso Range geothermal system, California: Geol. Soc. America, Absts. with Progs., v. 8, p. 761-762.

Brace, W. F., Orange, A. S., and Madden, T. R., 1965, The effect of pressure on the electrical resistivity of water saturated crystalline rocks: Jour. Geophys. Res., v. 70, p. 5669-5678.

Bruges, E. A., Latto, B., and Ray, A. K., 1966, New correlations and tables of the coefficient of viscosity of water and steam up to 1000 bar and 1000°C: Internatl. Jour. Heat & Mass Transf., v. 9, p. 465-480.

Combs, James, 1975, Heat flow studies, Coso geothermal area, China Lake, California: Tech. Rept. no. 2 for contract no. N00123-74-C-2099, Advanced Research Proj. Agency, 24 p.

Combs, J., 1975, heat flow and microearthquake studies, Coso geothermal area, China Lake, California: Final Rept., contract no. N00123-74-C-2099, Advanced Research Proj. Agency, ARPA order no. 2800.

Combs, James, ed., 1976a, the Coso geothermal project technical report no. 1: U.S. Energy Research and Development Administration, ERDA prime contract E(45-1)-1830, 18 p.

Combs, James, ed., 1976b, The Coso geothermal project technical report no. 2: U.S. Energy Research and Development Administration, ERDA prime contract E(45-1)-1830, 37 p.

Combs, Jim, and Rotstein, Yair, 1976, Microearthquake studies at the Coso geothermal area, China Lake, California, in Proc. of 2nd United Nations Symp. on the Development and Use of Geothermal Resources, v. 2, p. 909-916.

Duffield, Wendell A., 1975, Late Cenozoic ring faulting and volcanism in the Coso Range area of California: Geology, v. 3, p. 335-338.

Duffield, Wendell A., Bacon, Charles R., and Dalrymple, G. Brent, 1976, Late Cenozoic volcanism and structure of the Coso Range geothermal area, California: Geol. Soc. America, Absts. with Progs., v. 8, p. 845.

Everden, J. F., Savage, D. E., Curtis, G. H., and James, G. F., 1964, Potassium-argon dates and the Cenozoic mammalian chronology of North America: Am. Jour. Sci., v. 262, p. 145-198.

Fraser, H. J., Wilson, H. D. B., and Hendry, N. W., 1943, Hot springs deposits of the Coso Mountains, California: Jour. Mines and Geol., v. 38, p. 223-242.

Furgerson, R. B., 1973, Progress report on electrical resistivity studies, Coso geothermal area, Inyo County, California: Naval Weapons Center Tech. Paper 5497, 38 p.

Helgeson, Harold C., and Kirkham, David H., 1974, Theoretical prediction of the thermodynamic behavior of aqueous electrolytes at high pressures and temperatures: I. Summary of the thermodynamic/electrostatic properties of the solvent: Am. Jour. Sci., v. 274, p. 1098-1198.

Keenan, Joseph H., Keyes, Frederick G., Hill, Philip G., and Moore, Joan G., 1969, Steam Tables, Thermodynamic Properties of Water Including Vapor, Liquid, and Solid Phases: New York, John Wiley & Sons.

Knapp, Richard B., and Knight, Jerry E., 1977, Differential thermal expansion of pore fluids: Fracture propagation and microearthquake production in hot pluton environments: Jour. Geophys. Res., v. 82, p. 2515-2522.

Koenig, James B., Gawarecki, Stephen J., and Austin, Carl F., 1972, Remote sensing survey of the Coso geothermal area, Inyo County, California: Naval Weapons Center Tech. Pub. 5233, 32 p.

Lanphere, Marvin A., Dalrymple, G. Brent, and Smith, Robert L., 1975, K-Ar ages of Pleistocene rhyolitic volcanism in the Coso Range, California: Geology, v. 3, p. 339-341.

McSpadden, William R., 1975, The Marysville, Montana, Geothermal Project, Final Rept. to U.S. Energy Research and Development Administration: Richland, Washington, Batelle, Pacific Northwest Laboratories.

Moskowitz, B., and Norton, D., 1977, A preliminary analysis of intrinsic fluid and rock resistivity in active hydro-

thermal systems: Jour. Geophys. Res., in press.

Norton, Denis, 1977, Fluid circulation in the earth's crust: Am. Geophys. Union Mon. 20, in press.

Norton, Denis L., and Knapp, Richard B., 1977, Transport phenomena in hydrothermal systems: The nature of porosity: Am. Jour. Sci., v. 277, p. 913-936.

Norton, Denis L., and Knight, Jerry E., 1977, Transport phenomena in hydrothermal systems: Cooling plutons: Am. Jour. Sci., v. 277, p. 937-981.

Norton, Denis, 1978, Sourcelines, Sourceregions, and pathlines for fluids in hydrothermal systems related to cooling plutons: Econ. Geol., in press.

Peaceman, D. W., and Rachford, H. H., Jr., 1955, The numerical solution of parabolic and elliptic differential equations: Jour. Soc. Indust. Appl. Math., v. 3, no. 1, p. 28-41.

Schultz, John R., 1937, A Late Cenozoic vertebrate fauna from the Coso Mountains, Inyo County, California: Carnegie Inst., Washington, Pub. 487, p. 75-109.

Smith, R. L., and Shaw, H. R., 1973, Volcanic rocks as geologic guides to geothermal evaluation: EOS:Trans. Am. Geophys. Union, v. 54, p. 1213.

Snow, D. T., 1965, A parallel plate model of fractured permeable media: Unpublished Ph.D. dissertation, University of California, Berkeley, 331 p.

Teledyne Geotech, 1972, Geothermal noise survey of the Coso Hot Springs area, Naval Weapons Center, China Lake, California: Unpublished Tech. Rept. no. 72-6, produced under contract for the Naval Weapons Center, 18 p.

Timoshenko, S. P., and Goodier, J. H., 1951, Theory of elasticity: New York, McGraw-Hill, 2nd ed.

Villas, R. Netuno, and Norton, Denis L., 1977, Irreversible mass transfer between circulating hydrothermal fluids and the Mayflower stock: Econ. Geol., in press.

White, D. E., and Williams, D. L., eds., 1975, Assessment of geothermal resources of the United States: Geol. Survey Circ. 726, 155 p.

Zbur, R. T., 1963, A geophysical investigation of Indian Wells Valley, California: U.S. Naval Ordinance Testing Stations, China Lake, California: Naval Ordinance Test Station Tech. Paper 2795, 98 p.i

Zienkiewicz, O. C., 1971, The Finite Element Method in Engineering Science: London, McGraw-Hill, 521 p.

APPENDIX I

Operations Procedures for Interactive Graphics Programs Developed During this Study

Program ETCHG (Developed under ERDA Contract)

Program ETCHG is a user-oriented interactive graphics program which permits the user to analyze the output from the heat and mass transfer simulations and prepare final copies of figures for publication. The program is written in FORTRAN IV and utilizes the PLOT10 FORTRAN IV Tektronix programs for routine operations. ETCHG accepts input files of variables computed at a sequence of elapsed times for the thermal anomaly. These variables include temperature, pressure, streamfunction, horizontal and vertical mass fluxes, permeability, and thermal conductivity. The following is an abstracted user's manual which documents the capabilities of the program.

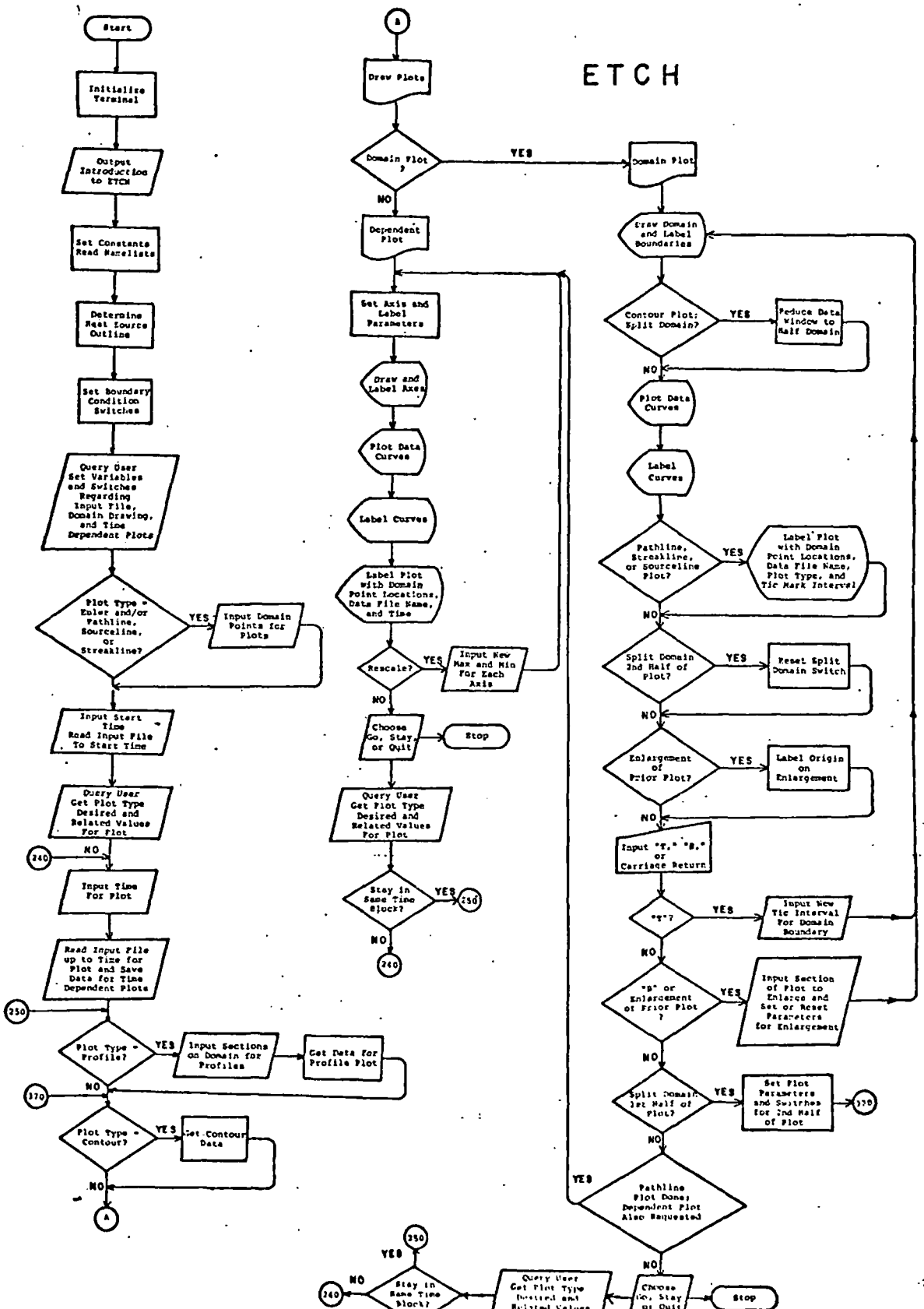
ETCH
Start
Initialize Terminal
Output Introduction to ETCH
Set Constants Read Namelists
Determine Heat Source Outline
Set Boundary Condition Switches
Query User Set Variables and Switches Regarding Input File, Domain Drawing, and Time Dependent Plots
Plot Type = Euler and/or Pathline, Sourceline, or Streakline?
YES
Input Domain Points for Plots
Input Start Time Read Input File To Start Time
Query User Get Plot Type Desired and Related Values For Plot
240
NO
Input Time For Plot
Read Input File up to Time for Plot and Save Data for Time Dependent Plots
250
Plot Type = Profile?
YES
Input Sections on Domain for Profiles
Get Data for Profile Plot
370
NO
Plot Type = Contour?
YES
Get Contour Data
NO
A
A
Draw Plots
Domain Plot ?
YES
Domain Plot
NO
Dependent Plot
Set Axis and Label Parameters
Draw and Label Axes
Plot Data Curves
Label Curves
Label Plot with Domain Point Locations, Data File Name, and Time
Rescale?
YES
Input New Max and Min for Each Axis
NO
Choose Go, Stay or Quit
Stop
Query User Get Plot Type Desired and Related Values For Plot
Stay in Same Time Block?
YES
250
NO
240
Draw Domain and Label Boundaries
Contour Plot: Split Domain?
YES
Reduce Data Window to Half Domain
NO
Plot Data Curves
Label Curves
Pathline, Streakline, or Sourceline Plot?
YES
Label Plot with Domain Point Locations, Data File Name, Plot Type, and Tic Mark Interval
NO
Split Domain 2nd Half of Plot?
YES
Reset Split Domain Switch
NO
Enlargement of Prior Plot?
YES
Label Origin on Enlargement
NO
Input "T," "B," or Carriage Return
"T"?
YES
Input New Tic Interval For Domain Boundary
NO
"B" or Enlargement of Prior Plot ?
YES
Input Section of Plot to Enlarge and Set or Reset Parameters for Enlargement
NO
Split Domain 1st Half of Plot?
YES
Set Plot Parameters and Switches for 2nd Half of Plot
370
NO
YES
Pathline Plot Done; Dependent Plot Also Requested
NO
Choose Go, Stay or Quit
Stop
Query User Get Plot Type Desired and Related Values For Plot
Stay in Same Time Block?
YES
250
NO
240

PROGRAM ETCH WITH INTERACTIVE GRAPHICS
J. KNIGHT, D. NORTON, B. MOSKOWITZ, AND E. NOAH
UNIVERSITY OF ARIZONA 1975-77

THIS PROGRAM USES TEKTRONIX PLOT-10 ROUTINES AS DESCRIBED IN THE TEKTRONIX ADVANCE GRAPHICS AND TCS MANUALS AND IS DESIGNED FOR USE ON A TEKTRONIX 4014 TERMINAL.

VERSION 1.0	JULY 1976
VERSION 2.0	MULTIPLE EULERS, ENLARGEMENTS, ERROR CHECKS REMOTE EXPONENTS ON DOMAIN PLOTS, RESCALE OPTION FOR DEPENDENT PLOTS. AUGUST 1976
VERSION 3.0	REORGANIZATION OF CODE TO MAKE PROGRAM MORE READABLE AND GENERAL. ADDED FLEXIBLE DOMAIN SIZE, LABELS READ FROM INPUT FILE, AND TIME EXPRESSED IN SECONDS. JULY 1977

ETCH PRODUCES PLOTS OF DATA FROM FLOW DATA FILES. IT WILL CONTOUR ANY OF 6 DATA BLOCKS IN THE FLOW FILE, WILL COMPUTE PATHLINES AND STREAKLINES ORIGINATING AT ANY POINT IN THE DOMAIN, WILL PLOT THE VARIATION OF 21 VARIABLES AGAINST TIME OR AGAINST DISTANCE ALONG VERTICAL OR HORIZONTAL SECTIONS CUT THROUGH THE DOMAIN.

RAW DATA IS OBTAINED FROM A DISK OR TAPE FILE GENERATED BY FLOW. (ETCH IS COMPATIBLE WITH VERSION 3 AND EARLIER VERSIONS OF PROGRAM FLOW.)
INITIAL NAMELISTS AND ARRAYS PRECEDE THE DATA TO SET VALUES FOR DATA DEPENDENT CONSTANTS AND SWITCHES. DATA IS READ IN E10.4 FORMAT FROM ARRAYS REPRESENTING PARAMETER VALUES AT GRID POINTS ON THE DOMAIN. DATA ARRAYS ARE PRECEDED BY A TITLE LINE GIVING NAME OF THE PARAMETER REPRESENTED. PLOT LABELS ARE OBTAINED FROM THIS LINE THRU A READ FORMATTED (2X,25R1). UP TO 6 ARRAYS ARE ALLOWED IN BLOCKS REPRESENTING TIME STEPS. THE TITLE LINE FOR THE FIRST ARRAY IN EACH TIME BLOCK INCLUDES THE TIME (EXPRESSED IN YEARS) AND IS GENERALLY READ THRU FORMAT (47X,E15.3). UP TO 200 TIME BLOCKS CAN BE PROCESSED FOR TIME DEPENDENT PLOTS.

TAPE53 FLOW OUTPUT FILE

TO EXECUTE THE ADVANCE GRAPHICS PACKAGE:

SET THE TERMINAL TO GRAPHICS MODE

```
.R SETTTY
TYPE TERMINAL? 4010
```

TO EXECUTE THE PROGRAM TYPE

```
.EX@ETCHG[6130,636]
```

INPUT FOR ETCH IS CARRIED OUT BY TYPING OPTIONS
AT THE TERMINAL IN RESPONSE TO QUESTIONS.
FOR MULTIPLE ANSWERS SEPARATE BY COMMAS.
AFTER EACH ANSWER END WITH A CARRIAGE RETURN.

AFTER EACH DIAGRAM THE TERMINAL WILL WAIT FOR A
CARRIAGE RETURN OR THE LETTER R OR B (SEE BELOW).
AT THIS TIME A HARD COPY CAN BE MADE.

AT THE START OF EXECUTION THE SCREEN WILL BE ERASED
AND ONE OF THE FOLLOWING RESPONSES IS REQUIRIED:

CR	INTRODUCTION TO ETCHG WILL BE DISPLAYED RETURN WITH TWO CARRIAGE RETURNS
S	SKIP INTRODUCTION AND CONTINUE TO OPTION INPUT

INITIAL QUESTIONS:

INPUT THERMAL CONDUCTIVITY

(PRE VERSION FLOW - ONLY)

INPUT TOTAL POROSITY

FRACTION OF ROCK WHICH IS FLUID.

INPUT ORDER OF DATA ARRAYS IN DATA BLOCKS

THERE ARE 6 POSSIBLE ARRAY POSITIONS PER DATA BLOCK
INPUT 1 S FOR POSITIONS TO BE FILLED BY DATA ARRAYS
INPUT Ø S FOR UNUSED POSITIONS
FOR EXAMPLE: Ø,Ø,1,1,1,1 WILL FILL THE LAST FOUR
POSITIONS IN EACH BLOCK WITH DATA ARRAYS

IF INPUT FILE CONTAINS MORE THAN 1 DATA BLOCK PER TIME
BLOCK, ORDER INPUT ABOVE APPLIES TO ALL BUT THE LAST
DATA BLOCK OF THE TIME BLOCK. INPUT ORDER
(AS ABOVE) OF DATA ARRAYS IN THE LAST DATA BLOCK.

IMPORTANT: SEE NOTES(*) IN LIST OF PARAMETER OPTION
NUMBERS REGARDING THE PLACEMENT OF CERTAIN DATA
ARRAYS TO ENABLE USE OF SOME PLOT OPTIONS AND
PARAMETER OPTIONS.

QUESTIONS FOR RESISTIVITY MODEL

PROGRAM WILL READ FROM A DATA FILE CONTAINING
FLUID RESISTIVITY DATA. TWO FILES ARE CURRENTLY USED
1. RHO1 .01 MOLAL NACL
2. RHO2 .1 MOLAL NACL

DO YOU WISH TO MODEL RESISTIVITY?
INPUT YES OR NO.

IF ANSWER WAS YES:

INPUT OLD OR NEW MODEL

IF OLD: INPUT RESISTIVITY FILE
FILENAME OF PRIOR RESISTIVITY MODEL
DATA SAVED TO BE READ IN

IF NEW: DO YOU WISH TO SAVE DATA?
INPUT YES OR NO. YES SAVES RESISTIVITY
AND POROSITY DATA ON FOR50.DAT TO USE
FOR RERUN OF MODEL.

DO YOU WISH TO MODEL POROSITY?
INPUT YES OR NO. YES CALCULATES POROSITY
AS A FUNCTION OF INCREASING TEMPERATURE.

RESISTIVITY INPUT FILE?
INPUT FILENAME OF FLUID RESISTIVITY DATA FILE.

IMPORTANT: IF OLD MODEL IS BEING USED AN EULER PLOT
OPTION MUST BE SPECIFIED FOR RESISTIVITY.

QUESTIONS FOR DOMAIN DRAWING:

DO YOU WANT TO CHANGE TERMINAL WINDOW DIMENSIONS?

INPUT YES OR NO.

IF YES: INPUT LEFT,RIGHT,BOTTOM,TOP
FOR NEW WINDOW IN SCREEN COORDINATES
(SCREEN IS 1074 X 780 UNITS)

INPUT TIC INTERVAL(KM) FOR X AND Y DIRECTIONS FOR DOMAIN

CONTROLS SPACING OF TIC MARKS DRAWN ON DOMAIN BOUNDARY.
IF DOMAIN WIDTH IS 20 KM AND TIC INTERVAL IS SPECIFIED
AS 2 FOR THE X DIRECTION, TIC MARKS WILL REPRESENT
2 KM INTERVALS ACROSS THE DOMAIN.

QUESTIONS FOR TIME DEPENDENT PLOTS:

DO YOU WANT EULER, PATHLINE, STREAKLINE OR SOURCELINE PLOTS?

SPECIFY ONLY EULER AND/OR ONE OF THE OTHERS.
(PATHLINE,STREAKLINE,OR SOURCELINE)
INPUT 1 S FOR OPTIONS DESIRED
INPUT Ø S FOR OPTIONS NOT WANTED
FOR EXAMPLE: 1,1,Ø,Ø ALLOWS USER TO OBTAIN EULER AND PATHLINE PLOTS.

NOTE: IF PATH, STREAK, OR SOURCELINE PLOTS ARE DESIRED ARRAY POSITIONS 3,4,5, & 6 IN DATA BLOCK 1 OF EACH TIME BLOCK MUST CONTAIN DATA FOR HORIZONTAL MASS FLUX, VERTICAL MASS FLUX, TEMPERATURE, & PRESSURE, RESPECTIVELY.
ALSO, SOURCELINE PLOTS REQUIRE THAT TIME BLOCKS IN THE FLOW DATA FILE BE ARRANGED IN ORDER OF DECREASING TIME (USE PROGRAM SHUF).

IF EULER PLOTS ARE SPECIFIED:

HOW MANY EULER PLOTS?

INPUT 1,2 OR 3 DEPENDING ON THE NUMBER OF DIFFERENT VARIABLES YOU WISH TO PLOT

INPUT OPTIONS FOR EULER PLOTS

INPUT PARAMETER OPTION NUMBERS (SEE LIST BELOW), SEPARATED BY COMMAS, FOR EACH VARIABLE TO PLOT.

INPUT DATA BLOCK NUMBERS

IF INPUT TAPE HAS MORE THAN ONE DATA BLOCK PER TIME BLOCK, INPUT DATA BLOCK NUMBERS SEPARATED BY COMMAS, FOR EACH PARAMETER IN THE SAME ORDER AS OPTION NUMBERS WERE INPUT.

IF PATHLINE,STREAKLINE,OR SOURCELINE PLOT SPECIFIED:

INPUT DEPENDENT PARAMETERS FOR PATHLINES: IXLIN,IYLIN

GIVE 2 PARAMETER OPTION NUMBERS (SEE LIST BELOW)

IXLIN = OPTION NUMBER OF VARIABLE TO BE REPRESENTED ON THE X-AXIS
= Ø IF DISTANCE ALONG PATHLINE IS TO BE SHOWN FOR X-AXIS OR IF NO DEPENDENT PLOT IS WANTED.
IYLIN = OPTION NUMBER OF VARIABLE TO BE REPRESENTED ON THE Y AXIS
= Ø IF NO DEPENDENT PLOT IS WANTED

INPUT DATA BLOCK NUMBERS

IF INPUT TAPE HAS MORE THAN ONE DATA BLOCK PER TIME BLOCK, INPUT DATA BLOCK NUMBERS SEPARATED BY COMMAS FOR IXLIN AND IYLIN.

INPUT TIC MARK INTERVAL

TICS WILL BE DRAWN ON LINE PLOTTED IN INCREMENTS OF THIS TIME. IF Ø.Ø NO TICS WILL BE DRAWN. INTERVAL SPECIFIED MUST BE GREATER THAN THE TIME INTERVAL BETWEEN TIME BLOCKS AND SHOULD BE A MULTIPLE OF THAT TIME INTERVAL FOR ACCURATE REPRESENTATION.

INPUT FREQUENCY OF PARTICLES TRACED FROM SOURCE OR STREAKLINES.

NEW POINTS ARE ADDED TO THE CALCULATION WITH THE VALUE OF THIS OPTION. RUN TIME IS DIVIDED BY THIS VALUE, BUT ACCURACY DECREASES.

INPUT DOMAIN POINTS FOR EULER, AND/OR PATHLINE, STREAKLINE, OR SOURCELINE PLOTS

INPUT UP TO 3 POINTS FOR EACH PLOT BY POSITIONING CROSSHAIRS ON DOMAIN AND TYPING A CHARACTER OTHER THAN A SMALL "E" OR CARRIAGE RETURN.
IF FEWER THAN 3 POINTS ARE DESIRED INPUT A SMALL "E" AND CARRIAGE RETURN AFTER THE BELL FOLLOWING THE LAST POINT TO BE INPUT.

INITIAL CONDITION DOMAIN

WHEN THIS DOMAIN IS DRAWN, THE USER MAY TURN THE TERMINAL TO LOCAL AND WRITE ANYTHING UPON THIS DIAGRAM. ONCE ON LINE, THE TERMINAL WILL WAIT FOR EITHER:

CR	PROCEED
H	REDETERMINE POINTS AND REDRAW

INPUT STARTING TIME IN YEARS

TIME TO START READING TIME BLOCKS FOR ACTUAL PLOTTING (USUALLY Ø.Ø FOR IPLOT1-5). FOR IPLOT=6, TMIN= FINAL TIME

INPUT PLOT TYPE OPTION NUMBER:

OPTION NUMBER:	PLOT TYPE:	DESCRIPTION.
1:		CONTOUR PLOT: PLOTS CONTOURS OF A VARIABLE WITHIN THE DOMAIN SPLIT-DOMAIN CONTOUR PLOT: PLOTS CONTOURS OF ONE VARIABLE ON LEFT HALF OF DOMAIN AND CONTOURS OF ANOTHER VARIABLE ON RIGHT HALF.
2:		PATHLINE PLOT: COMPUTES AND PLOTS PATHS TAKEN BY FLUID PACKETS STARTING AT ANY POINT IN THE DOMAIN. WILL ALSO PLOT THE VALUE OF A PARAMETER ALONG THE PATHLINE VS DISTANCE ALONG THE PATHLINE OR VS ANOTHER VARIABLE.
3:		STREAKLINE PLOT: COMPUTES AND PLOTS A LINE GOING THROUGH THE FINAL POSITIONS OF ALL FLUID PACKETS PASSING THROUGH A POINT IN THE DOMAIN.
4:		EULER PLOT: PLOTS VALUE OF A PARAMETER AT A FIXED POINT IN THE DOMAIN AGAINST TIME.
5:		PROFILE PLOT: COMPUTES AND PLOTS THE VALUE OF A PARAMETER AGAINST ITS DEPTH IN THE DOMAIN (VERTICAL PROFILE) OR DISTANCE FROM THE EDGE (HORIZONTAL PROFILE).
6:		SOURCELINE PLOT: COMPUTES AND PLOTS A LINE GOING THROUGH THE INITIAL POSITIONS OF ALL FLUID PACKETS PASSING THROUGH A POINT IN THE DOMAIN. THIS OPTION REQUIRES THE TIME BLOCKS IN THE FLOW DATA FILE BE ARRANGED IN ORDER OF DECREASING TIME. FOR THIS OPTION TMIN IS GREATER THAN TMAX. (USE PROGRAM SHUF)

ADDITIONAL QUESTIONS ABOUT PLOT REQUESTED

FOR CONTOUR PLOT:

INPUT PARAMETER OPTION NUMBER (AND DATA BLOCK NUMBER) FOR PARAMETER TO CONTOUR, AND NUMBER OF CURVES TO PLOT (MAXIMUM IS 5).

SEE LIST BELOW FOR PARAMETER OPTION NUMBERS. CONTOUR PLOTS ARE RESTRICTED TO OPTIONS 1 - 6, 25 & 27. DATA BLOCK NUMBER IS ASKED FOR ONLY IF DATA FILE HAS MORE THAN ONE DATA BLOCK PER TIME BLOCK.

INPUT VALUE FOR EACH CONTOUR.

IF DATA HAS A RECTANGULAR BLOCK OF GRID POINTS WITH THE SAME VALUE, DONT USE THAT EXACT VALUE WHEN REQUESTING CONTOUR. USE SOME VALUE BETWEEN IT AND ADJACENT GRID VALUES.

INPUT SECOND OPTION TO CONTOUR (AND DATA BLOCK NUMBER), AND NUMBER OF CURVES TO PLOT (MAXIMUM IS 5).

INPUT 0,0,0 IF ONLY ONE OPTION IS TO BE CONTOURED ON THE DOMAIN,
OR
INPUT PARAMETER OPTION NUMBER (1 - 6, 25 & 27) TO BE CONTOURED ON THE RIGHT SIDE OF THE DOMAIN. DATA BLOCK NUMBER IS ASKED FOR ONLY IF INPUT FILE HAS MORE THAN ONE DATA BLOCK PER TIME BLOCK. OPTION WITH HIGHEST BLOCK NUMBER WILL BE PLOTTED ON THE RIGHT SIDE OF THE DOMAIN.

INPUT VALUE FOR EACH CONTOUR FOR SECOND OPTION.

SEE NOTE FOR 1ST OPTION CONTOUR VALUES

FOR PATHLINE PLOT:

IF IXLIN WAS NOT 0:

INPUT MIN. AND MAX. FOR DEPENDENT VARIABLE ON X AXIS AND AXIS TYPE SWITCH. (USE 1 FOR LOG(BASE 10) SCALED AXIS. USE 0 FOR NORMAL AXIS).

IF IYLIN WAS NOT 0:

INPUT MIN. AND MAX. FOR DEPENDENT VARIABLE ON Y AXIS AND AXIS TYPE SWITCH. USE 1 FOR LOG(BASE 10) SCALED AXIS. USE 0 FOR NORMAL AXIS.

FOR EULER PLOT:

IF MORE THAN ONE EULER PLOT WAS SPECIFIED EARLIER, WHICH PLOT IS WANTED NOW? INPUT 1,2, OR 3 AS DIRECTED.

INPUT MIN AND MAX FOR DEPENDENT VARIABLE.
AND AXIS TYPE SWITCH. (USE 1 FOR LOG(BASE 10)
SCALED AXIS. USE 0 FOR NORMAL AXIS).

FOR PROFILE PLOT:

HORIZONTAL OR VERTICAL PROFILE SECTION? INPUT H OR V.

INPUT PARAMETER OPTION NUMBER (AND DATA BLOCK NUMBER)
FOR PARAMETER TO PROFILE, AND NUMBER OF CURVES TO PLOT.

SEE LIST BELOW FOR PARAMETER OPTION NUMBERS.
DATA BLOCK NUMBER IS ASKED FOR ONLY IF DATA FILE
HAS MORE THAN ONE DATA BLOCK PER TIME BLOCK.

INPUT MIN AND MAX FOR DEPENDENT VARIABLE
AND AXIS TYPE SWITCH. (USE 1 FOR LOG(BASE 10)
SCALED AXIS. USE 0 FOR NORMAL AXIS).

IF IYLIN WAS NOT 0:

INPUT MIN. AND MAX. FOR DEPENDENT VARIABLE ON Y AXIS
AND AXIS TYPE SWITCH. (USE 1 FOR LOG(BASE 10)
SCALED AXIS. USE 0 FOR NORMAL AXIS).

INPUT NUMBER OF INTERPOLATIONS BETWEEN DATA POINTS.
RECOMMENDED VALUE IS 2.

THE PARAMETER OPTION NUMBERS ARE:

1 - 6 REPRESENT THE PARAMETER AVAILABLE IN ARRAY POSITIONS 1 - 6 RESPECTIVELY.

* PATHLINE, SOURCELINE, AND STREAKLINE PLOTS REQUIRE DATA IN POSITIONS 3-6 IN FIRST DATA BLOCK OF EACH TIME BLOCK AS LISTED BELOW:

3 HORIZONTAL MASS FLUX
4 VERTICAL MASS FLUX
5 TEMPERATURE
6 PRESSURE

* THE FOLLOWING OPTIONS REQUIRE THAT ARRAY POSITIONS 5 & 6 CONTAIN TEMPERATURE AND PRESSURE DATA RESPECTIVELY.
* OPTIONS 14,15, & 20 ALSO REQUIRE VERTICAL FLUX IN ARRAY POSITION 4.
* OPTION 19 ALSO REQUIRES HORIZONTAL FLUX IN ARRAY POSITION 3.
* OPTIONS 12 & 21 ALSO REQUIRE HORIZONTAL FLUX AND VERTICAL FLUX IN ARRAY POSITIONS 3 & 4 RESPECTIVELY.

7 DENSITY
8 COEFFICIENT OF ISOBARIC THERMAL EXPANSION
9 ENTHALPY
10 HEAT CAPACITY
11 VISCOSITY
12 MASS FLUX
13 CONDUCTIVE HEAT FLUX
14 CONVECTIVE HEAT FLUX
15 TOTAL HEAT FLUX
16 ROCK HEAT
17 FLUID HEAT
18 TOTAL HEAT
19 HORIZONTAL DARCY VELOCITY
20 VERTICAL DARCY VELOCITY
21 DARCY VELOCITY

* THE FOLLOWING OPTIONS ARE AVAILABLE ONLY IF FLUID RESISTIVITY DATA FILE OR PREVIOUS RESISTIVITY MODEL DATA FILE HAS BEEN NAMED FOR INPUT (SEE RESISTIVITY MODEL QUESTIONS ABOVE). THESE OPTIONS REQUIRE TEMPERATURE AND PRESSURE IN ARRAY POSITIONS 5 & 6 IN FIRST DATA BLOCK OF EACH TIME BLOCK:

25 RESISTIVITY
26 DIELECTRIC CONSTANT
27 POROSITY

INPUT TIME IN YEARS FOR PLOT.

INPUT TIME SLIGHTLY LESS THAN ACTUAL TIME DESIRED
FROM DATA FILE

FOR STEADY STATE OPTIONS TIME INCREASES
FROM STARTING TIME IN YEARS UNTIL END OF FILE
IS ENCOUNTED OR TERMINATION OF PROGRAM.
WITH THIS YOU CAN TIME STEP THROUGH DATA FILE
PLOTTING STEADY STATE OPTIONS(IPLOT=1,5).

FOR TIME DEPENDENT OPTIONS PLOT WILL BE FROM
TMIN TO TIME GIVEN HERE.

END OF FILE ENCOUNTERED
FINAL TIME WILL BE USED

MESSAGE IS OUTPUT WHEN TIME GIVEN EXCEEDS THE
FINAL TIME IN THE DATA FILE.
A CARRIAGE RETURN WILL ALLOW THE PLOT TO BE DRAWN.
IF DATA FILE HAS MORE THAN ONE DATA BLOCK PER TIME
BLOCK,FINAL TIME IS NOT USED. PROGRAM STOPS.

INPUT DOMAIN SECTIONS FOR PROFILES

FOR VERTICAL SECTION PROFILE:

POSITION CURSOR AT MAXIMUM Y VALUE
(MAXIMUM DEPTH FOR PROFILE)
AND TYPE IN ANY CHARACTER EXCEPT CARRIAGE RETURN.

POSITION CURSOR AT X COORDINATE FOR VERTICAL SECTION
(POINT ON DOMAIN ON X DIRECTION FOR VERTICAL
PROFILE) AND TYPE IN ANY CHARACTER EXCEPT CARRIAGE
RETURN.

FOR HORIZONTAL SECTION PROFILE:

POSITION CURSOR AT MAXIMUM X VALUE (MAXIMUM DISTANCE
FROM LEFT EDGE OF DOMAIN FOR HORIZONTAL PROFILE) AND
TYPE IN ANY CHARACTER EXCEPT CARRIAGE RETURN.

POSITION CURSOR AT Y COORDINATE FOR HORIZONTAL SECTION
(POINT ON DOMAIN ON Y DIRECTION FOR HORIZONTAL
SECTION) AND INPUT ANY CHARACTER EXCEPT CARRIAGE RETURN.

OPTIONS AFTER PLOT IS DRAWN

PROGRAM WAITS FOR A CARRIAGE RETURN OR OPTION
SELECTION FOR ENLARGEMENT, RESCALE, OR NEW TICS.
AT THIS TIME A HARD COPY CAN BE GENERATED.

CONTOUR PLOT, WHOLE DOMAIN:

INPUT CARRIAGE RETURN TO ERASE AND CHOOSE GO, STAY, OR QUIT (SEE BELOW).

INPUT "T" TO REDRAW PLOT WITH DIFFERENT TIC MARKS ON DOMAIN BOUNDRY (SEE NEW TIC OPTION BELOW).

INPUT "B" TO ENLARGE A PORTION OF THE PLOT (SEE ENLARGEMENT OPTION BELOW).

CONTOUR PLOT, SPLIT DOMAIN:

AFTER LEFT HAND SIDE OF PLOT IS DRAWN INPUT A CARRIAGE RETURN TO GO ON WITH THE RIGHT HAND SIDE OF THE PLOT.

AFTER RIGHT HAND SIDE OF PLOT IS DRAWN A CARRIAGE RETURN ERASES THE SCREEN AND PRESENTS USER WITH OPTIONS (GO,STAY,QUIT). RESCALE AND ENLARGEMENT OPTIONS ARE NOT AVAILABLE.

PATHLINE PLOT, DOMAIN PLOT:

IF IYDEP=Ø, A CARRIAGE RETURN WILL ERASE SCREEN AND PRESENT USER WITH OPTIONS (GO,STAY,QUIT).
IF IYDEP NON ZERO, CARRIAGE RETURN WILL ERASE AND DRAW DEPENDENT PLOT.

INPUT "T" TO SET NEW TIC MARK INTERVAL FOR DOMAIN BOUNDRY (SEE NEW TIC OPTION BELOW)

INPUT "B" TO ENLARGE A PORTION OF THE PLOT (SEE ENLARGEMENT OPTION BELOW)

PATHLINE PLOT, DEPENDENT PLOT:

INPUT CARRIAGE RETURN TO ERASE AND CHOOSE OPTIONS (GO, STAY, QUIT).

INPUT "R" TO RESCALE AXIS (SEE RESCALE OPTION BELOW)

STREAKLINE OR SOURCELINE PLOT, DOMAIN PLOT:

INPUT CARRIAGE RETURN TO ERASE AND CHOOSE (GO,STAY,QUIT).

INPUT "T" TO REDRAW PLOT WITH DIFFERENT TIC MARKS ON DOMAIN BOUNDRY(SEE NEW TIC OPTION BELOW).

INPUT "B" TO ENLARGE A PORTION OF THE PLOT (SEE ENLARGEMENT OPTION BELOW).

EULER OR PROFILE PLOT, DEPENDENT PLOT:

INPUT CARRIAGE RETURN TO ERASE AND CHOOSE (GO,STAY,QUIT)

INPUT "R" TO RESCALE AXIS (SEE RESCALE OPTION BELOW).

(GO,STAY, OR QUIT) OPTION

GO-	WILL PROCEED TO NEXT TIME
STAY	CONTINUE AT PRESENT TIME WITH STEADY STATE PLOTTING
QUIT	TERMINATION OF PROGRAM

RESCALE OPTION

USED ONLY FOR IPLOT = 2,4,OR 5
ASKS USER FOR NEW MIN AND MAX FOR EACH AXIS.

ENLARGEMENT OPTION

USED ONLY FOR IPLOT=1,2,3,OR 6
IF B IS CHOSEN THE CROSSHAIRS WILL APPEAR. TO ENLARGE AN AREA POSITION THE CROSSHAIR AT THE LOWER LEFT HAND CORNER OF THE DESIRED AREA AND INPUT A CAPTIAL P. THEN MOVE TO THE UPPER RIGHT HAND CORNER OF THE AREA AND INPUT CAPITAL P AGAIN. A BOX WILL BE DRAWN AROUND THE AREA FOR ENLARGEMENT.
ONCE THE BOX IS DRAWN, THE TERMINAL WILL WAIT FOR A CARRIAGE RETURN, AT THIS TIME A HARD COPY CAN BE GENERATED. AFTER THE CARRIAGE RETURN,THE USER IS ASKED TO INPUT TIC INTERVAL FOR THE DOMAIN. THIS INTERVAL IS TEMPORARY AND AFFECTS THE ENLARGEMENT ONLY. INPUT A CARRIAGE RETURN AFTER NEW TIC INTERVAL TO GO ON WITH PLOT.

NEW TIC OPTION

USER IS ASKED TO SPECIFY A NEW TIC INTERVAL FOR DOMAIN BOUNDRY. THIS PERMANENTLY RESETS TIC INTERVAL SPECIFIED EARLIER.

ERROR MESSAGES ARE FEW AND SELF EXPLANATORY.

BIBLIOGRAPHY

Alexander, G. B., Heston, W. M., and Iller, R. K., 1954, The solubility of amorphous silica in water: Jour. Phys. Chem., v. 58, p. 453-455.

Apps, J. A., 1970, The stability field of analcine: Ph.D. dissertation, Harvard University, Cambridge, Massachusetts.

Archie, G. E., 1942, The electrical resistivity log as an aid in determining some reservoir characteristics: Trans. AIME, Petrol. Br., v. 146, p. 54-62.

Atwater, R., 1970, Relationship of plate tectonics to Cenozoic tectonics of western North America: Geol. Soc. America Bull., v. 81, p. 3513-3536.

Austin, Carl F., and Pringle, J. Kenneth, 1970, Geologic investigations at the Coso thermal area: Naval Weapons Center Tech. Pub. 4878, 40 p.

Babcock, James W., and Wise, William S., 1973, Petrology of contemporaneous Quaternary basalt and rhyolite in the Coso Mountains, California: Geol. Soc. America, Absts. with Progs., v. 5, p. 6.

Babcock, James W., 1975, Volcanic rocks in the Coso Mountains, California: Geol. Soc. America, Absts. with Progs., v. 5, p. 6.

Bacon, Charles R., and Duffield, Wendell A., 1976, Phenocryst mineralogy of Pleistocene rhyolites and heat content of the Coso Range geothermal system, California: Geol. Soc. America, Absts. with Progs., v. 8, p. 761-762.

Bailey, R. A., 1976, Volcanism, structure, and geochemistry of Long Valley Caldera, Mono County, Calif.: Jour. Geophys. Res., v. 81, no. 5, p. 725-744.

Baker, A. A., Calkins, F. C., Crittenden, M. D., Jr., and Bromfield, C. S., 1966, Geologic Map of the Brighton Quadrangle, Utah: U.S. Geol. Survey.

Barker, C., 1972, Aquathermal pressuring--role of temperature in development of abnormal-pressure zones: Am. Assoc. Pet. Geol. Bull., v. 56, p. 2068-2071.

Barnes, M. P., and Simos, J. G., 1968, Ore deposits of the Park City District, with a contribution on the Mayflower Lode, in Ore Deposits of the United States, 1933-1967, Ridge, J. R., Jr., ed., The Granton-Sales Volume, no. 2, AIME, p. 1002-1126.

Bath, M., 1966, Earthquake energy and magnitude: Physics and Chemistry of the Earth, v. 7, p. 117-165.

Beane, R. E., 1972, A thermodynamic analysis of the effect of solid solution on the stability of biotite: Unpublished Ph.D. dissertation, Northwestern University, 195 p.

Beane, R., 1974, Biotite stability in porphyry copper environment: Econ. Geol., v. 69, no. 2, p. 241-256.

Bear, Jacob, 1972, Dynamics of fluids in porous media: New York, Am. Elsevier, 764 p.

Belytschko, T., and Kennedy, J. M., 1975, Finite element study of pressure wave attenuation by reactor fuel subassemblies: Jour. Pres. Vessel Tech., v. 97, p. 172-177.

Benard, M., 1901, Les tourbillons cellularies dans une nappe liquide transportant de la chaleur par convection en regime permanent: Am. Chim. Phys., v. 23, p. 62-144.

Bianchi, L., and Snow, D. T., 1969, Permeability of crystalline rocks interpreted from measured orientations and apertures of fractures: The Arid Zone Research of India, Jodphur (Rajasthan), Annals of Arid Zone, v. 8, no. 2, p. 231-245.

Birch, F., 1966, Compressibility, elastic constants, in Clark, S. P., ed., Handbook of Physical Constants, Geol. Soc. America Mem. 97: New York, Geol. Soc. America, p. 97-174.

Boardman, C. R., and Skrove, J., 1966, Distribution in fracture permeability of a granitic rock mass following a contained nuclear explosion: Jour. Petrol. Tech., v. 18, p. 619-623.

Boutwell, J. M., 1912, Geology and Ore Deposits of the Park City District, Utah, With Contributions by L. H. Woolsey: U.S. Geol. Survey Prof. Paper #77, 231 p.

Bowden, C., 1975, The impact of energy development on water resources in arid lands: Arid Lands Res. Info. Paper, no. 6, 278 p.

Brace, W. F., 1971, Resistivity of saturated crustal rocks to 40 km based on laboratory measurements, in Heacock, J. G., ed., The Structure and Physical Properties of the Earth's Crust: Am. Geophys. Union Mon. 14, p. 243-255.

Brace, W. F., 1977, Permeability from resistivity and pore shape: Jour. Geophys. Res., v. 82, p. 3343-3347.

Brace, W. F., Orange, A. S., and Madden, T. R., 1965, The effect of pressure on the electrical resistivity of water

saturated crystalline rocks: Jour. Geophys Res., v. 70, p. 5669-5678.

Brace, W. F., Walsh, J. B., and Frangos, W. T., 1968, Permeability of granite under high pressure: Jour. Geophys. Res., v. 73, no. 6, p. 2225-2236.

Brace, W. F., and Orange, A. S., 1968a, Electrical resistivity changes in saturated rocks during fracture and frictional sliding: Jour. Geophys. Res., v. 73, p. 1433-1445.

Brace, W. F., and Orange, A. S., 1968b, Further studies of the effect of pressure on electrical resistivity of rocks: Jour. Geophys. Res., v. 73, p. 5407-5420.

Brock, T. D., and Mosser, J. L., 1975, Rate of sulfuric acid production in Yellowstone National Park: Geol. Soc. America Bull., v. 86, p. 194-198.

Bromfield, C. S., Baker, A. A., and Crittenden, M.D., Jr., 1970, Geologic Map of the Heber Quadrangle, Wasatch and Summit Counties, Utah: U.S. Geol. Survey.

Brown, T. H., 1970, Theoretical predictions of equilibria and mass transfer in the system CaO-MgO-Si_2-H_2O-CO_2-NaCl-HCl: Unpublished Ph.D. dissertation, Northwestern University.

Browne, P. R. L., and Ellis, A. J., 1970, The Ohaki-Broadlands hydrothermal area, New Zealand: Mineralogy and related geochemistry: Am. Jour. Sci., v. 269, p. 97-131.

Bruges, E. A., Latto, B., and Ray, A. K., 1966, New Correlations and tables of the coefficient of viscosity of water and steam up to 1000 bar and 1000°C: Internatl. Jour. Heat and Mass Transf., v. 9, p. 465-480.

Burnham, C. W., Holloway, J. R., and Davis, N. F., 1969, Thermodynamic properties of water to 1000°C and 10,000 bars: Geol. Soc. America Spec. Paper 132, 96 p.

Burnham, C. W., and Davis, N. F., 1971, The Role of H_2O in silicate melts I. P-V-T relations in the system $NaAlSi_3O_8$-H_2O to 10 kilobars and 1000°C: Am.. Jour. Sci., v. 270, p. 54-79.

Butler, B. S., 1919, Primary (hypogene) sulfate minerals in ore deposits: Econ. Geol., v. 14, p. 581-609.

Butler, B. S., 1956, Mineralizing solutions that carry and deposit iron and sulfur: Mining Eng., p. 1012-1017.

Cadek, J., Hazdrova, M., Kacura, G., Krasny, J., and Malkovsky, M., 1869, Hydrogeology of the thermal waters at Teplice and Usti nad Labem: Sbornik Geolog. Ved, Hydrogeol., Inzenyrska

Geol., Rada Hig, sv. 6, p. 1-184.

Calkins, F. C., and Butler, B. S., 1943, Geology and Ore Deposits of the Cottonwood-American Fork Area, Utah, With Contributions by V. C. Heikes: U.S. Geol. Survey Prof. Paper #201, 152 p.

Chambers, J. F., 1958, The conductance of concentrated aqueous solutions of potassium iodide at 25°C and of potassium and sodium chlorides at 50°C: Jour. Phys. Chem., v. 62, p. 1136.

Cheng, W. T., 1970, Geophysical exploration in the Tatun volcanic region, Taiwan: Geothermics Spec. Issue 2, U.N. Symp. on the Development and Utilization of Geothermal Resources, Pisa, v. 2, part 1, p. 910-917.

Christiansen, R. L., and Lipman, P. W., 1972, Cenozoic volcanism and plate-tectonic evolution of the western United States I. Late Cenozoic: Phil. Trans. R. Soc. Land., v. 217A, p. 249-284.

Clark, S. P., Jr., ed., 1966, Handbook of Physical Constants, rev. ed.: New York, Geol. Soc. America Mem. 97, 587 p.

Combs, J., 1975, Heat flow and microearthquake studies, Coso geothermal area, China Lake, California: Final rept. to Adv. Res. Proj. Agency, ARPA, order no. 2800, 65 p.

Combs, James, 1975, Heat flow studies, Coso geothermal area, China Lake, California: Tech. Rept. no. 2 for contract no. NOO123-74-C-2099, Advanced Research Proj. Agency, 24 p.

Combs, James, Ed., 1976a, The Coso geothermal project technical report no. 1: U.S. Energy Research and Development Administration, ERDA prime contract E(45-1)-1830, 18 p.

Combs, James, ed., 1976b, The Coso geothermal project technical report no. 2: U.S. Energy Research and Development Administration, ERDA prime contrast E(45-1)-1830, 37 p.

Combs, Jim, and Rotstein, Yair, 1976, Microearthquake studies at the Coso geothermal area, China Lake, California, in Proc. of 2nd United Nations Symp. on the Development and Use of Geothermal Resources, v. 2, p. 909-916.

Cook, K. L., 1966, Rift system in the basin and range province, in the World Rift System, Irvine, T. N., ed.: Paper, Geol. Survey Canada, no. 66, p. 280-289.

Cooper, John R., 1957, Metamorphism and volume losses in carbonate rocks near Johnson Camp, Cochise County, Arizona: Geol. Soc. America Bull., v. 68, p. 577-610.

Craig, J. R., and Barton, P. B., 1973, Thermochemical approximations for sulfosalts: Econ. Geol., v. 68, p. 493-506.

Criss, C. M., and Cobble, J. W., 1964a, The thermochemical properties of high temperature aqueous solutions IV. Entropies of the ions to 200° and the correspondence principle: Am. Chem. Soc. Jour., v. 86, p. 5385-5390.

Criss, C. M., and Cobble, J. W., 1964b, The thermochemical properties of high temperature aqueous solutions V. The calculation of ionic heat capacities up to 200°C: Entropies and heat capacities above 200°: Am. Chem. Soc. Jour., v. 86, p.

Crittenden, M. D., Jr., 1965, Geologic map of the Dromedary Peak Quadrangle, Utah: U.S. Geol. Survey.

Crittenden, M. D., Jr., Stockless, J. S., Kistler, R. W., and Stern, T. W., 1973, Radiometric dating of intrusive rocks in the Cottonwood Area, Utah: Jour. Res., U.S. Geol. Survey, v. 1, n. 2, p. 173-178.

Damon, P. E., Shafigullah, M., and Leventhal, J. S., 1974, K/Ar chronology for the San Francisco volcanic field and rate of erosion of the Little Colorado River, in Geology of Northern Arizona, Part 1, Regional Studies: Geol. Soc. America, p. 221-235, Rocky Mt. Sec. Mtg., Flagstaff.

Damon, P. E., and Bikerman, M., 1966, K/Ar chronology of the Tucson Mountains, Pima County, Arizona: Geol. Soc. America Bull., v. 77, p. 1225-1234.

Davis, S. N., 1969, Porosity and permeability of natural materials, in DeWiest, R. J. M., ed., Flow through porous media: New York, Academic Press, p. 54-90.

DeWiest, R. J. M., 1965, Geohydrology: New York, John Wiley & Sons, Inc., 366 p.

Dellechaie., Frank, 1975, A hydrochemical study of the south Santa Cruz Basin near Coolidge, Arizona (abs.): 2nd United Nations Symp. on the Development and Use of Geothermal Resources, San Francisco, California, May 20-2.

Donaldson, I. G., 1962, Temperature gradients in the upper layers of the earth's crust due to convective water flows: Jour. Geophys. Res., v. 67, no. 9, p. 28-48.

Donaldson, I. G., 1968, The flow of stream water mixtures through permeable beds: a simple simulation of a natural undisturbed hydrothermal region: New Zealand Jour. Sci., v. 11, no. 1, p. 3-23.

Duffield, Wendell A., 1975, Late Cenozoic ring faulting and volcanism in the Coso Range area of California: Geology, v. 3, p. 335-338.

Duffield, Wendell A., Bacon, Charles R., and Dalrymple, G. Brent, 1976, Late Cenozoic volcanism and structure of the Coso Range geothermal area, California: Geol. Soc. America, Absts. with Progs., v. 8, p. 845.

Elder, J. W., 1965, Physical processes in geothermal areas, chap. 8, in Lee, W. H. K., ed., Terrestrial Heat Flow: Am. Geophys. Union Mon. 8, p. 211-239.

Elder, J. W., 1967, Steady free convection in a porous medium heated from below: Jour. Fluid Mech., v. 27, p. 29-84.

Ellis, A. J., and Mahon, W. A. J., 1967, National hydrothermal systems and experimental hot water/rock interactions (Part II): Geochim. et Cosmochim. Acta, v. 31, p. 519-538.

Everden, J. F., Savage, D. E., Curtis, G. H., and James, G. F., 1964, Potassium-argon dates and the Cenozoic mammalian chronology of North America: Am. Jour. Sci., v. 262, p. 145-198.

Fatt, I., 1956, The network model of porous media: AIME, Petroleum Trans., v. 207, p. 141-181.

Forgac, J., 1972, Genesis of alunite and metamorphic rocks near Dekys (Stiavnicke Porhorie Mountains): Geol. PR., v. 58, p. 189-199 (in Slovic): Chem. Abst. CA07904021557H.

Fournier, R. O., and Rowe, J. J., 1966, Estimation of underground temperature from the silica content of water from hot springs and wet-steam wells: Am. Jour. Sci., v. 264, p. 685-697.

Fournier, R. O., and Truesdell, A. H., 1973, An empirical Na-K-Ca geothermometer for natural waters: Geochim. et Cosmochim. Acta, v. 37, p. 1255-1275.

Fraser, H. J., Wilson, H. D. B., and Hendry, N. W., 1943, Hot springs deposits of the Coso Mountains, California: Jour. Mines and Geol., v. 38, p. 223-242.

Furgerson, R. B., 1973, Progress report on electrical resistivity studies, Coso geothermal area, Inyo County, California: Naval Weapons Center Tech. Paper 5497, 38 p.

Garrels, R. M., Dreyer, Z. M., and Howland, D. L., 1949, Diffusion of ions through intergranular spaces in water saturated rocks: Geol. Soc. America Bull., v. 60, p. 1809-1828.

Gilluly, James, 1946, The Ajo mining district: U.S. Geol. Survey Prof. Paper #209.

Gilluly, J., 1963, The tectonic evolution of the western United States: Q. Jl, Geol. Soc. Land., v. 119, p. 133-174.

Gonzales, Arsenio Geronimo, 1959, Geology and genesis of the Lepanto Copper Deposit, Mankayan, Mountain Province, Philippines: Unpublished Ph.D. dissertation, Stanford University.

Goranson, R. W., 1938, Silicate-Water Systems: Phase Equilibria in the $NaAlSi_3O_8$-H_2O and $KAlSi_3O_8$-H_2O Systems at High Temperatures and Pressures: Am. Jour. Sci., 5th Series, v. 35A, p. 71-91.

Graton, L. C., and Bowditch, Samuel I., 1936, Alkaline acid solutions in hypogene zoning at Cerro de Pasco: Econ. Geol., v. 31, p. 651.

Greenberg, R. J., and Brace, W. F., 1969, Archie's Law for rocks modeled by simple networks: Jour. Geophys. Res., v. 74, p. 2099-2102.

Grindley, G. W., 1965, The geology, structure, and exploration of the Wairakei geothermal field, Taupo, New Zealand: New Zealand Geol. Survey Bull. n.s. 75, 131 p.

Grindley, G. W., 1970, Subsurface structures and relation to steam production in the Broadlands geothermal field, New Zealand: Geothermics Spec. Issue 2, U. N., Symp. on the Development and Utilization of Geothermal Resources. Pisa, v. 2, pt. 1, p. 248-261.

Gunning, H. E., and Gordon, A. R., 1942, The conductance and ionic mobilities for aqueous solutions of K and NaCl at T = 15°C - 45°C: Jour. Chem. Phys., v. 10.

Gustafson, L. B., 1963, Phase equilibria in the system Cu-Fe-As-S: Econ. Geol., v. 58, p. 667-701.

Gustafson, L. B., and Hunt, John P., 1975, The porphyry copper deposit at El Salvador, Chile: Econ. Geol., v. 70, p. 857-912

Haas, H., 1972, Equilibria in the system Al_2O_3-SiO_2-H_2O involving the stability limits of diaspore and pyrophyllite, and thermodynamic data of these minerals: Am. Mineralogist, v. 57, p. 1375-1385.

Hamilton, W., and Myers, W. B., 1966, Cenozoic tectonics of the western United States: Rev. Geophys., v. 4, p. 509-550.

Harbour, J., 1966, Stratigraphy and sedimentology of the upper Safford Basin sediments: Unpublished Ph.D. dissertation, University of Arizona.

Heacock, J. G., 1971, Intermediate and deep properties of the earth's crust, a possible electromagnetic wave guide, in Heacock, J. G., ed., The Structure and Physical Properties of the Earth's Crust: Am. Geophys. Union Mon. 14, p. 1-11.

Heard, H. C., 1967, The influence of environment on the brittle failure of rocks, in Failure and Breakage of Rocks, Eighth Symposium on Rock Mechanics, AIME (New York), p. 82-93.

Helgeson, H. C., 1968, Evaluation of irreversible reactions in geochemical processes involving minerals and aqueous solutions - I. Thermodynamic relations: Geochim. et Cosmochim. Acta, v. 32, p. 853-877.

Helgeson, H. C., 1969, Thermodynamics of hydrothermal systems at elevated temperatures and pressures: Am. Jour. Sci., v. 267, p. 729-804.

Helgeson, H. C., 1970, A chemical and thermodynamic model of ore deposition in hydrothermal systems: Min. Soc. of Am. Spec. Paper #3, p. 155-186.

Helgeson, H. C., Brown, T. H., Nigrini, A., and Jones, T. A. 1970, Calculation of mass transfer in geochemical processes involving aqueous solutions: Geochim et Cosmochim. Acta, v. 34, p. 569-592.

Helgeson, H. C., Garrels, R. M., and Mackenzie, F. T., 1969, Evaluation of irreversible reactions in geochemical processes involving minerals and aqueous solutions - II. Applications: Geochim. et Cosmochim. Acta, v. 33, p. 455-481.

Helgeson, H. C., and Kirkham, D. H., 1974a, Theoretical predictions of the thermodynamic behavior of aqueous electrolytes at high pressures and temperatures; I. Summary of the thermodynamic/electrostatic properties of the solvent: Am. Jour. Sci., v. 274, p. 1098-1198.

Helgeson, H. C., and Kirkham, D. H., 1974b, Theoretical predictions of the thermodynamic behavior of aqueous electrolytes at high pressures and temperatures; II. Debye-Huckel parameters for activity coefficient and relative partial molal properties of the source: Am. Jour. Sci., v. 274, p. 1199-1261.

Hemley, J. J., Hostetler, P. B., Gude, A. J., and Mountjoy, W. T., 1969, Some stability relations of alunite: Econ. Geol., v. 64, p. 599-612.

Henley, R. W., 1973, Some fluid dynamics and ore genesis: Trans/section B, Inst. Min. and Metall., v. 2, p. B1-B8.

Holst, P. H., and Aziz, K., 1972, Transient three-dimensional natural convection in confined porous media: Internatl. Jour. Heat and Mass Transf., v. 15, p. 73-90.

Horikoshi, E., 1969, Volcanic activity related to the formation of the Kuroko-type deposits in the Kosaka District, Japan: Mineralium Deposita, v. 4, p. 321-345.

Horn, M. K., and Adams, J. A. S., 1966, Computer-derived geochemical balances and elemental abundances: Geochim. et Cosmochim. Acta, v. 30, p. 279-297.

Huang, C. K., 1955, Gold-copper deposits of the Chinkaushih Mine, Taiwan, with special reference to the mineralogy: ACTA Geol. Taiwanica, no. 7, p. 1.

Hubbert, M. K., 1940, The theory of ground-water motion: Jour. Geol., v. 48, p. 785-944.

Hubbert, M. K., and Willis, D. G., 1957, Mechanics of hydraulic fracturing: Petrol. Trans., AIME, v. 210, p. 153-166.

Hubbert, M. K., and Rubey, 1959, W. W., Role of fluid pressure in mechanics of overthrust faulting. I: Geol. Soc. America Bull., v. 70, p. 115-166.

Ishihara, S., Kanehira, K., Sasaki, A., Sato, T., and Shimazaki, Y., eds., 1974, Geology of Kuroko deposits, Japan: Soc. Mining Geol. Japan, Spec. Issue 6, 435 p.

Jackson, D. B., 1966, Deep resistivity probes in the southwestern United States: Geophysics, v. 31, p. 1123-1144.

Jacobs, D. C., and Parry, W. T., 1976, A comparison of the geochemistry of biotite from some Basin and Range stocks: Econ. Geol., v. 71, no. 6, p. 1027-1035.

Jaeger, J. C., 1968, Cooling and solidification of igneous rocks, in Hess, H., ed., Basalts, v. II: New York, John Wiley & Sons, p. 504-535.

Jaques, A. L., and Webb, A. Q., 1975, Geochronology of porphyry copper intrusives from Manus Island Papua New Guinea: Geol. Survey of Papua New Guinea, rpt. 75/5.

Jarzabek, D., and Combs, J., 1976, Microearthquake survey of the Dunes KGRA, Imperial Valley, Southern California: Geol. Soc. Am., Absts. with Progs., v. 8, p. 939.

Johnson, D. M., and Combs, J., 1976, Microearthquake survey of the

Kilbourne Hole KGRA, South Central New Mexico: Geol. Soc. Am., Absts. with Progs., v. 9, p. 942.

Kajiwara, Y., 1973, A simulation of the Kuorko type mineralization in Japan: Geochem. Jour., v. 6, p. 193-209.

Keenan, J. H., Keyes, F. G., Hill, P. G., and Moore, J. G., 1969, Steam Tables: New York, John Wiley & Sons, 162 p.

Keller, G. V., 1970, Induction methods in prospecting for hot water: Geothermics Spec. Issue 2, U.N. Symp. on the Development and Utilization of Geothermal Resources, Pisa, v. 2, pt. 1, p. 318-332.

Keller, G. V., Anderson, L. A., and Pritchard, J. I., 1966, Geological survey investigations of the electrical properties of the crust and upper mantle: Geophysics, v. 31, p. 1078-1087.

Keller, G. V., 1971, Electrical studies of the crust and upper mantle in Heacock, J. G., ed., The Structure and Physical Properties of the Earth's Crust: Am. Geophys. Union Mon. 14, p. 107-126.

Keller, G. V., and Frischknecht, F. C., 1966, Electrical methods in geophysical prospecting: Oxford, Pergamon Press.

Kelley, K. K., 1960, Contributions to the data on theoretical metallurgy. XIII. High-temperature heat content, heat capacity, and entropy data for the elements and inorganic compounds: U.S. Bur. Mines Bull. 584, 232 p.

Kelley, K. K., Shomate, C. Y., Young, F. E., Naylor, B. F., Salo, A. E., and Huffman, E. H., 1946, Thermodynamic properties of ammonium and potassium alums and related substances with reference to extraction of alumina from clay and alunite: U.S. Bur. Mines, Tech. Paper 688.

Kelley, Vincent C., 1935, Paragenesis of the Colorado copper sulfides, Cananea, Mexico: Econ. Geol., v. 30, p. 663.

Kennedy, G. C., 1950, A portion of the system silica-water: Econ. Geol., v. 45, p. 629-653.

Kerr, Paul F., 1951, Alteration features at Silver Bell, Arizona: Geol. Soc. America Bull., v. 62, p. 451.

Kim, Gung Rae, I. K. Song Kim, Man Ung Pak, and Gyung Tae Shin, 1971, Metasomatic zonality of low-temperature hydrothermal secondary quartzites and argillaceous rocks with alunite: Chijil Kwa Chiri, v. 11, p. 21-25 (in Korean): Chem. Abst. CA07614074817N.

King, P. B., 1959, The evolution of North America: Princeton

University Press, 189 p.

Kitahara, S., 1960, The polymerization of silicic acid obtained by the hydrothermal treatment of quartz and the solubility of amorphous silica: Rev. Phys. Chem. Japan, v. 30, p. 131-137.

Knapp, R. B., 1975, An analysis of the porosities of fractured crystalline rocks: Unpublished M.S. thesis, University of Arizona, 160 p.

Knapp, R., and Knight, J., 1977, Decrease in effective pressure by differential thermal expansion of pore fluids: Jour. Geophys. Res., accepted for publication.

Knapp, R., and Knight, J., 1977, Permeability of rocks in hydrothermal systems: Fracture propagation by pore fluid expansion: Jour. Geophys. Res., in press.

Knapp, Richard B., and Knight, Jerry E., 1977, Differential thermal expansion of pore fluids: fracture propagation and microearthquake production in hot pluton environments: Jour. Geophys. Res., v. 82, p. 2515-2522.

Knight, Jerry E., 1976, A thermochemical study of alunite and copper arsenic sulfosalt deposits: Unpublished M.S. thesis, University of Arizona.

Koenig, James B., Gawarecki, Stephen J., and Austin, Carl F., 1972, Remote sensing survey of the Coso geothermal area, Inyo County, California: Naval Weapons Center Tech. Pub. 5233, 32 p.

Kofman, R. G., 1971, Interrelations between alunitization and kaolinitization in the Zaglik Deposits: Tr. Kavhar. Inst. Miner. Syr'ya No. 9 Geol. Tekhnol, p. 195-207. (in Russian): Chem. Abst. CA0780 6032584V.

Kramer, J. R., 1969, subsurface brines and mineral equilibria: Chem. Geol., v. 4, p. 38-50.

Krieger, M. H., 1969, Ash-flow tuffs in the norther Galiuro Mountains, Arizona (abs): Geol. Soc. America Spec. Paper no. 121, p. 523.

Lachenbruch, A. H., 1970, Crustal temperature and heat production: Implications of the linear heat-flow relation: Jour. Geophys. Res., v. 75, p. 3291-3300.

Lachenbruch, A. H., and others, 1976, Geothermal setting and simple heat conduction models for the Long Valley Caldera: Jour. Geophys. Res., v. 81, no. 5, p. 769-784.

Lambert, J. B., and Sato, T., 1974, The Kuroko and associated

ore deposits of Japan: A review of their features and metallogenesis: Econ. Geol., v. 69, p. 1215-1236.

Landisman, M., Mueller, S., and Mitchell, B. J., 1971, Review of evidence for velocity inversions in the continental crust, in Heacock, J. G., ed., The Structure and Physical Properties of the Earth's Crust: Am. Geophys. Union Mon. 14, p. 11-34.

Lanphere, Marvin A., Dalrymple, G. Brent, and Smith, Robert L., 1975, K-Ar ages of Pleistocene rhyolitic volcanism in the Coso Range, California: Geology, v. 3, p. 339-341.

Lapwood, E. R., 1948, Convection of a fluid in a porous medium: Proc., Cambridge Phil. Soc. 44, p. 508-521.

Laughlin, G. F., and Behre, C. H., Jr., 1933, Classification of ore deposits, in Ore deposits of the Western States: Amer. Inst. of Mining and Metallur. Eng., New York, 797 p.

Leeman, W. P., and Rogers, J. J. W., 1970, Late Cenozoic alkali-olivine basalts of the basin-range province, USA: Contr. Mineral. and Petrol., v. 25, p. 1-24.

Lindgren, Waldemar, 1905, The copper deposits of the Clifton-Morenci District, Arizona: U.S. Geol. Survey Prof. Paper #43.

Lindgren, W., 1907, The relation of ore deposition to physical conditions: Econ. Geol., v. 2, p. 105-127.

Lister, C. R. B., 1974, On the penetration of water into hot rock: Royal Astr. Soc., Jour. Geophys., v. 39, p. 465-509.

Lodder, W., 1966, Gold-alunite deposits and zonal wall-rock alteration near Rodalaguilar, S.E. Spain: Unpublished Ph.D. dissertation, University of Amsterdam.

Lovering, T. S., 1935, Theory of heat conduction applied to geological problems: Geol. Soc. America Bull., v. 46, p. 69-94.

Lowell, R. P., 1975, Circulation in fractures, hot springs, and convective heat transport on mid-ocean ridge crests: Royal Astr. Soc., Jour. Geophys., v. 40, p. 351-365.

McSpadden, William R., 1975, The Marysville, Montana, Geothermal Project, Final Rept. to U.S. Energy Research and Development Administration: Richland, Wasington, Batelle, Pacific Northwest Laboratories.

Maini, Y. N. T., 1971, In situ hydraulic parameters in jointed

rock--their measurement and interpretation: Unpublished Ph.D. dissertation, University of London, 312 p.

Marine, I. W., 1966, Hydraulic correlation of fracture zones in buried crystalline rock at the Savannah River plant, near Aiken, South Carolina: U.S. Geol. Survey Prof. Paper #550-D, p. 223-227.

Marlowe, J. I., 1960, Late Cenozoic geology of the lower Safford Valley--a preliminary report: Arizona Geol. Soc. Digest, v. 3, p. 127-129.

Maske, S., and Skinner, B. J., 1971, Studies of the sulfosalts of copper. I. Phases and phase relations in the system Cu-As-S: Econ. Geol., v. 66, p. 901-918.

McKee, B. H., and Anderson, C. A., 1971, Age and chemistry of Tertiary volcanic rocks in north-central Arizona, and their relationship to the Colorado Plateaus: Geol. Soc. America Bull., v. 82, p. 2767-2782.

Mehnert, Harold H., Lipman, Peter W., and Sleven, Thomas A., 1973, Age of mineralization at Summitville, Colorado, as indicated by K-Ar dating of alunite: Econ. Geol., v. 68, p. 399.

Meidav, T., and Furgerson, R., 1972, Resistivity studies of the Imperial Valley geothermal area, California: Geothermics, v. 1, p. 47-62.

Meyer, C., Shea, E. P., Goddard, C. C., Jr., and staff, 1968, Ore deposits at Butte Montana, in Ore deposits of the United States: Amer. Inst. of Mining, Metal. and Petro. Eng., New York, p. 1373-1416.

Meyer, Charles, 1950, Hydrothermal wall rock alteration at Butte, Montana: Ph.D. dissertation, Harvard, 329 p.

Minakami, T., Utibori, S., Yamaguchi, M., Gyoda, N., Utsunomiya, T., Hagiwara, M., and Hirai, K., 1969, The Ebino earthquake swarm and the seismic activity in the Kirisima volcanoes, in 1968-1969, Part I. Hypocentral distribution of the 1968 Ebino earthquakes inside the Kakuto Caldera: Bull. Earthquake Res. Inst., v. 47, p. 721-743.

Mitchell, B. J., and Landisman, M., 1971, Geophysical measurements in the southern great plains, in Heacock, J. G., ed.: The Structure and Physical Properties of the Earth's Crust: Am. Geophys. Union Mon. 14, p. 77-95.

Moskowitz, Bruce M., 1977, Numerical analysis of electrical resistivity in hydrothermal systems: Unpublished M.S. thesis, University of Arizona.

Moskowitz, B., and Norton, D., 1977, A preliminary analysis of intrinsic fluid and rock resistivity in active hydrothermal systems: Jour. Geophys. Res., in review.

Muller, A. B., Battaile, J. R., Bond, L. A., Lamson, P. W., 1973, An analysis of the water quality problems of the Safford Valley, Arizona: Repts. on Natural Resource Systems, Rept. no. 15, 126 p.

Nash, T. J., 1973, Geochemical Studies in the Park City District: I. Ore Fluids in the Mayflower Mine: Econ. Geol., v. 68, no. 1, p. 34-59.

Nield, D. A., 1968, Onset of thermohaline convection in a porous medium: Water Resources Res., v. 4, p. 553-560.

Nielson, Richard L., 1968, Hypogene texture and mineral zoning in a copper-bearing granodiorite porphyry stock, Santa Rita, New Mexico: Econ. Geol., v. 63, no. 1, p. 37-50.

Nolan, T. B., 1943, The basin and range province in Utah, Nevada, and California: U.S. Geol. Survey Prof. Paper #197-D, p. 141-196.

Norris, R. J., and Henley, R. W., 1976, Dewatering of a metamorphic pile: Geology, v. 4, p. 333-336.

Norton, D., 1972, Concepts relating anhydrite deposition to solution flow in hydrothermal systems: 24th IGC, sec. 10, p. 237-244, Ottawa.

Norton, D. L., and Cathles, L. M., 1975, An analysis of the physics and chemistry of pluton environments, Part II: Applications: Unpublished manuscript.

Norton, D., and Gerlach, T., 1975a, Preliminary analysis of the energy and water requirements for developing geothermal energy in Arizona, in Proceedings of a Symposium on Water Requirements for Lower Colorado River Basin Energy, ed., Foster, K: Office of Arid Lands Studies, Univ. of Arizona, in press.

Norton, D., and Gerlach, T., 1975b, Characteristics useful in exploration for thermal energy resources as suggested by field observation and computer models (abs.): 2nd United Nations Symposium on the Development and Use of Geothermal Resources, San Francisco, California, May 20-29.

Norton, D., Gerlach, T., DeCook, K. J., and Sumner, J. S., 1975, Geothermal water resources in Arizona: Feasibility study: Technical Completion Rept., Office of Water Research and Technology, Project A-054-ARIZ.

Norton, D., and Knapp, R., 1977, Transport Phenomena in

Hydrothermal Systems: Nature of Porosity: Am. Jour. Sci., v. 277, p. 913-936.

Norton, D., and Knight, J. E., 1977, Transport phenomena in hydrothermal systems: Cooling plutons: Am. Jour. Sci., v. 277, p. 937-981.

Norton, Denis, 1977, Fluid circulation in the earth's crust: Am. Geophys. Union Mon. 20, in review.

Norton, Denis, 1978, Sourcelines, sourceregions, and pathlines for fluids in hydrothermal systems related to cooling plutons: Econ. Geol., in press.

Nur, A., and Simmons, G., 1969, The effect of saturation on velocity in low porosity rocks: Earth and Planet Sci. Letts., v. 17, p. 183-193.

Nur, A., and Simmons, G., 1970, The origin of small cracks in igneous rocks: Int. Jour. Rock Mech. Min. Sci., v. 7, p. 307-314.

Ohle, E. L., 1951, The influence of permeability on ore distribution in limestone and dolomite: Econ. Geol., v. 46, p. 667-706.

Ohmoto, H., and Rye, R. O., 1974, Hydrogen and oxygen isotope compositions of fluid inclusions in the Kuroko deposits, Japan: Econ. Geol., v. 69, p. 947-953.

Okamoto, G., Okura, T., and Goto, K., 1957, Properties of silica water: Geochim. et Cosmochim. Acta, v. 12, p. 123-132.

Osmond, J. C., 1960, Tectonic history of the basin and range province in Utah and Nevada: Mining Eng. v. 12, p. 251-265.

Parkhomenko, E. I., 1967, Electrical Properties of Rocks, Keller, G. V., ed. and trans.: New York, Plenum Press, 314 p.

Peaceman, D. W., and Rachford, H. H., Jr., 1955, The numerical solution of parabolic and elliptic differential equations: Soc. Indust. Appl. Math. Jour., v. 3, no. 1, p. 28-41.

Percious, J. K., 1968, Geology and Geochronology of the Del Bac Hills, Pima County, Arizona, in Titley, S. R., ed., Southern Arizona Guidebook: Arizona Geol. Soc., p. 199-208.

Peterson, D. W., 1960, Geology of the Haunted Canyon quadrangle, Arizona: U.S. Geol. Survey Geol. Quad. Map, GQ-128.

Peterson, D. W., 1968, Zoned ash-flow sheet in the region around Superior, Arizona, in Titley, S. R., ed., Southern

Arizona Guidebook III: Arizona Geol. Soc., p. 215-222.

Peterson, D. W., 1969, Geologic map of the Superior quadrangle, Pinal County, Arizona: U.S. Geol. Survey Geol. Quad. Map GQ-818.

Peterson, N. P., 1962, Geology and ore deposits of the Globe-Miami District, Arizona: U.S. Geol. Survey Prof. Paper #342, 151 p.

Plauff, D., 1966, Magneto-telluric soundings in the southwestern United States: Geophysics, v. 31, p. 1145-1152.

Porath, H., 1971, A review of the evidence on low resistivity layers in the earth's crust, in Heacock, J. G., ed., The Structure and Physical Properties of the Earth's Crust: Am. Geophys. Union Mon. 14, p. 127-145.

Pratt, H. R., Black, A. D., Brace, W. F., and Norton, D. L., 1974, In situ joint permeability in a granite: EOS, Trans. Am. Geophys. Union, v. 55, p. 433.

Quillen, R., and Combs, J., 1976, Microearthquake survey of the Radium Springs KGRA, South Central New Mexico: Geol. Soc. America, Absts. with Progs., v. 8, p. 1055.

Quinlan, J. J., and Simos, J. G., 1968, The Mayflower Mine, in Park City District, Utah: A. J. Erickson, ed., Utah Geol. Guidebook n. 22, p. 40-55.

Quist, A. S., Franck, E. U., Jolley, H. R., and Marshall, W. L., 1963, Electrical conductances of aqueous conditions at high temperature and pressure, 1, The conductances of potassium sulfate water solutions from 25 to 200 and at pressures up to 4000 bars: Jour. Phys. Chem., v. 67, p. 2453-2459.

Quist, A. S., and Marshall, W. L., 1968, Electrical conductances of aqueous sodium chloride solutions from 0°C to 200°C and at pressures to 4000 bars: Jour. Phys. Chem., v. 72, p. 684-703.

Quist, A. S., and Marshall, W. L., 1969, The electrical conductances of some alkali metal halides in aqueous solutions from 0 to 800 and at pressures to 4000 bars: Jour. Phys. Chem., v. 73, p. 978-985.

Ransome, F. L., 1909, The geology and ore deposits of Goldfield, Nevada: U.S. Geol. Survey Prof. Paper #66.

Ransome, F. L., 1919, The copper deposits of Ray and Miami, Arizona: U.S. Geol. Survey Prof. Paper #115.

Ratte, j. C., Landis, E. R., and Gaskill, D. L., 1969, Mineral

resources of the Blue Range Primitive Area, Greenlee county, Arizona, and Catron County, New Mexico: U.S. Geol. Survey Bull. no. 1261-E, 91 p.

Rayleigh, Lord, 1916, On convection currents in a horizontal layer of fluid, when the higher temperature is on the underside: Phis. Mag. Ser. 6, v. 32, p. 529-545.

Raymahashay, B. C., 1968, A geochemical study of rock alteration by hot springs in the Paint Pot Hill area, Yellowstone National Park: Geochim. et Cosmochim. Acta, v. 32, p. 499-522.

Ribando, R. J., Torrance, K. E., and Turcotte, D. L., 1976, Numerical models for hydrothermal circulation in the oceanic crust: Jour. Geophys. Res., v. 81, p. 3007-3012.

Ribando, R. J., and Torrance, K. E., 1975, Natural convection in a porous medium: effects of confinement, variable permeability, and thermal boundary conditions: ASME preprint 75-KW/HT-73, 9 p.

Risk, G. F., MacDonald, W. J. P., and Dawson, G. B., 1970, D.C. resistivity surveys of the Broadlands geothermal region, New Zealand: Geothermics Spec. Issue 2, U.N. Symp. on the Development and Utilization of Geothermal Resources, Pisa, v. 2, pt. 1, p. 287-294.

Roache, Patrick J., 1972, Computational fluid dynamics: Albuquerque, N.M., Hermosa Publishers, 434 p.

Robie, R. A., and Waldbaum, D. R., 1968, Thermodynamic properties of minerals and related substances at 298.15° K (25°C) and one atmosphere (10^{13} bars) pressure and at higher temperatures: U.S. Geol. Survey Bull. 1259.

Robinson, H. H., 1913, The San Francisco volcanic field, Arizona: U.S. Geol. Survey Prof. Paper #76, 213 p.

Rubin, H., 1973, Effect of nonlinear stabilizing salinity profiles on thermal convection in a porous medium layer: Water Resources Res., v. 9, p. 211-221.

Rye, R. O., and Ohmoto, H., 1974, Sulfur and carbon isotopes and ore genesis: A review: Econ. Geol., v. 6, p. 826-842.

Sato, K., 1970, The present state of geothermal development in Japan: Geothermics Spec. Issue 2, U.N. Symp. on the Development and Utilization of Geothermal Resources, Pisa, v. 2, pt. 1, p. 155-184.

Schmidt, E., 1969, Properties of water and steam in Si-units: New York, Springer-Verlag, 205 p.

Schoen, R., White, D. E., Man Ung Pak, and Tae Gyung, 1971, Metasomatic zonality of low-temperature hydrothermal secondary quartzites and argillaceous rocks with alunite: Chiji Kwa Chiri, v. 11, p. 21-25. (in Korean): Chem. Abst. CA07614074817N.

Schultz, John R., 1937, A Late Cenozoic vertebrate fauna from the Coso Mountains, Inyo County, California: Carnegie Inst., Washington, Pub. 487, p. 75-109.

Schwartz, George M., 1953, Geology of the San Manuel Copper Deposit, Arizona: U.S. Geol. Survey Prof. Paper #256.

Shankland, T. J., and Waff, H. S., 1974, Conductivity in fluid bearing rocks: Jour. Geophys. Res., v. 79, p. 4863-4868.

Shaw, D. R., 1965, Strike-slip control of basin-range structure indicated by historical faults in western Nevada: Geol. Soc. America Bull., v. 76, p. 1361-1378.

Shaw, H. R., and Swanson, D. A., 1970, Eruption and flow rates of flood basalts, in Gilmour, E. H., and Stradlin, G. D., eds., Proc. 2nd Columbia River Basalt Symp.: Pullman East., Wash. State College Press, p. 271-299.

Sheridan, M. F., and Fodor, R. V., 1969, Orogin of silicic ash-flow tuffs and lavas in the Goldfield Mountains, Arizona (abs.): Geol. Soc. America Spec. Paper no. 121, p. 557-558.

Sheridan, M. F., and Stuckless, J. S., 1969, Volcanics related to Black Mesa Caldera, central Arizona (abs.): Geol. Soc. America Spec. Paper no. 121, p. 60-61.

Simmons, G., and Nur, A., 1968, Granites: Relation of properties in situ laboratory measurements: Science, v. 162, p. 789-791.

Simmons, G., and Nur, A., 1969, The effect of saturation on velocity in low porosity rocks: Earth and Planet. Sci. Letts., v. 7, p. 183-193.

Simons, F. S., 1964, Geology of the Klondike Quadrangle, Graham and Pinal counties, Arizona: U.S. Geol. Survey Prof. Paper #461, 173 p.

Skinner, B. J., 1960, Assemblage enargite-famatinite, a possible geologic thermometer (abs.): Geol. Soc. America Bull., v. 71, p. 1975.

Skinner, B. J., 1966, Thermal expansion, in Clark, S. P., ed., Handbook of Physical Constants, Geol. Soc. America Mem. 97: New York, Geol. Soc. America, p. 75-96.

Smiley, T. L., 1958, The geology and dating of Sunset Crater, Flagstaff, Arizona, in New Mexico Geol. Soc. Guidebook: 9th Field Conf., Black Mesa Basin, p. 186-190.

Smith, J. H., 1970, Geothermal development in New Zealand: Geothermics Spec. Issue 2, U. N. Symp. on the Development and Utilization of Geothermal Resources, Pisa, v. 2, pt. 1, p. 232-247.

Smith, R. B., and Sbar, M. L., 1974, Contemporary tectonics and seismicity of the western United States with emphasis on the Intermountain Seismic Belt: Geol. Soc. America Bull., v. 85, p. 1205-1218.

Smith, R. L., and Shaw, H. R., 1973, Volcanic rocks as geologic guides to geothermal evaluation: EOS:Trans. Am. Geophys. Union, v. 54, p. 1213.

Snow, D. T., 1965, A parallel plate model of fractured permeable media: Unpublished Ph.D. dissertation, University of California, Berkeley, 331 p.

Snow, D. T., 1968, Rock fracture spacings, openings, and porosities: Jour. Soil Mech. and Foundations Div., ASCE, v. 94, p. 73-91.

Snow, D. T., 1970, The frequency and aperture of fractures in rocks: Jour. Rock Mech., v. 7, p. 23-40.

Ssu-hsiao, 1250, in Brower, ed., Of All Things Most Yielding: San Francisco, California, McGraw-Hill, Friends of the Earth, 128 p.

Summers, W. K., 1965, Chemical characteristics of New Mexico thermal waters: New Mexico Bureau of Mines Circ. 83, 87 p.

Takahashi, T., and Kiyonori, S., 1974, Geology and ore deposits of the Hanaoka belt, Akita Prefecture: Soc. Mining Geologists Japan, Spec. Issue 6, p. 101-113.

Takashima, I., 1972, Hydrothermal rock alteration in Takenoyu geothermal area, Kumamoto Prefecture, Japan: Chishitsu Chosajo Geppo, v. 23, p. 721-732 (in Japanese): Chem. Abst. CA07908044422Z.

Tatsumi, T., ed., 1970, Volcanism and ore genesis: Tokyo, University of Tokyo Press, 448 p.

Taylor, H. P., Jr., 1971, Oxygen isotope evidence for large-scale interaction between meteoric ground waters and Tertiary granodiorite intrusions, Western Cascade Range, Oregon:

Jour. Geophys. Res., v. 76, p. 7755-7873.

Taylor, Hugh P., Jr., 1974, The application of oxygen and hydrogen isotope studies to problems of hydrothermal alteration and ore deposition: Econ. Geol., v. 69, no. 6, p. 843-883.

Teledyne Geotech, 1972, Geothermal noise survey of the Coso Hot Springs area, Naval Weapons Center, China Lake, California: Unpublished Tech. Rept. no. 72-6, produced under contract for the Naval Weapons Center, 18 p.

Tellier, A. H., 1973, Geothermal waters of Arizona: Unpublished M.S. thesis, Arizona State University, 31 p.

Thoenin, J. R., 1941, Alunite resources of the United States: U.S. Bur. of Mines Res. Rept. 3561, 48 p.

Thompson, G. A., 1960, Problem of the Late Cenozoic structure of the Basin Ranges: 20th IGC, pt. 18, p. 62-68.

Timoshenko, S. P., and Goodier, J. H., 1951, Theory of elasticity: New York, McGraw-Hill, 2nd ed.

Tono, N., 1974, Minor elements distribution around Kuroko deposits of northern Akita, Japan: Soc. Mining Geologists Japan, Spec. Issue 6, p. 399-420.

Ulbrich, H. H., and Merino, E., 1974, Examination of standard enthalpies of formations of selected minerals in the SiO_2-Al_2O_3-Na_2O-K_2O-H_2O system: Am. Jour. Sci., v. 274, p. 510-542.

Van Hise, C. R., 1901, Some principles controlling the deposition of ores: Am. Inst. Min. Eng. Trans., v. 30, p. 27.

Veronis, G., 1968, Effect of stabilizing gradient of solute on thermal convective: Jour. Fluid Mech., v. 34, p. 315-336.

Villas, Netuno R., 1975, Fracture analysis, hydrodynamic properties, and mineral abundance in altered igneous rocks at the Mayflower Mine, Park City District, Utah: Unpublished Ph.D. dissertation, University of Utah.

Villas, R. N., and Norton, D., 1977, Irreversible mass transfer between circulating hydrothermal fluids and the Mayflower stock: Econ. Geol., v. 72, in press.

Wagmen, D. D., Evans, W. H., Parker, V. B., Halow, I., Vailey, S. M., and Schumm, R. H., 1968, Selected values of chemical thermodynamic properties: Natl. Bur. Standards, Tech. Note 270-3, 264 p.

Walsh, J. B., 1965, The effects of cracks on the compressibility of rock: Jour. Geophys. Res., v. 70, p. 381-389.

Walsh, J. B., and Brace, W. F., 1966, Cracks and pores in rocks: Internatl. Cong. Rock. Mech., Lisbon, p. 643-646.

Ward, S. H., and Fraser, D. C., 1967, Conduction of electricity in rocks, in Mining Geophysics: Soc. Expl. Geol., p. 197-222.

White, D. E., 1964, Saline waters of sedimentary rocks: Am. Assoc. Pet. Geol. Bull., v. 48, p. 342-365.

White, D. E., 1974, Diverse origins of hydrothermal ore fluids: Econ. Geol., v. 69, no. 6, p. 954-973.

White, D. E., and Williams, D. L., eds., 1975, Assessment of geothermal resources of the United States: Geol. Survey Circ. 726, 155 p.

Willden, R., 1964, Geology of the Christmas Quadrangle, Gila and Pinal counties, Arizona: U.S. Geol. Survey Bull., no. 1161-E., 64 p.

Williams, H., 1932, History and character of volcanic domes: Univ. Calif. Pub., Dept. Geol. Sci., Bull. 21, p. 51-146.

Williams, N. C., 1952, Wall rock alteration, Mayflower Mine, Park City, Utah: Unpublished Ph.D. dissertation, Columbia University, 58 p.

Wilson, J. C., 1967, Geology of the Alta Stock, Utah: Unpublished Ph.D. dissertation, California Institute of Technology, 236 p.

Winograd, I. J., 1971, Hydrogeology of ash flow tuff: a preliminary statement: Water Resources Res., v. 7, p. 994-1006.

Wong, C. M., 1970, Geothermal energy and desalination: Patterns in progress: Geothermics Spec. Issue 2, U. N. Symp. on Development and Utilization of Geothermal Resources, Pisa, v. 2, pt. 1, p. 892-895.

Wooding, R. A., 1957, Steady state free thermal convection of liquid in a saturated permeable medium: Jour. Fluid Mech., v. 2, p. 273-285.

Wright, J. J., 1971, The occurrence of thermal groundwater in the Basin and Range Province of Arizona, in Hydrology and Water Resources in Arizona and the Southwest: Proc. 1971 Mtgs., Arizona Sec., Tempe, Arizona, April 22-23.

Zbur, R. T., 1963, A geophysical investigation of Indian Wells Valley, California: U.S. Naval Ordinance Testing Stations,

China Lake, California: Naval Ordinance Test Station Tech. Paper 2795, 98 p.

Zen, E., 1972, Gibbs free energy, enthalpy, and entropy of ten rock-forming minerals: Calculations, discrepancies, implications: Am. Miner., v. 57, p. 524-553.

Zienkiewicz, O. C., 1971, The finite element method in engineering science: London, McGraw-Hill, 521 p.

Zohdy, A. A. R., Anderson, L. A., and Muffler, L. J. P., 1973, Resistivity, self potential, and induced polarization surveys of a vapor-dominated geothermal system: Geophysics, v. 38, p. 1130-1144.